Model Development Report: Navarro River Watershed

SUBMITTED TO:

State Water Resources Control Board
1001 I Street, 14th Floor
Sacramento, CA 95814

PREPARED BY:

Paradigm Environmental
9320 Chesapeake Drive, Suite 100
San Diego, CA 92123

APRIL 28, 2025

THIS PAGE INTENTIONALLY LEFT BLANK

Contents

Figures

Tables

1 INTRODUCTION

This report provides a detailed discussion of the development and configuration of a hydrology model which was developed for the Navarro River watershed to support decision making by the California State Water Resources Control Board (Water Board) regarding water supply, demand, and use. In April 2021, Governor Gavin Newsom issued a state of emergency proclamation for specific watersheds across California in response to exceptionally dry conditions throughout the state. The April 2021 proclamation, as well as subsequent proclamations, directed the Board to address these emergency conditions to ensure adequate, minimal water supplies for critical purposes. To support Water Board actions to address emergency conditions, hydrologic modeling and analysis tools are being developed to contribute to a comprehensive decision support system that assesses water supply and demand, and the flow needs for watersheds throughout California.

This model development report builds on the Navarro River watershed modeling work plan[1], which has additional information on the model background and overarching model approach; the Loading Simulation Program in C++ (LSPC) was used to simulate hydrology within the watershed. The model provides an evaluation platform for (1) simulating existing instream flows that integrate current water management activities and consumptive uses and (2) evaluating the range of impacts of alternative management scenarios. Key components necessary for the development of this model are detailed in this report. Model development refers to basic building blocks for defining the surface water model domain. It includes catchments delineation, reach segments (cross-sections, hydraulic characteristics, and routing network), and Hydrologic Response Units (HRUs). Model development also includes creating and assigning representative climate forcing inputs. The final sections of this report provide details on the model calibration approach and present calibration and validation results.

- Section 2.1 describes the Catchment Delineation. Catchments are the highest-resolution spatial boundaries in the model. Delineated catchments were compiled from best-available topographic layers and refined to align outlets with monitoring gauges.
- Section 2.2 describes the Hydraulic Network. Hydraulic routing features include reaches, lakes/reservoirs, and other network routing elements that convey flow and pollutants from one catchment to another.
- Section 3 describes the Hydrologic Response Units. HRUs are the smallest spatial unit within the model, representing unique combinations of spatial data layers, including land use/land cover, hydrologic soil group, and slope.
- Section 4 describes the climate-forcing inputs. Forcing inputs that drive the model's rainfall-runoff response include precipitation and potential evapotranspiration.
- Section 5 describes the surface water demand data, withdrawals, and irrigation demand.
- Section 6 describes the model calibration approach and results.
- Section 7 presents the model validation results.

[1] The Navarro River watershed modeling work plan is available online at: https://www.waterboards.ca.gov/waterrights/water_issues/programs/supply-and-demand/navarro-river.html

2 CATCHMENT NETWORK

2.1 Catchment Delineation

The United States Geological Survey (USGS) delineates watersheds nationwide based on surface hydrological features and organizes the drainage units into a nested hierarchy using hydrologic unit codes (HUC). These HUCs have a varying number of digits to denote scale ranging from 2-digit HUCs (largest) at the regional scale to 12-digit HUCs (smallest) at the subwatershed scale. The Navarro River watershed is defined as a HUC-10 watershed that comprises 9 HUC-12 subwatersheds.

For units smaller than HUC-12 subwatersheds, the National Hydrography Dataset Plus v2 (NHDPlus) has further discretized the watershed into catchments ranging in size between 0.001 square miles to over 5 square miles. Figure 2-1 is a map of HUC-12 subwatersheds and NHDPlus catchments within the Navarro River watershed (HUC-10). Table 2-1. presents summary statistics of NHDPlus catchment sizes by HUC-12 subwatershed.

Where necessary, catchments were either merged to eliminate divergences in the stream network (e.g., islands in the mainstem) or sub-delineated using the hydrologically conditioned 30-meter resolution digital elevation model (DEM), flow direction, and flow accumulation rasters available with the NHDPlus dataset to represent points of interest better. Catchments were merged in two cases in the Navarro River watershed to eliminate divergences on the mainstem of the Navarro River. Sub-delineation was necessary in one case in the Navarro River watershed, where a catchment had disconnected reach segments with points of diversion; this catchment was split into three catchments as shown in Figure 2-2. Figure 2-3 shows the final delineated catchments for the LSPC model and highlights areas that were refined from the original NHDPlus catchment layer.

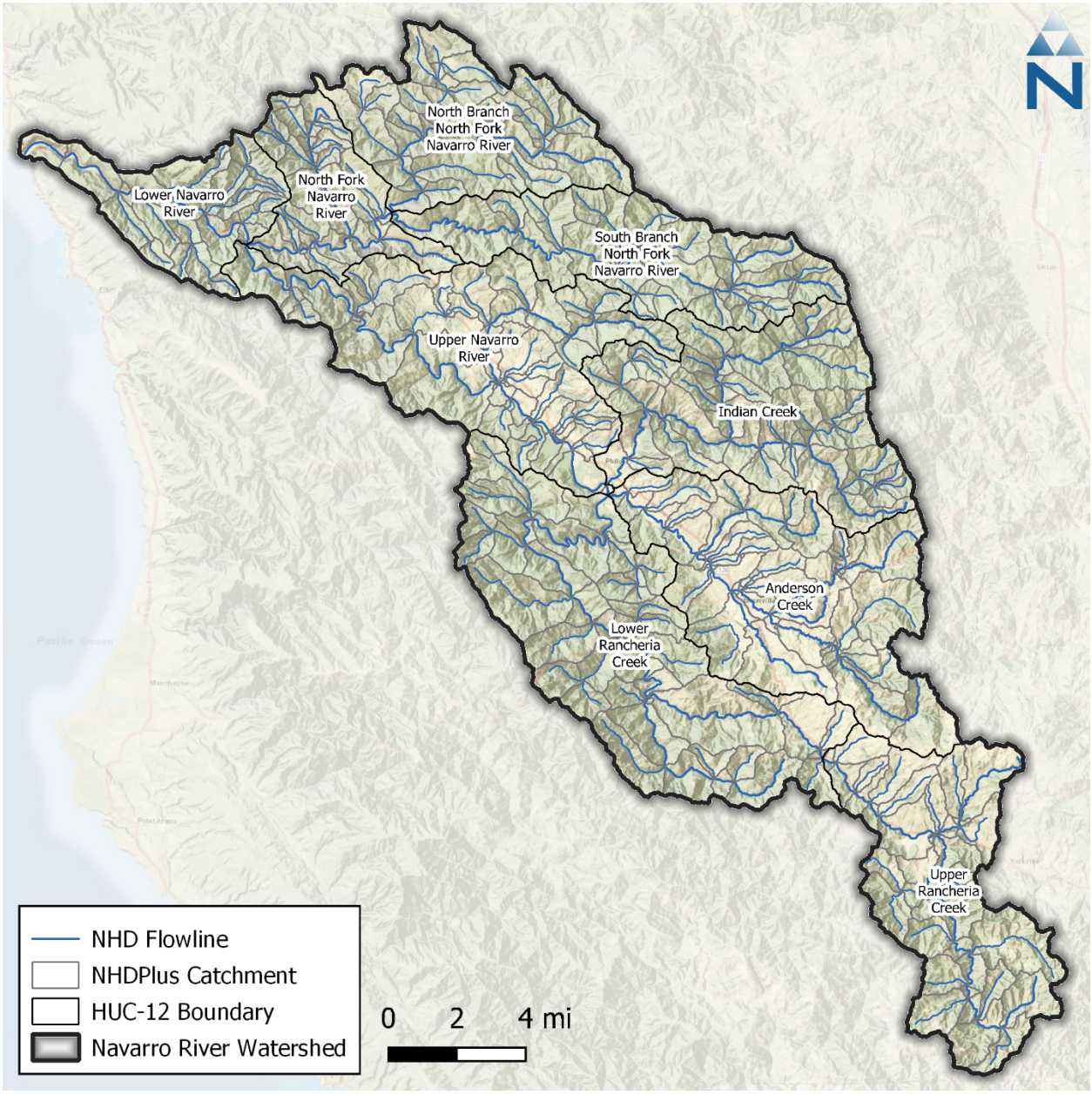

Figure 2-1. Initial NHDPlus catchment segmentation for the Navarro River watershed.

Table 2-1. Summary of final NHDPlus catchments within the Navarro River watershed HUC-12 subwatersheds

HUC-12	HUC-12 Name	Catchment Count	Catchment Area (ac)			
			Minimum	Average	Maximum	Total
180101080401	Upper Rancheria Creek	37	6.9	643.9	2,439.62	23,822.8
180101080402	Lower Rancheria Creek	50	1.1	707.0	3,706.10	35,352.0
180101080403	Anderson Creek	53	5.6	555.0	2,354.88	29,414.0
180101080404	Indian Creek	49	2.2	515.3	1,993.66	25,249.9
180101080405	North Branch North Fork Navarro River	34	55.4	535.0	1,874.28	18,190.6
180101080406	South Branch North Fork Navarro River	34	19.1	552.7	2,710.58	18,791.3
180101080407	North Fork Navarro River	28	15.8	375.0	1,677.28	10,501.1
180101080408	Upper Navarro River	53	0.9	540.8	3,712.73	28,660.3
180101080409	Lower Navarro River	26	9.3	438.2	1,208.65	11,394.0
	Total	**364**	**--**	**--**	**--**	**201,368**

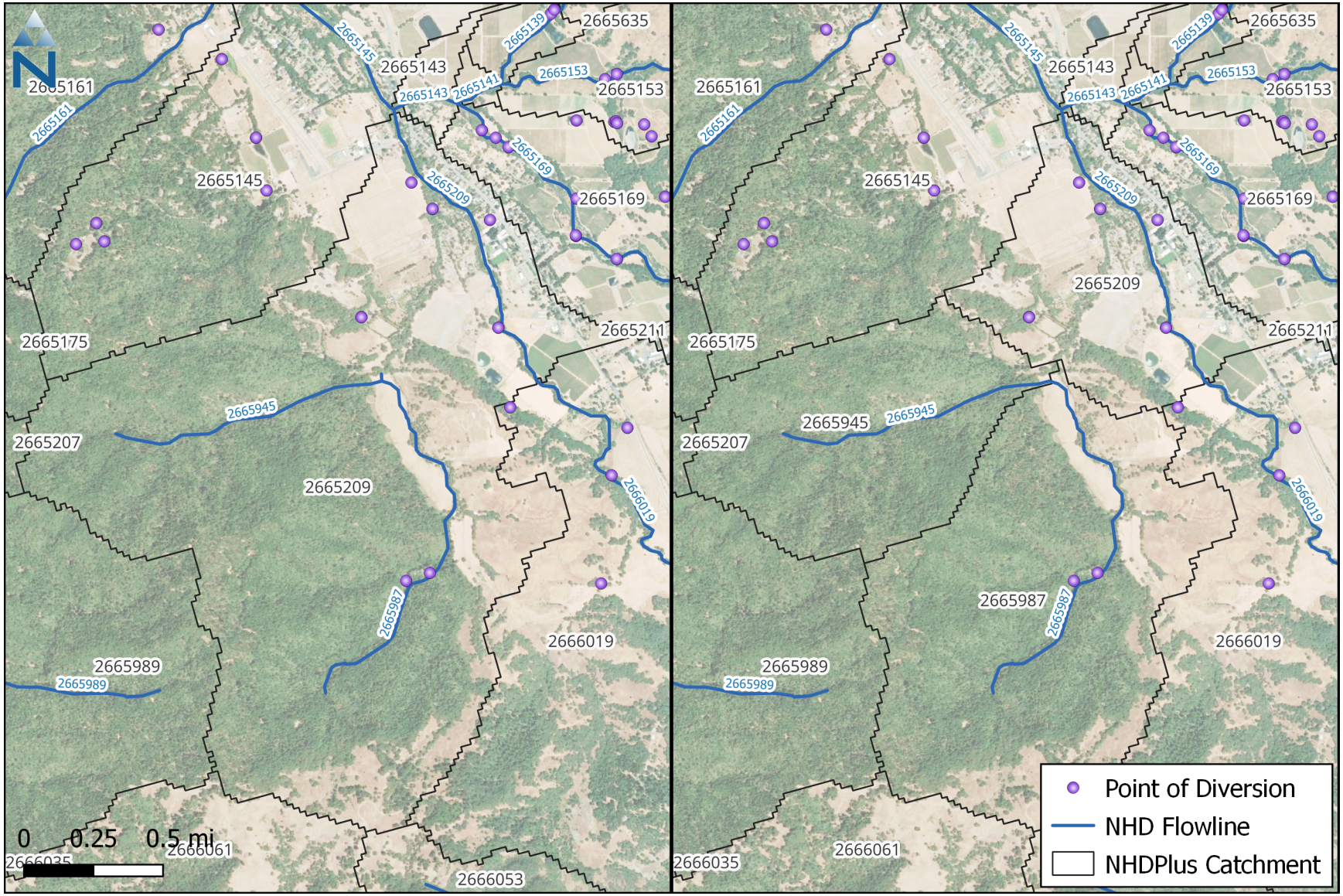

Figure 2-2. Map depicting disconnected flowlines (left) in catchment 2665209 and the delineated catchments represented in LSPC (right).

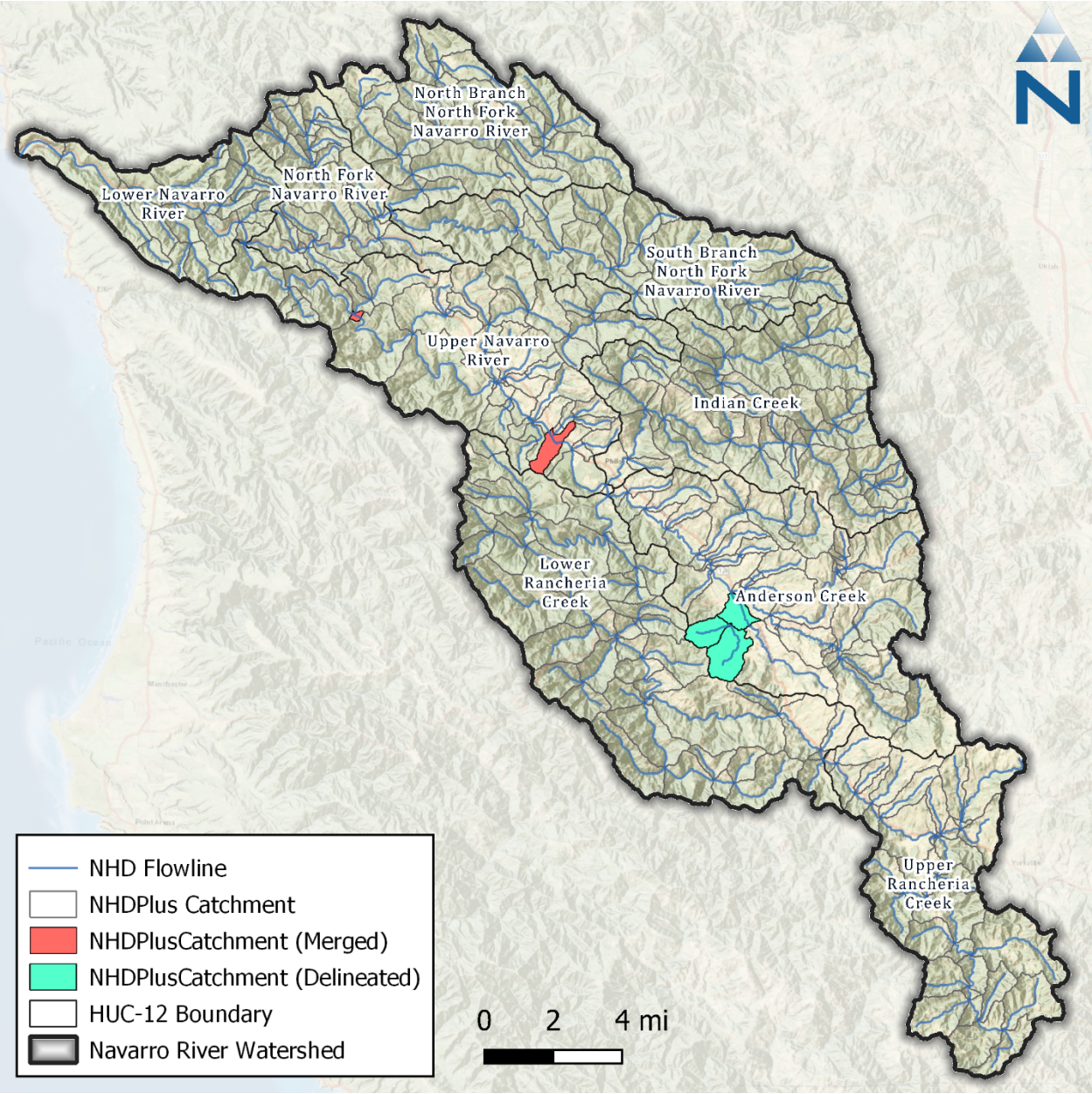

Figure 2-3. Final NHDPlus catchment segmentation for the Navarro River watershed.

2.2 Routing and Connectivity

Once catchments have been delineated, the connectivity of flow within and between each catchment needs to be specified so that water can be routed from upstream to downstream areas. Within the Navarro River watershed model, surface flow is conveyed through a reach network with one representative reach segment for each catchment. Within a catchment, water from all other upstream physical conveyance is routed directly to the top of and through the representative stream segment.

The reach network for the Navarro River watershed is based on the NHD flowlines available with the NHDPlus dataset. As described in Section 2.1, these flowlines were edited to eliminate braiding and are shown in Figure 2-3. Within the NHDPlus schema, catchments can be related to flowlines through the catchment *FEATUREID* and flowline *COMID*. The flowline *COMID* was joined to the

PlusFlowlineVAA (value-added attributes) table available with the NHDPlus dataset to determine flow routing.

2.3 Stream Characteristics

The discharge for each stream segment is calculated in LSPC using the Manning equation, presented below as Equation 1:

$$Q = VA = (1.49/n)\, AR^{2/3}\sqrt{S}$$

where (A) is the cross-sectional area in square feet, (R) is the hydraulic radius in feet, (V) is the velocity in feet per second, (S) is the longitudinal slope in feet/feet, and (n) is the channel roughness coefficient.

Length and slope are derived from the NHDPlus Value-Added Attribute table (VAA), which includes precalculated reach characteristics based on local conditions. For reaches that were merged, split, or edited, the slope was recalculated based on the new reach length and the difference between the minimum and maximum elevation (derived from the DEM described in Section 3.4). The default cross-section representation in LSPC is a symmetrical trapezoidal channel defined using the terms shown in Figure 2-4. Stream segments are represented in the model as having the same cross-section for the entire reach length. Numerous studies have developed empirical relationships between stream channel geometry and upstream contributing area (Bent and Waite 2013; McCandless 2003a, 2003b; McCandless and Everett 2002); these were used to derive channel geometry for each stream segment in LSPC. An initial estimate of $n = 0.04$ representing natural streams with vegetation was used for all reach segments and may be updated as needed during model calibration (Arcement and Schneider 1989).

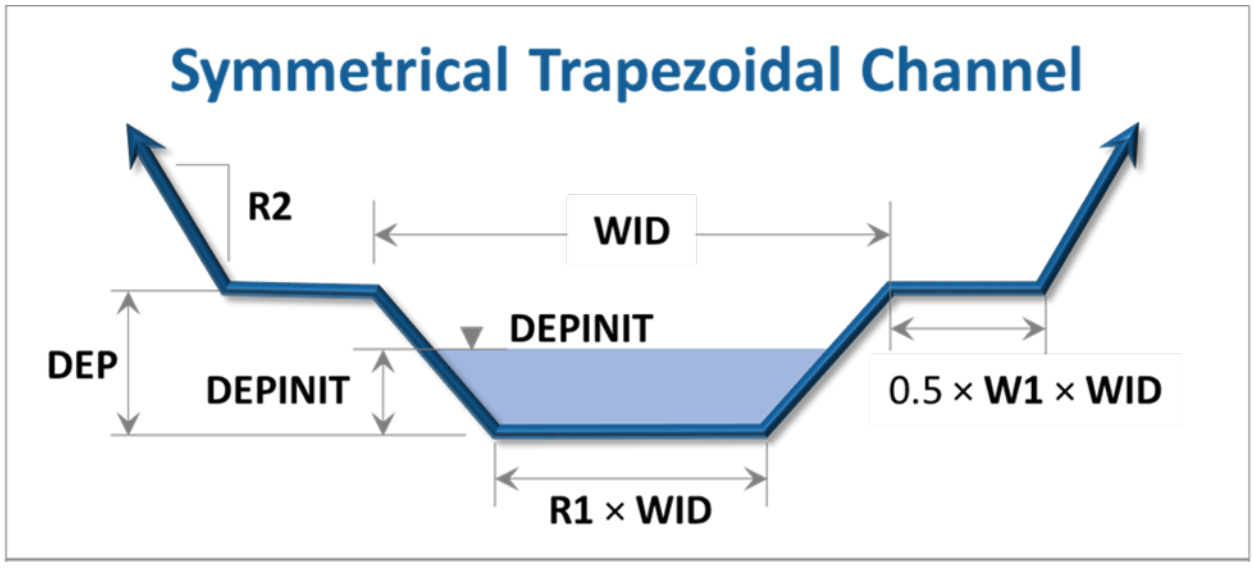

WID	Estimated Bankfull-Width	**R1**	Ratio of channel bottom width to **WID**
DEP	Estimated Bankfull-Depth	**R2**	Side slope for floodplain
DEPINIT	Initial water depth	**W1**	Floodplain width parameter

Figure 2-4. Example cross-section representation in LSPC.

3 HYDROLOGIC RESPONSE UNITS

Within LSPC, land is categorized into HRUs, which are the core hydrologic modeling land units in the watershed model. Each HRU represents areas of similar physical characteristics attributable to certain processes. The HRU development process uses data types that are typically closely associated with hydrology (and water quality, when applicable) in the watershed. For the Navarro River watershed, this includes data such as land cover, cropland, soil type, and slope. The HRUs are developed by overlaying these datasets in raster format and identifying the unique combinations over catchments. Ultimately, some consolidation of HRUs was implemented to balance the model computational efficiency and optimal spatial resolution, resulting in a set of meaningful HRUs for model configuration. Secondary attributes such as tree canopy cover are summarized by HRU to estimate initial values for the interception storage and lower-zone evapotranspiration rate for model configuration.

Table 3-1 lists the spatial data used in the HRU analysis along with the corresponding data sources. The following subsections summarize the data that were used to develop each of these spatial layers and the processes for consolidating them as HRUs.

Table 3-1. Summary of input datasets detailing data source and type

GIS Layer	Data Source	Site	Description	Date Downloaded
Digital Elevation Model	USGS 3D Elevation Program (3DEP)	Science Base	2020 – 27.89m resolution grid	March 29, 2024
Land Cover	MRLC (NLCD)	MRLC	2021 – 30m resolution grid	June 30, 2023
Cropland	USDA (CDL)	USDA	2022 – 30m resolution grid	January 2, 2023
Percent Imperviousness	MRLC (NLCD)	MRLC	2021 – 30m resolution grid	June 30, 2023
Percent Tree Canopy	MRLC	MRLC	2021 – 30m resolution grid	October 5, 2023
Soil Survey Geographic Database (SSURGO)	USDA (NRCS)	USDA	2022 – polygon layer	October 5, 2023

3.1 Land Cover

The land cover data were obtained from the 2021 National Land Cover Database (NLCD) maintained by the Multi-Resolution Land Consortium (MRLC), a joint effort between multiple federal agencies. The primary objective of the MRLC NLCD is to provide a current data product in the public domain with a consistent characterization of land cover across the United States. The 2021 NLCD provides a 16-class scheme at a 30-meter grid resolution.

Table 3-2 summarizes the NLCD 2021 land cover distribution for the Navarro River watershed; Figure 3-1 shows the land cover for the Navarro River watershed. Evergreen forest is the dominant land cover classification covering approximately 67% of the watershed area. When combined, evergreen forest,

the undeveloped categories of deciduous forest, mixed forest, shrub/scrub, and grassland/herbaceous account for close to 95% of the total watershed area. Developed land cover makes up less than 5% of the total watershed area and is classified mostly as "Developed, Open Space," which suggests that much of the developed area is dispersed. Approximately 0.3% of the total watershed area is categorized as cultivated cropland. For HRU development, similar NLCD classes (e.g., forest) were grouped.

Table 3-2. Distribution of 2021 NLCD land cover classes within the Navarro River watershed

NLCD Class	Description	Model Group	Area	
			Acres	%
22	Developed, Low Intensity	Developed_Low_Intensity	411.2	0.20%
23	Developed, Medium Intensity	Developed_Medium_Intensity	141.4	0.07%
24	Developed, High Intensity	Developed_High_Intensity	24.5	0.01%
21	Developed, Open Space	Developed_Open_Space	9,267.4	4.60%
31	Barren Land (Rock/Sand/Clay)	Barren	22.2	0.01%
41	Deciduous Forest	Forest	603.4	0.30%
42	Evergreen Forest	Forest	134,393.6	66.74%
43	Mixed Forest	Forest	9,203.8	4.57%
52	Shrub/Scrub	Scrub	32,939.0	16.36%
71	Grassland/Herbaceous	Grassland	12,431.4	6.17%
81	Pasture/Hay	Pasture	141.0	0.07%
82	Cultivated Crops	Agriculture	638.7	0.32%
90	Woody Wetlands	Forest	817.1	0.41%
95	Emergent Herbaceous Wetlands	Grassland	237.3	0.12%
11	Open Water	Water	96.5	0.05%
		Total	**201,368**	**100%**

Color Gradient: Lowest | Low | Med | High | Highest

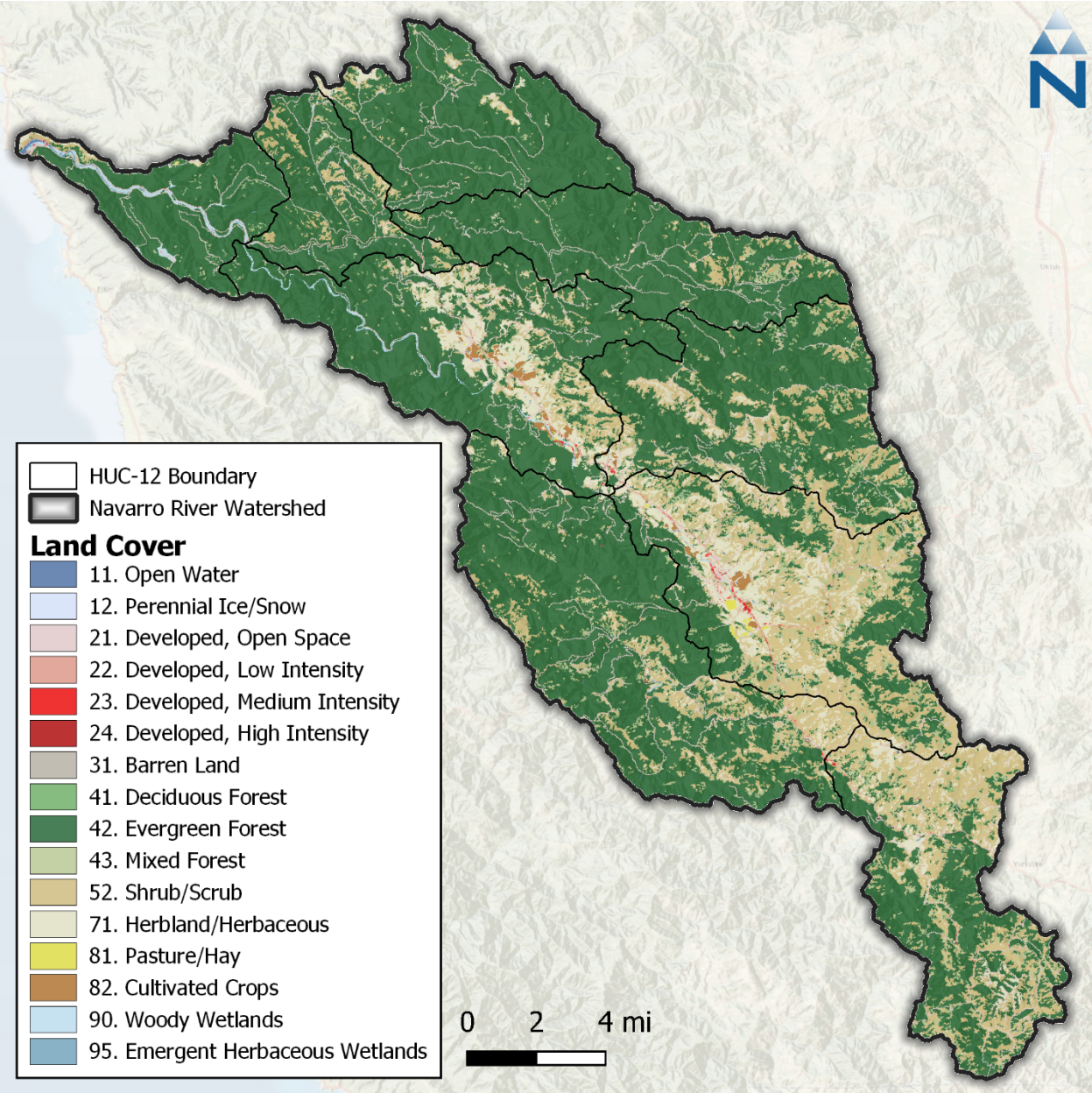

Figure 3-1. NLCD 2021 land cover within the Navarro River watershed.

3.2 Agriculture and Crops

Land cover data for the Navarro River watershed (see Section 3.1) was analyzed to identify predominant cropland vegetation classes. This analysis revealed that less than 0.07% of the Navarro River watershed area is classified as Pasture/Hay (class 81) and 23% of the watershed was classified as either Shrub/Scrub (class 52) or Grassland/Herbaceous (class 71); of these areas, a portion may include areas of cultivated crops that were not automatically recognized through processing of the remote sensing data or include cultivated crops on a rotating schedule. To reflect these situations, supplemental information published by the United States Department of Agriculture (USDA) was used.

The USDA Cropland Data Layer (CDL) (USDA 2024) is an annually updated raster dataset that geo references crop-specific land use. The dataset comes as a 30-meter resolution raster with a linked lookup table of 85 standard crop types that can be used to classify agricultural land. Figure 3-2 shows the spatial distribution of these classes through the study area, and Table 3-3 summarizes their areal coverage. The CDL layer was intersected with the NLCD Land Cover layer, and CDL Agriculture and Pasture land use classifications overwrote the original NLCD classifications. The combined Land Use/Land Cover (LULC) increased "Cropland" to 2,400 acres (1.2% of total watershed area), which was classified as "Agriculture" in the final HRU layer—"Pasture" area was also updated to match CDL land use. The LULC intersection redistributes HRU area between originally classified Grassland, Pasture, and Agriculture categories from NLCD.

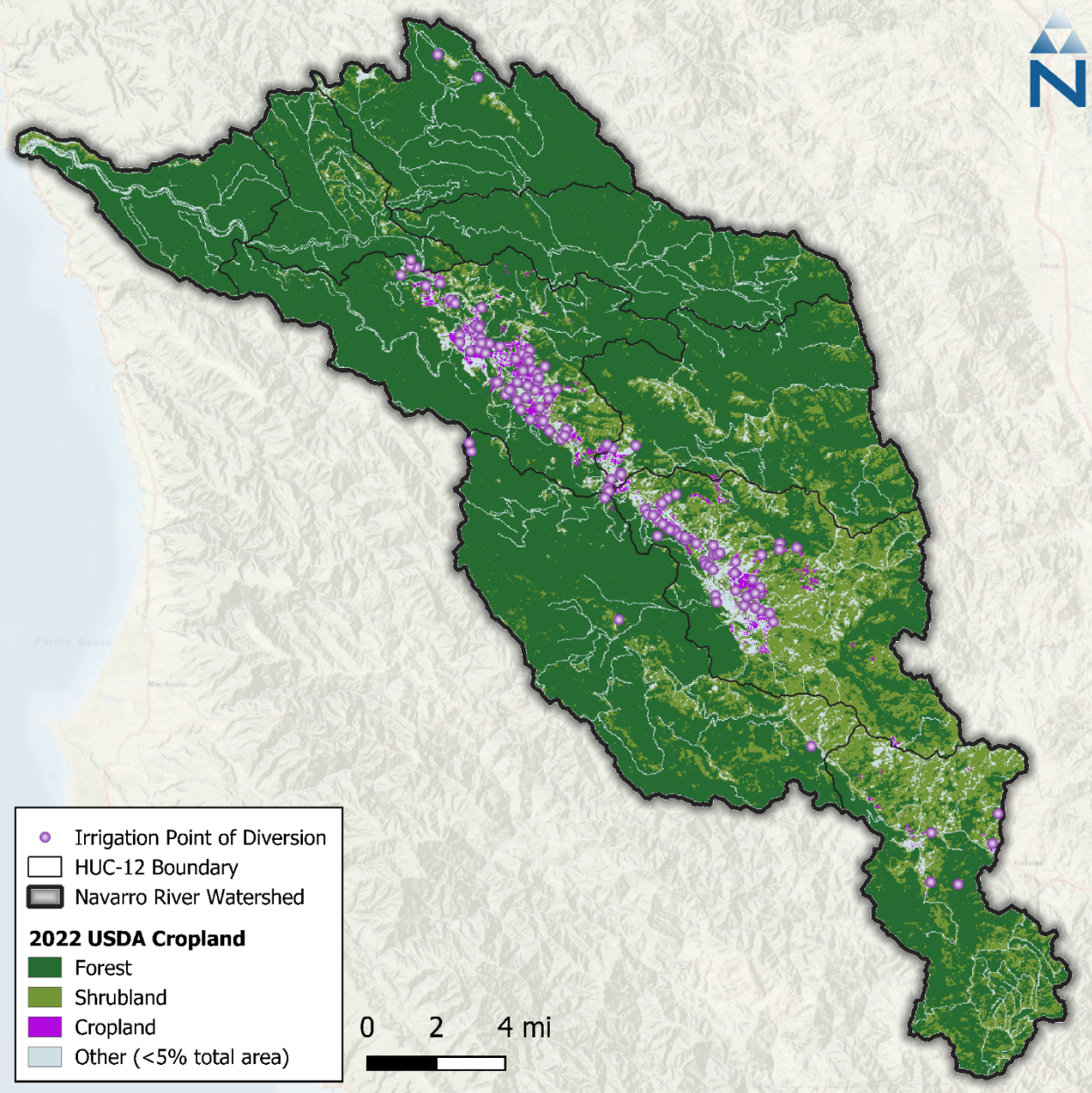

Figure 3-2. USDA 2022 Cropland Data within the Navarro River watershed.

Table 3-3. USDA 2022 Cropland Data Summary within the Navarro River watershed

Crop Type	Area (ac)	Area (%)
Forest	144,443.5	71.73%
Shrubland	37,207.4	18.48%
Cropland	2,286.7	1.14%
Other (<5% Total Area)	17,430.8	8.66%
Total	**201,368**	**100%**

Color Gradient: Lowest | Low | Medium | High | Highest

3.3 Soils

Soil data for the Navarro River watershed were obtained from the Soil Survey Geographic Database (SSURGO) published by the Natural Resource Conservation Service (NRCS). Four primary hydrologic soil groups (HSG) are used to characterize soil runoff potential. Group A generally has the lowest runoff potential, whereas Group D has the highest runoff potential. The SSURGO soils database is composed of a GIS polygon layer of map units and a linked tabular database with multiple layers of soil properties.

Table 3-4 and Figure 3-3 present summaries of the SSURGO hydrologic soil groups for the Navarro River watershed. The dominant soil group in the watershed is Group B (51%), containing moderately well to well-drained silt loams and loams. Group C (36%) is the next most common soil group in the watershed, containing sandy clay loam that typically has low infiltration rates. Group D, with the lowest infiltration rates, makes up approximately 12% of the watershed. Less than 1% of the watershed areas have mixed soils. For modeling purposes, mixed soils will be grouped with the nearest primary group as follows: A/D → B, B/D → C, and C/D → D. Less than 1% of the watershed HSG area is classified as unknown in the SSURGO database. Since most of the soil in the watershed is Group B, the unknown soil areas are also considered to be Group B in the analysis.

Table 3-4. NRCS Hydrologic soil groups in the Navarro River watershed

Soil Group	Model Group	Area (acre)	Area (%)
A	A	1,580.1	0.8%
A/D	B	134.5	0.1%
B	B	101,690.7	50.5%
C	C	72,413.9	36.0%
C/D	D	408.3	0.2%
D	D	23,745.4	11.8%
Unclassified	B	1,395.3	0.7%
	Total	**201,368**	**100%**

Color Gradient: Lowest | Low | Medium | High | Highest

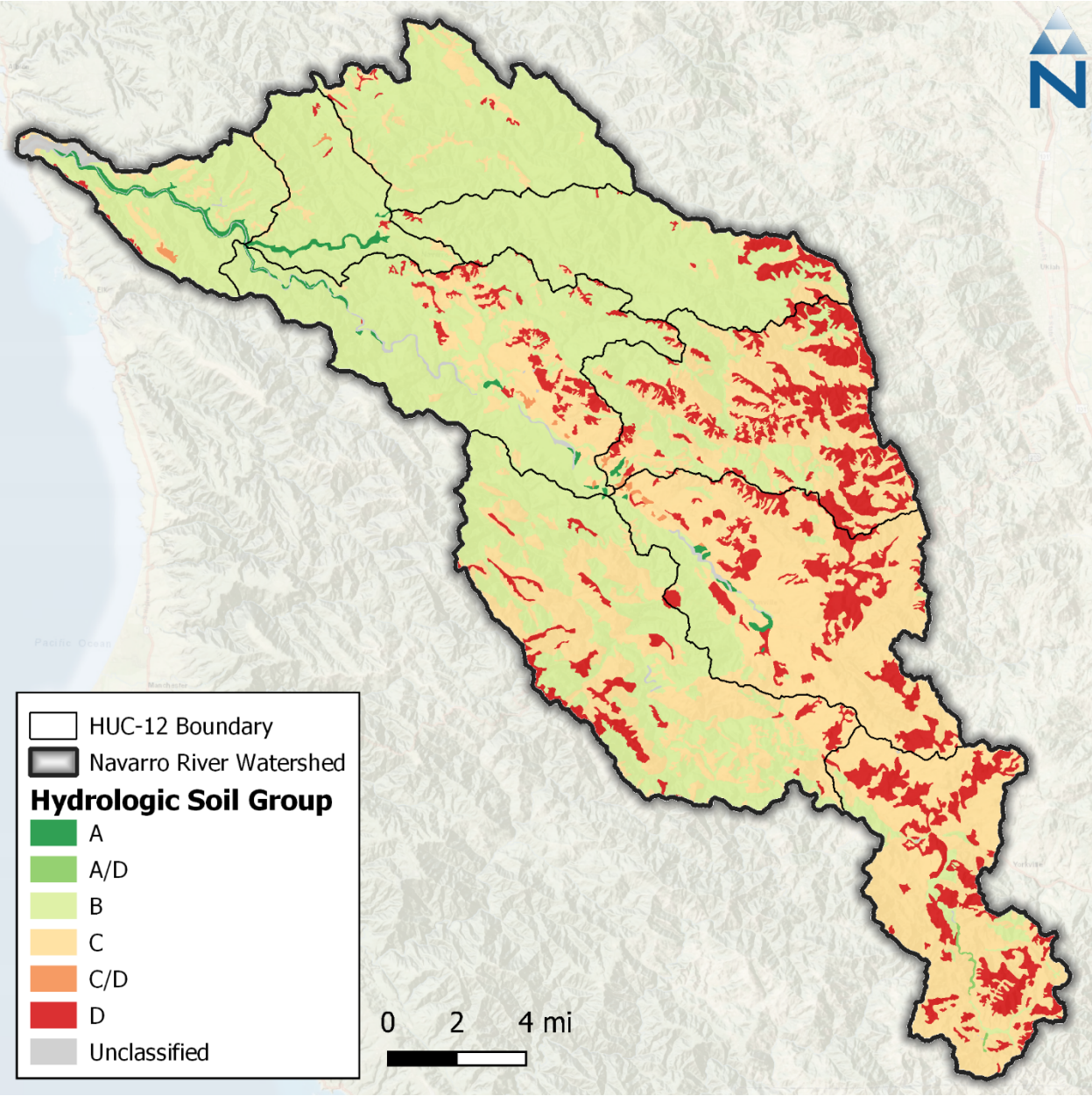

Figure 3-3. SSURGO hydrologic soil groups within the Navarro River watershed.

3.4 Elevation and Slope

The United States Geological Survey (USGS) 3D Elevation Program (3DEP) publishes DEMs expressing landscape elevation through a raster grid data product with a 1 arc-second (approximately 30-meter) horizontal resolution. The 1 arc-second data covering the Navarro watershed had a resolution of 27.89-meters and thus was resampled to 30-meters for consistency with the rest of the datasets for the HRU analysis. The Navarro watershed ranges in elevation from less than 100 meters along the riverbed in the northern part of the watershed to over 1,000 meters at several of the highest elevation peaks in the southern portion of the watershed along the eastern edge.

The 30-meter DEM was used to generate a slope (percent rise) raster for the watershed. Figure 3-4 illustrates the cumulative distribution function (CDF) of the slope raster values across the model

domain as a percentage of the total watershed land area (i.e., excluding major water bodies). The CDF was used to identify appropriate bins for HRU slope categories during the HRU definition process. Slopes were categorized as low (< 5%), medium (5 to 15%), and high (>15%) according to their distribution and overlap with the land cover layer. Table 3-5 and Figure 3-5 present the distribution of slope categories within the watershed. These slope categories are used to group HRUs across the model domain; however, within LSPC, slope varies by catchment and HRU based on the average slope for each catchment-HRU combination.

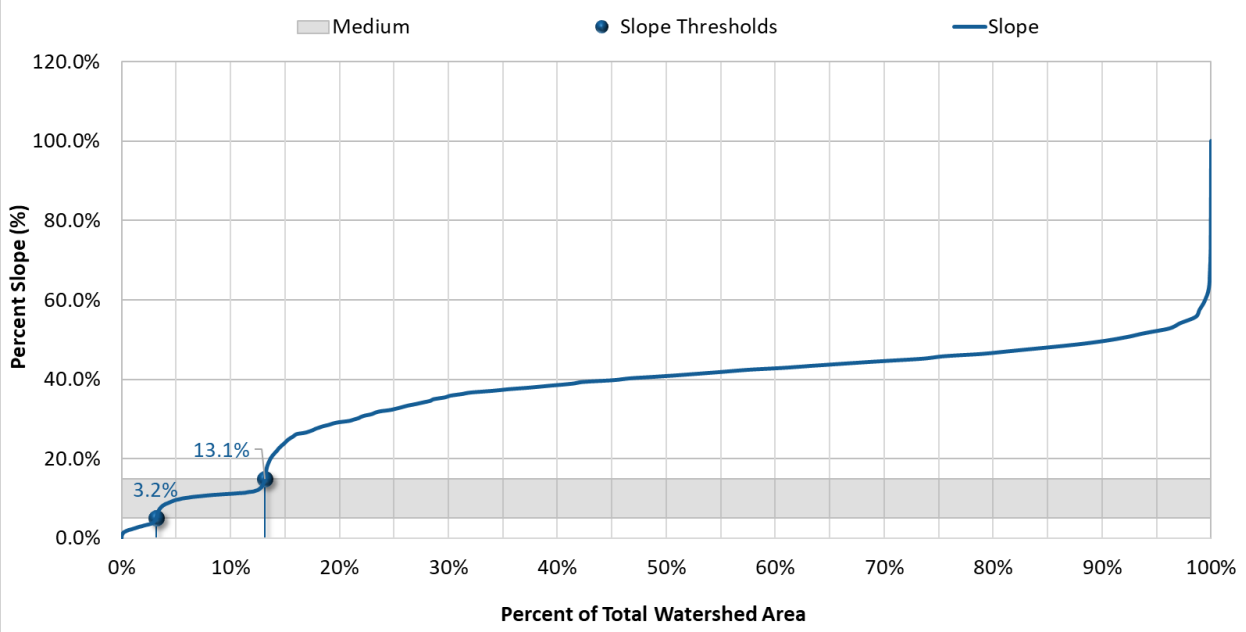

Figure 3-4. Cumulative distribution of slope categories within the Navarro River watershed.

Table 3-5. Distribution of slope categories within the Navarro River watershed

Slope (%)	Slope Category	HRU Group	Area (ac)	Area (%)
0-5	Low	Low	6,404.3	3.18%
5-15	Medium	Med	20,069.1	9.97%
>15	High	High	174,895.1	86.85%
		Total	**201,368**	**100%**

Color Gradient: Lowest | Low | Medium | High | Highest

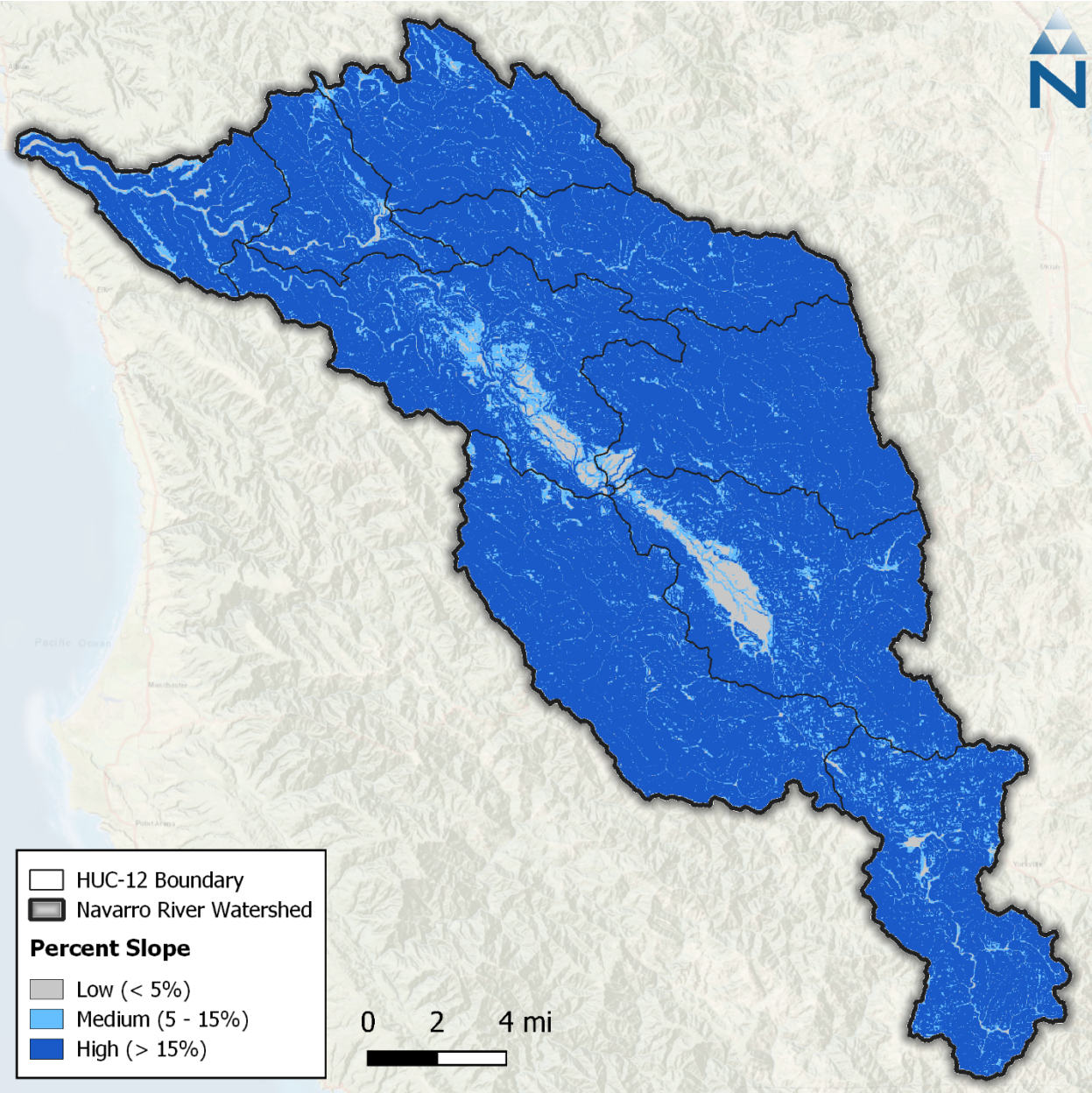

Figure 3-5. Percent Slope derived from the DEM within the Navarro River watershed.

3.4.1 Length and Slope of Overland Flow

Overland flow lengths on high slopes are generally shorter and more direct and have faster travel times on high slopes, but generally longer and less direct with slower travel times on lower slopes. It was found during previous modeling efforts that using an empirical relationship shown in Figure 3-6, derived by inversely scaling length of overland flow (LSUR) with slope of overland flow (SLSUR), improved model prediction of peak flow timing. Figure 3-7 is the resulting cumulative distribution of LSUR and SLSUR in the Navarro River watershed. Longer flow lengths on shallow sloped areas increase the opportunity for attenuation, surface storage, and infiltration. On the other hand, shorter flow lengths on steeper slopes retain the flashiness where applicable. Similar modeling efforts have historically used discrete/fixed values and ranges for SLSUR and LSUR to better manage the degrees

of freedom among model variables. However, because SLSUR can be measured by HRU from remotely-sensed data, applying a relationship to also estimate LSUR as a function of SLSUR preserves some natural variability throughout the watershed that (1) can provide some improvement relative to initial hydrology prediction using constant values and (2) helps to reduce the chance of adjusting other parameters during calibration that are better explained by the influence of LSUR and SLSUR.

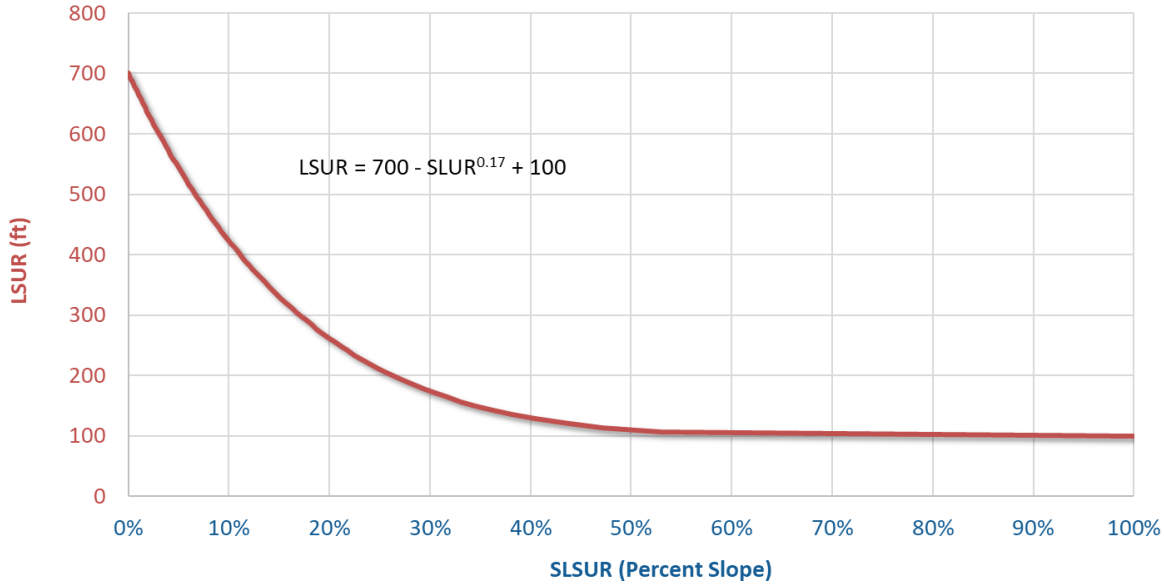

Figure 3-6. Empirical relationship of LSUR vs. SLSUR.

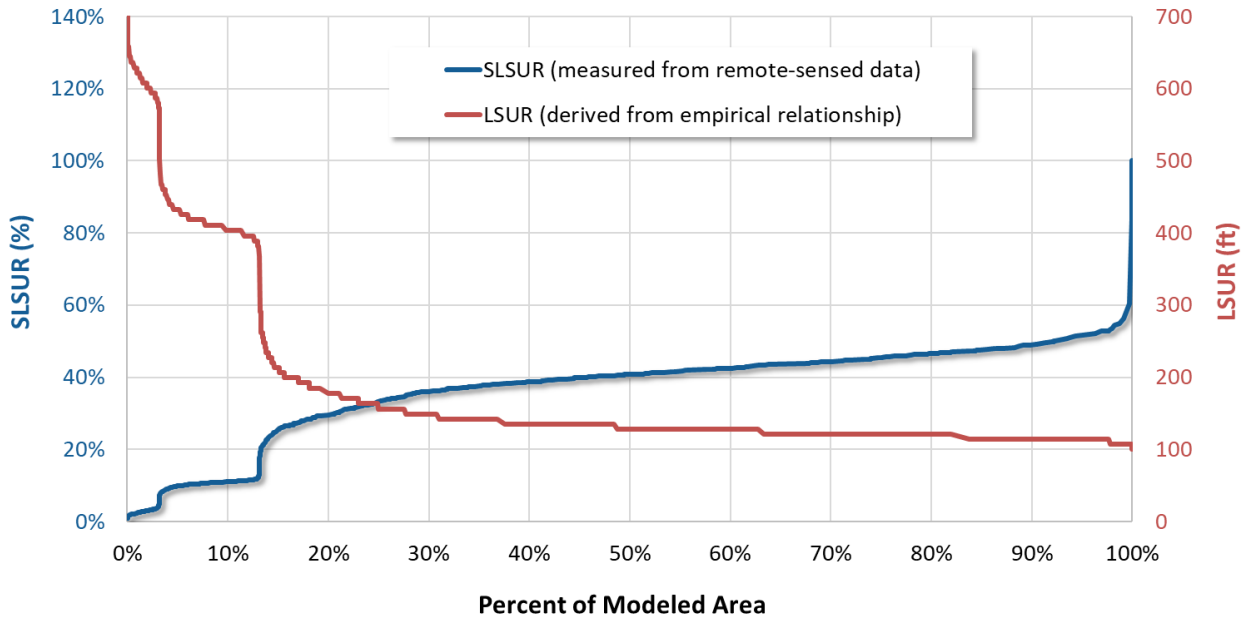

Figure 3-7. Cumulative distribution of LSUR and SLSUR in the Navarro River watershed derived from the generalized empirical relationship.

3.5 Secondary Attributes

Secondary attributes can be included in the HRU development process to provide additional information not directly mapped in the HRU categories. Secondary attributes used for the Navarro River watershed include impervious and tree canopy cover percentages. The impervious cover percentage is used for the translation of mapped impervious cover to effective impervious cover, while percent canopy estimates can inform certain hydrologic parameters but won't be represented in the HRUs as a category.

3.5.1 Impervious Cover

MRLC publishes a developed impervious cover dataset as a companion to the NLCD land cover. This dataset is also provided as a raster with a 30-meter grid resolution. Impervious cover is expressed in each raster pixel as a percentage of the total area ranging from 0 to 100 percent. Figure 3-8 shows the NLCD impervious 2021 cover dataset for the Navarro River watershed. Because this dataset provides impervious cover estimates for areas classified as developed, non-zero values closely align with developed areas (NLCD classification codes 21 through 24).

The percentage impervious cover was used in HRU development to further group developed land cover classes into pervious or impervious and to distinguish between mapped impervious area (MIA) and effective impervious area (EIA), as discussed in Section 3.6.1.

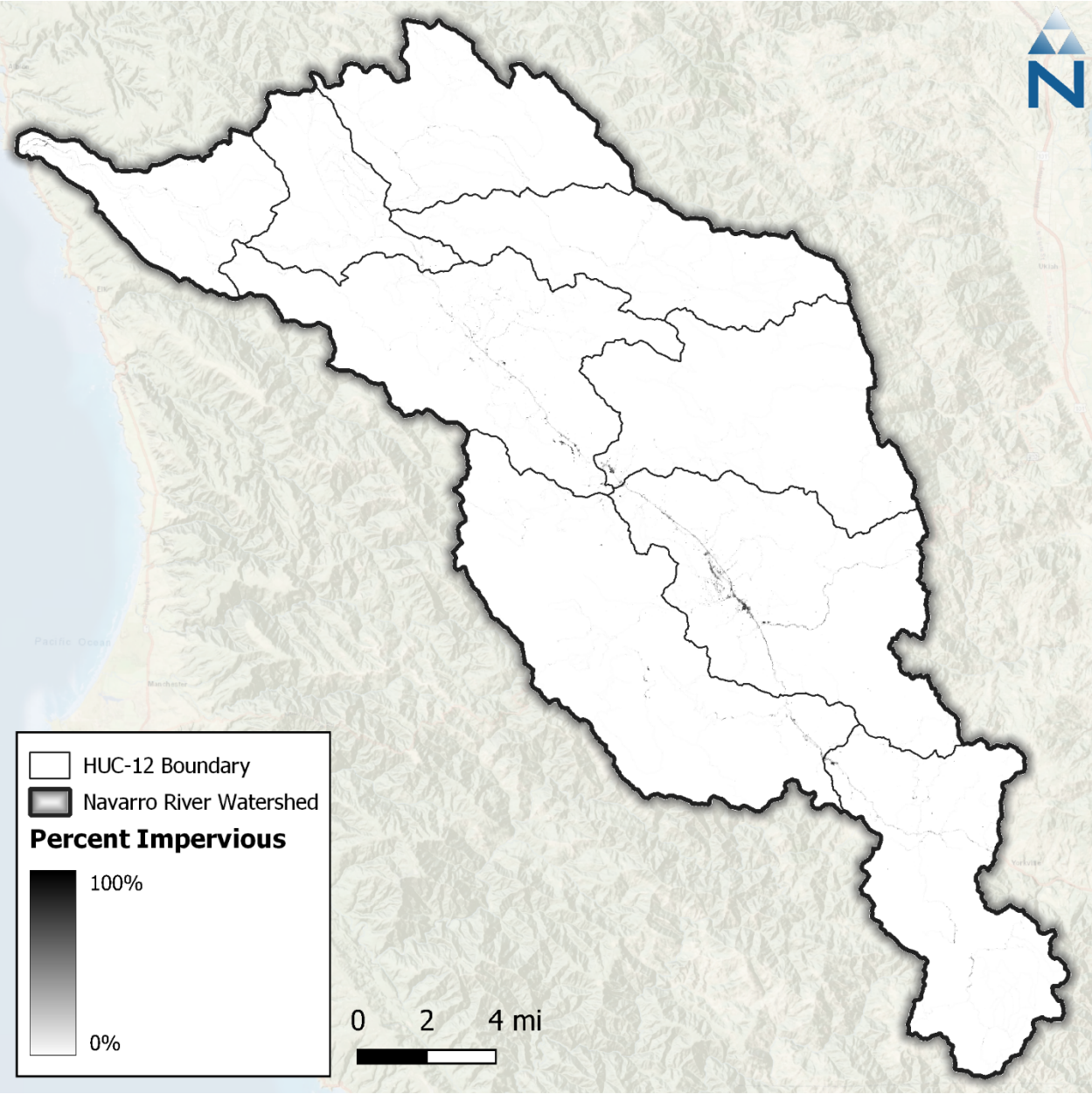

Figure 3-8. NLCD 2021 percent impervious cover in the Navarro River watershed.

3.5.2 Tree Canopy

MRLC publishes a tree canopy dataset as a companion to the NLCD land cover dataset that estimates the percentage of tree canopy cover spatially. The United States Forest Service (USFS) developed the underlying data model, which is available through its partnership with the MRLC. This dataset is also provided as a raster with a 30-meter grid resolution. Similar to the impervious cover dataset, each raster grid cell expresses the percentage of grid cell area covered by tree canopy with values ranging from 0 to 100 percent. The Navarro watershed has the highest canopy coverage of 89% toward the north and southeastern border (Figure 3-9). Tree canopy cover data was used to estimate model parameters such as interception storage and lower-zone evapotranspiration rates.

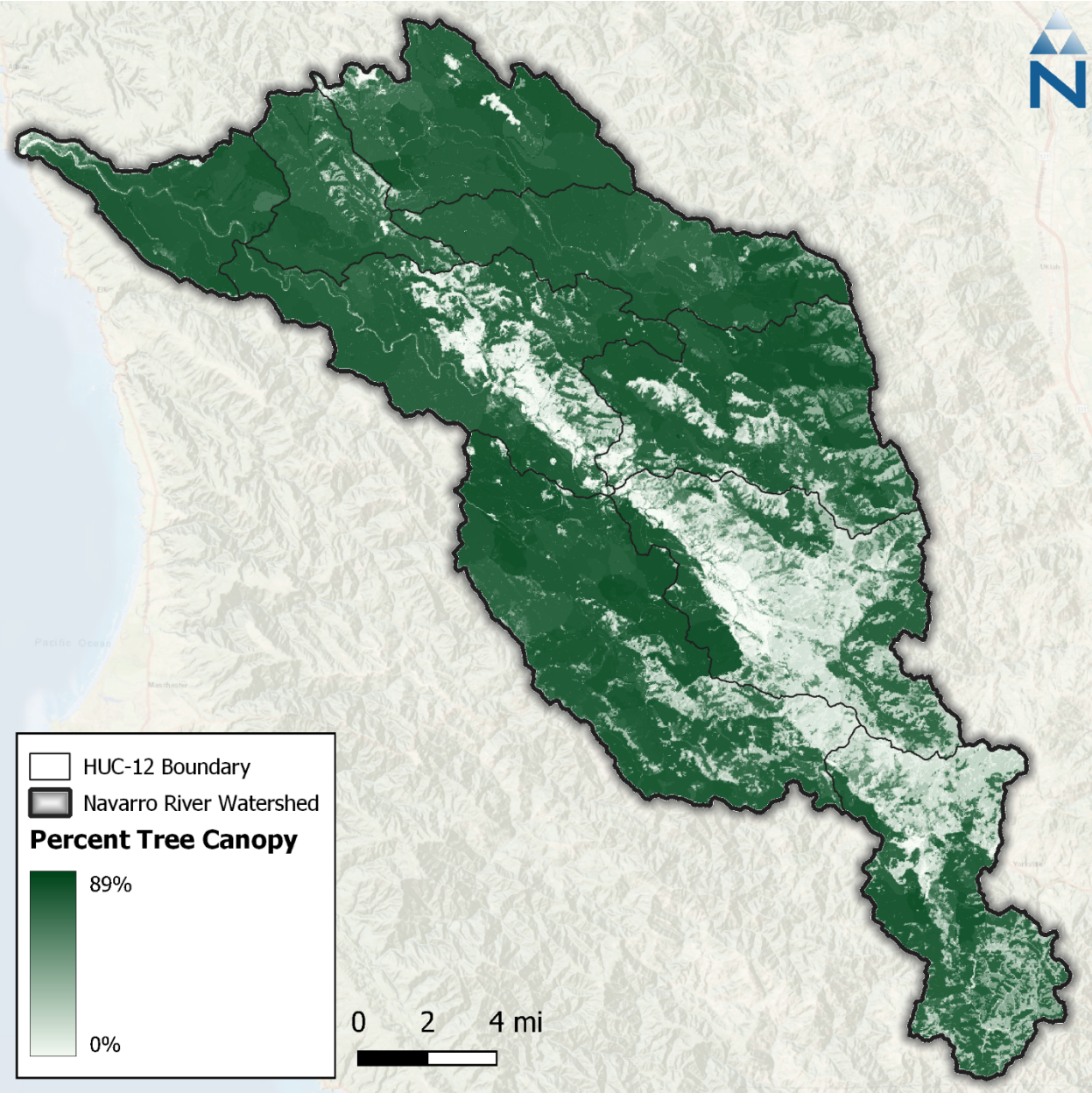

Figure 3-9. NLCD 2021 percent tree canopy cover in the Navarro River Watershed.

3.6 HRU Consolidation

The five spatial datasets described above (land cover, cropland, impervious cover, soils, and slope) were spatially overlayed in GIS to derive a composite raster where each grid cell shows the combination of the values from the overlayed datasets. A zonal statistics operation was then performed in GIS to generate a summary table identifying unique grid cell values (i.e., HRUs) from the composite raster and corresponding areas across catchments. The combination of these datasets resulted in 132 potential HRUs. To balance model computational efficiency, the impervious HRUs were consolidated for soil and slope combinations to reduce the overall number of unique HRUs. This step was necessary to develop a model with a reasonable run time while maintaining the optimal model resolution to characterize hydrologic conditions adequately. The HRU refinement process involves analyzing the

percentage of the model area attributed to each unique HRU combination as shown in Table 3-6. The spatial distribution of mapped HRUs across the watershed is shown in Figure 3-10. Additionally, the impervious percentage is used to group developed land cover classes (Section 3.6.1) and agricultural areas located in catchments with points of diversion were assigned as Irrigation HRUs (Section 5.1). The final 98 modeled HRU categories described in Section 3.6.2.

Table 3-6. Percent land cover distribution by mapped HRU category for the Navarro River watershed

LULC	Total Area (%)	Soil Group (% LULC Area)				Slope (% LULC Area)		
		A	B	C	D	0-5	5-15	>15
Developed_Low_Intensity	0.2%	5.4%	27.7%	52.9%	14.0%	36.4%	30.5%	33.1%
Developed_Medium_Intensity	0.1%	9.9%	32.9%	41.8%	15.4%	56.8%	22.4%	20.8%
Developed_High_Intensity	0.0%	6.1%	24.2%	49.5%	20.2%	74.7%	13.1%	12.1%
Developed_Open_Space	4.5%	3.8%	53.5%	29.4%	13.3%	7.0%	22.4%	70.6%
Barren	0.0%	12.5%	63.6%	19.3%	4.5%	43.2%	34.1%	22.7%
Forest	71.9%	0.6%	63.5%	28.9%	6.9%	1.4%	6.8%	91.8%
Scrub	15.8%	0.1%	12.9%	59.2%	27.7%	2.1%	12.0%	85.9%
Grassland	3.0%	1.7%	16.2%	52.0%	30.2%	11.9%	24.1%	64.1%
Pasture	3.3%	1.6%	9.9%	60.1%	28.4%	18.9%	25.5%	55.7%
Agriculture	1.2%	2.9%	17.1%	66.5%	13.5%	35.1%	42.8%	22.1%
Water	0.0%	0.7%	70.1%	24.0%	5.2%	62.0%	18.3%	19.7%
Total	**100.0%**	**0.8%**	**51.3%**	**36.0%**	**12.0%**	**3.2%**	**10.0%**	**86.8%**

Color gradients indicate more Watershed Area and an increasing percentage of Soil and Slope, respectively.

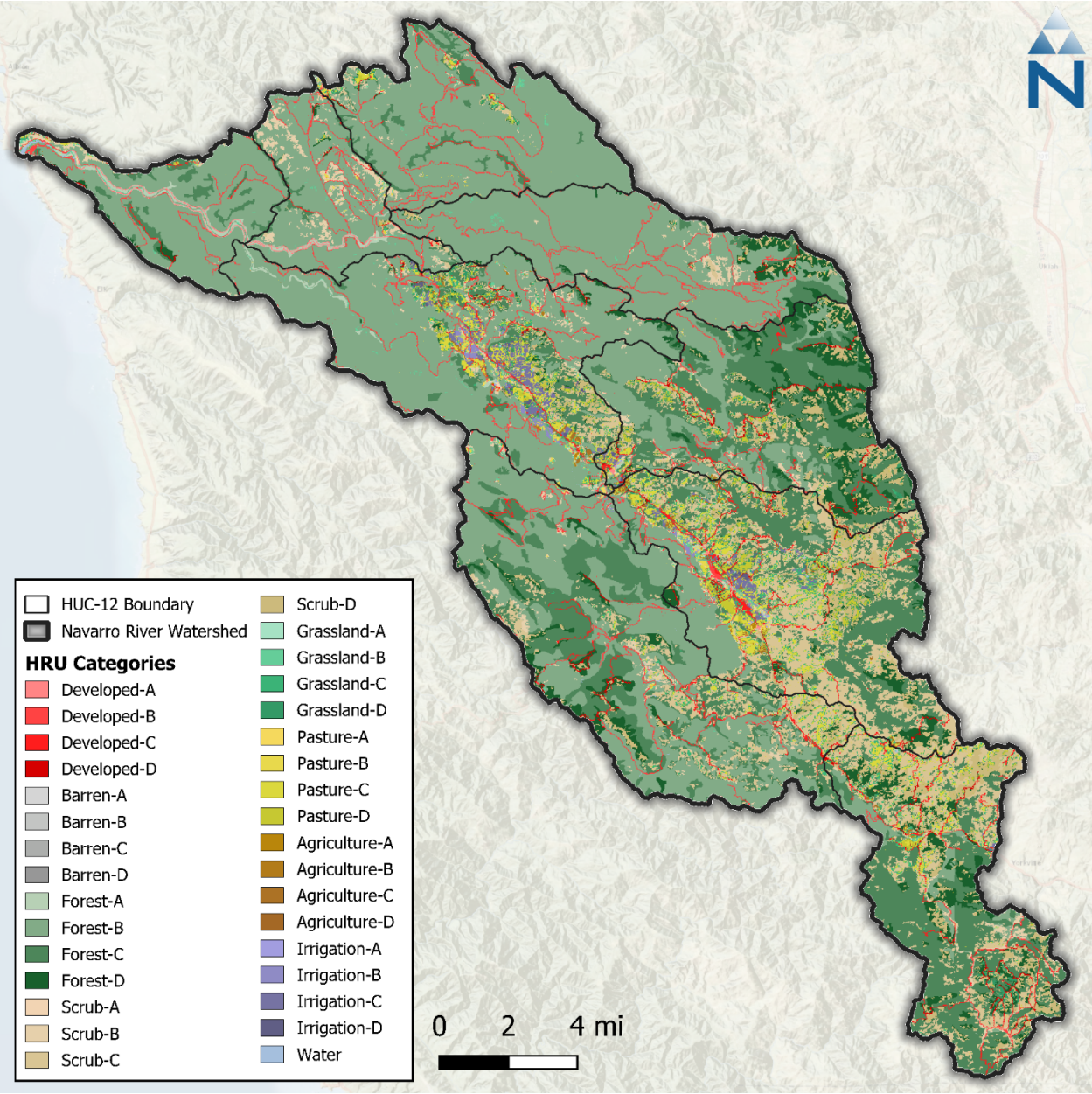

Figure 3-10. Mapped HRU categories within the Navarro River watershed. Note that slope categories are grouped for visual clarity.

3.6.1 Directly Connected Impervious Area

The HRU approach not only highlights the predominant composition of an area within the catchment but also provides additional texture and physical basis for parameterizing and representing natural processes. Within a given modeled catchment, HRU segments are modeled as being parallel to one another. Each HRU segment flows directly to the routing stream segment without any interaction with neighboring HRU segments. However, in the physical environment, the lines between impervious and pervious land are not as clearly distinguished—impervious land may flow downhill over pervious land on route to a storm drain or watercourse.

For modeling purposes, Effective Impervious Area (EIA) represents the portion of the total, or Mapped Impervious Area (MIA), that routes directly to the stream segments. It is derived as a function of the percent Directly Connected Impervious Area (DCIA), with other adjustments as needed to account for other structural and non-structural management practices in the flow network. Figure 3-11 illustrates the transitional sequence from MIA to DCIA. Impervious areas that are not connected to the drainage network can flow onto pervious surfaces, infiltrate, and become part of the pervious subsurface and overland flow. Because segments are modeled as being parallel to one another in LSPC, this process can be approximated using a conversion of a portion of impervious land to pervious land. On the open landscape, runoff from disconnected impervious surfaces can overwhelm the infiltration capacity of adjacent pervious surfaces during large rainfall/runoff events creating sheet flow over the landscape—therefore, the MIA→EIA translation is not actually a direct linear conversion. Finding the right balance between MIA and EIA can be an important part of the hydrology calibration effort.

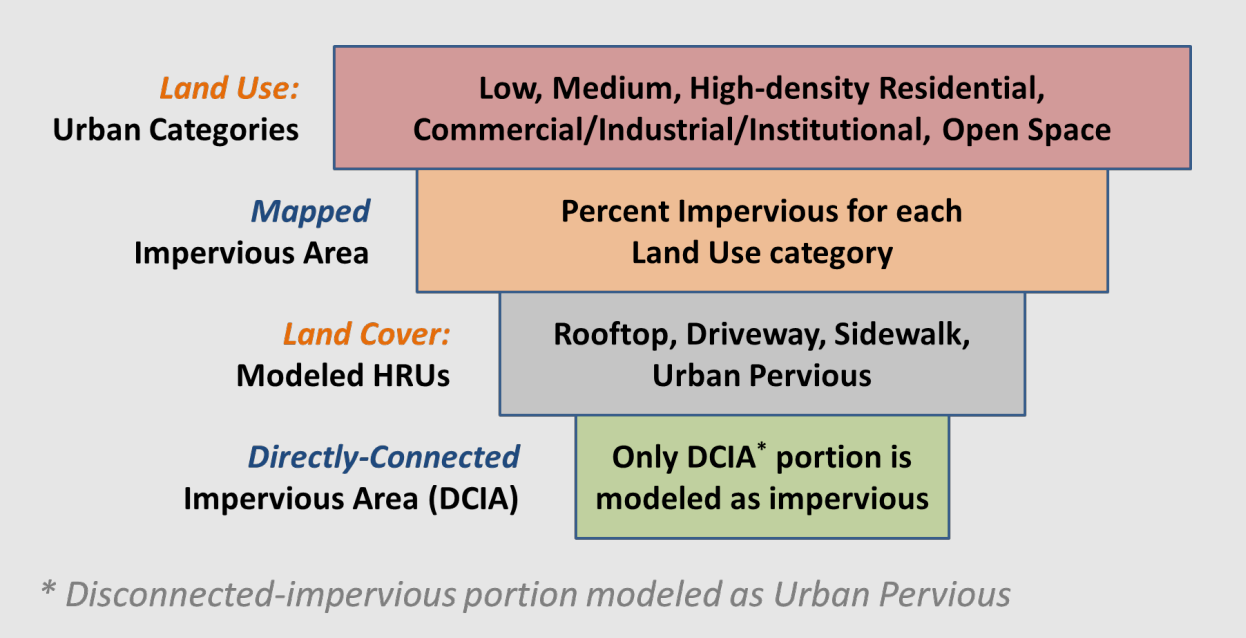

Figure 3-11. Generalized translation sequence from MIA to DCIA.

Empirical relationships like the Sutherland Equations (Sutherland, 2000) presented in Figure 3-12 show a strong correlation between the *density* of developed areas and DCIA. The curve for high-density developed land trends closer to the line of equal value than the curve for less developed areas. Similarly, as the density of the mapped impervious area approaches 100%, the translation to DCIA also approaches 100%. An initial estimate of EIA is equal to MIA × DCIA. This empirical approximation can be further refined during model calibration to account for other flow disconnections resulting from structural or non-structural Best Management Practices (BMP) practices or other inline hydraulic routing features.

For the Navarro River watershed, each developed land cover category was assigned a DCIA curve as shown in Table 3-7. The MIA, which is the impervious portion of each grid, was converted to EIA areas using these equations. Sutherland (2000) notes that areas with less than 1% MIA effectively behave like 100% pervious areas; therefore, EIA adjustments were only applicable to "Developed" areas. Table 3-8 is a summary of resampled MIA and calculated EIA by the land cover groups.

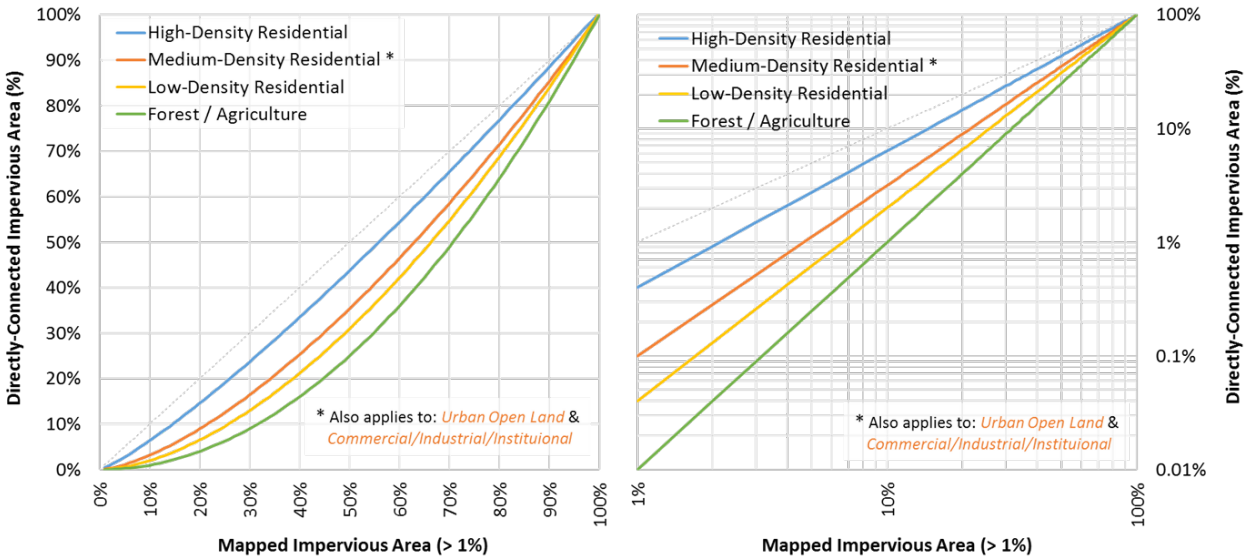

Figure 3-12. Mapped and directly connected impervious area relationships (Sutherland, 2000).

Table 3-7. Assignment of DCIA curves by land cover category

Land Cover	MIA	EIA	EIA:MIA	Equation
High Density Developed	74.0%	73.4%	95%	$DCIA=0.4(MIA)^{1.2}$
Medium Density Developed	50.4%	36.6%	73%	$DCIA=0.1(MIA)^{1.5}$
Low Density Developed	27.5%	11.5%	42%	$DCIA=0.04(MIA)^{1.7}$
Open Space	2.2%	0.1%	3%	$DCIA=0.01(MIA)^{2.0}$
Undeveloped*	0.04%	0.00%	0%	DCIA=0

* Assume no DCIA (100% disconnection, EIA = 0)

Color Gradient: Lowest | Low | Medium | High | Highest

Table 3-8. Distribution of impervious area by grouped NLCD land cover class

Model Group	Total Area		Impervious (acre)		Impervious (%)	
	Acre	%	MIA	EIA	MIA	EIA
Developed_Low_Intensity	383.4	0.19%	105.38	43.93	27.5%	11.5%
Developed_Medium_Intensity	130.3	0.06%	65.63	47.73	50.4%	36.6%
Developed_High_Intensity	22.0	0.01%	16.29	15.49	74.0%	70.4%
Developed_Open_Space	9,065.9	4.50%	196.16	5.89	2.2%	0.1%
Barren	19.6	0.01%	0.27	0.00	1.4%	0.0%
Forest (Deciduous)	594.2	0.30%	0.28	0.00	0.0%	0.0%
Forest (Evergreen)	134,251.0	66.67%	21.09	0.00	0.0%	0.0%
Forest (Mixed)	9,164.2	4.55%	1.43	0.00	0.0%	0.0%
Scrub	31,757.9	15.77%	15.83	0.00	0.0%	0.0%
Grassland (Herbaceous)	5,789.6	2.88%	10.01	0.00	0.2%	0.0%
Pasture	6,677.2	3.32%	22.83	0.00	0.3%	0.0%
Agriculture	2,399.9	1.19%	9.16	0.00	0.4%	0.0%
Forest (Woody Wetlands)	806.2	0.40%	1.77	0.00	0.2%	0.0%
Grassland (Herbaceous Wetland)	213.5	0.11%	0.81	0.00	0.4%	0.0%
Water	93.6	0.05%	0.18	0.00	0.2%	0.0%
Total	**201,368**	**100%**	**467**	**113**	**--**	**--**

Color gradients indicate model groups with more Watershed Area and Imperviousness, respectively.

3.6.2 Modeled HRU Categories

The combinations of LULC, HSG, and slope represent the physical characteristics that influence hydrology. After accounting for DCIA, the developed land cover classes were grouped into either a single "Developed Impervious" category or "Developed Pervious" stratified by HSG and slope. Agriculture HRUs (i.e., 4 HSGs × 3 slopes = 12 combinations) were further divided into irrigated and non-irrigated counterparts for a total of 24 HRUs. Altogether, a total of 98 HRU categories comprised the basic building blocks used in LSPC to represent hydrologic responses in the watershed. The "Agricultural" HRU areas within catchments where streamflow was withdrawn for irrigation were re-assigned to their "Irrigation" HRU counterparts. Irrigation was simulated for those HRUs as described in Section 5.1. The final HRU distribution in the watershed is shown in Table 3-9.

Table 3-9. Modeled HRU distribution within the Navarro River watershed

HRU ID	Land Use - Land Cover	HSG	Slope	Area	
				Acre	%
1000	Developed_Impervious	All	All	113.0	0.1%
2110	Developed_Pervious	A	Low	95.2	0.0%
2120	Developed_Pervious	A	Med	89.6	0.0%
2130	Developed_Pervious	A	High	188.9	0.1%
2210	Developed_Pervious	B	Low	242.5	0.1%
2220	Developed_Pervious	B	Med	991.8	0.5%

HRU ID	Land Use - Land Cover	HSG	Slope	Area	
				Acre	%
2230	Developed_Pervious	B	High	3,736.1	1.9%
2310	Developed_Pervious	C	Low	355.5	0.2%
2320	Developed_Pervious	C	Med	796.0	0.4%
2330	Developed_Pervious	C	High	1,726.6	0.9%
2410	Developed_Pervious	D	Low	109.1	0.1%
2420	Developed_Pervious	D	Med	278.2	0.1%
2430	Developed_Pervious	D	High	879.1	0.4%
3110	Barren	A	Low	1.3	0.0%
3120	Barren	A	Med	1.1	0.0%
3130	Barren	A	High	0.0	0.0%
3210	Barren	B	Low	5.1	0.0%
3220	Barren	B	Med	3.8	0.0%
3230	Barren	B	High	3.6	0.0%
3310	Barren	C	Low	1.6	0.0%
3320	Barren	C	Med	1.8	0.0%
3330	Barren	C	High	0.4	0.0%
3410	Barren	D	Low	0.4	0.0%
3420	Barren	D	Med	0.0	0.0%
3430	Barren	D	High	0.4	0.0%
4110	Forest	A	Low	288.7	0.1%
4120	Forest	A	Med	259.8	0.1%
4130	Forest	A	High	323.4	0.2%
4210	Forest	B	Low	1,107.1	0.5%
4220	Forest	B	Med	6,331.6	3.1%
4230	Forest	B	High	84,552.0	42.0%
4310	Forest	C	Low	494.8	0.2%
4320	Forest	C	Med	2,638.0	1.3%
4330	Forest	C	High	38,789.3	19.3%
4410	Forest	D	Low	111.0	0.1%
4420	Forest	D	Med	665.8	0.3%
4430	Forest	D	High	9,254.3	4.6%
5110	Scrub	A	Low	20.9	0.0%
5120	Scrub	A	Med	13.3	0.0%
5130	Scrub	A	High	11.3	0.0%
5210	Scrub	B	Low	187.3	0.1%
5220	Scrub	B	Med	617.6	0.3%

HRU ID	Land Use - Land Cover	HSG	Slope	Area	
				Acre	%
5230	Scrub	B	High	3,302.8	1.6%
5310	Scrub	C	Low	346.9	0.2%
5320	Scrub	C	Med	2,411.2	1.2%
5330	Scrub	C	High	16,045.7	8.0%
5410	Scrub	D	Low	108.5	0.1%
5420	Scrub	D	Med	761.9	0.4%
5430	Scrub	D	High	7,930.3	3.9%
6110	Grassland	A	Low	45.4	0.0%
6120	Grassland	A	Med	41.4	0.0%
6130	Grassland	A	High	14.9	0.0%
6210	Grassland	B	Low	211.7	0.1%
6220	Grassland	B	Med	317.4	0.2%
6230	Grassland	B	High	443.7	0.2%
6310	Grassland	C	Low	338.5	0.2%
6320	Grassland	C	Med	863.1	0.4%
6330	Grassland	C	High	1,917.0	1.0%
6410	Grassland	D	Low	116.1	0.1%
6420	Grassland	D	Med	223.1	0.1%
6430	Grassland	D	High	1,470.9	0.7%
7110	Pasture	A	Low	72.9	0.0%
7120	Pasture	A	Med	25.8	0.0%
7130	Pasture	A	High	6.9	0.0%
7210	Pasture	B	Low	193.0	0.1%
7220	Pasture	B	Med	244.4	0.1%
7230	Pasture	B	High	220.6	0.1%
7310	Pasture	C	Low	665.4	0.3%
7320	Pasture	C	Med	1,172.2	0.6%
7330	Pasture	C	High	2,177.2	1.1%
7410	Pasture	D	Low	328.5	0.2%
7420	Pasture	D	Med	258.9	0.1%
7430	Pasture	D	High	1,311.2	0.7%
8110	Agriculture	A	Low	40.0	0.0%
8120	Agriculture	A	Med	11.9	0.0%
8130	Agriculture	A	High	3.1	0.0%
8210	Agriculture	B	Low	82.1	0.0%
8220	Agriculture	B	Med	109.3	0.1%

HRU ID	Land Use - Land Cover	HSG	Slope	Area	
				Acre	%
8230	Agriculture	B	High	61.5	0.0%
8310	Agriculture	C	Low	315.6	0.2%
8320	Agriculture	C	Med	431.0	0.2%
8330	Agriculture	C	High	219.9	0.1%
8410	Agriculture	D	Low	65.9	0.0%
8420	Agriculture	D	Med	72.9	0.0%
8430	Agriculture	D	High	70.6	0.0%
9000	Water	All	All	93.6	0.0%
10110	Irrigation	A	Low	9.6	0.0%
10120	Irrigation	A	Med	4.1	0.0%
10130	Irrigation	A	High	0.7	0.0%
10210	Irrigation	B	Low	59.8	0.0%
10220	Irrigation	B	Med	75.3	0.0%
10230	Irrigation	B	High	21.7	0.0%
10310	Irrigation	C	Low	230.8	0.1%
10320	Irrigation	C	Med	282.9	0.1%
10330	Irrigation	C	High	115.9	0.1%
10410	Irrigation	D	Low	38.8	0.0%
10420	Irrigation	D	Med	40.0	0.0%
10430	Irrigation	D	High	36.4	0.0%
			Total	**201,368**	**100%**

Color Gradient: Lowest | Low | Med | High | Highest

4 CLIMATE FORCING INPUTS

The Navarro River watershed LSPC model uses hourly climate data forcing inputs to drive the hydrology module. In general, hydrologic models are highly dependent on the quantity and quality of meteorological input data (Quirmbach and Schultz 2002). Conventionally, meteorological boundary conditions for stormwater modeling rely on ground-based stations across an area; however, challenges arise when trying to associate point-sampled weather station data over complex and/or large terrain (Henn et al. 2018). Model representation of precipitation in regions with low station density is susceptible to distortion when using linearized downscaling methods (e.g., Thiessen polygons).

The hybrid approach supplements spatial and temporal gaps in observed meteorological data with gridded meteorological products from the Parameter-elevation Regressions on Independent Slopes Model (PRISM) and North American Land Data Assimilation System-2 (NLDAS). NLDAS and PRISM are Land Surface Model (LSM) datasets with 1/8th degree and 4-km spatial resolution, respectively, which are ideal for supplementing spatial gaps in the observed station network as well as

patching missing or erroneous temporal gaps in the observed time series data. The use of a hybrid approach that blends ground-based stations with remotely sensed precipitation products (i.e., increasing the rainfall gage density over the watershed) has been shown to improve the representation of rainfall and increase forecast accuracy more than using ground-based stations alone (Kim et al. 2018; Looper and Vieux 2012; Xia et al. 2012a, 2012b). This approach has been applied for large watershed-scale modeling applications in Los Angeles County (LACFCD 2020).

Potential evapotranspiration (PEVT) is another critical forcing input for hydrology simulation. Section 4.2 describes how PEVT was derived for this modeling effort.

4.1 Precipitation

Figure 4-1 presents a summary of the hybrid approach to blend observed precipitation with gridded meteorological products. Observed data and gridded products were first processed in parallel (1) to identify the highest quality gage data and (2) to merge gridded products to produce continuous hourly time series. Next, gridded products were used to fill spatial and temporal gaps in the observed precipitation coverage. The final coverage shown in Figure 4-2 comprises the highest quality observed time series, supplemented by gridded products only where spatial and temporal gaps occurred in the observed coverage. The parallel processing of observed and gridded precipitation is presented in Section 4.1.1. Section 4.1.2 describes how those outputs were synthesized into the model's final set of precipitation time series.

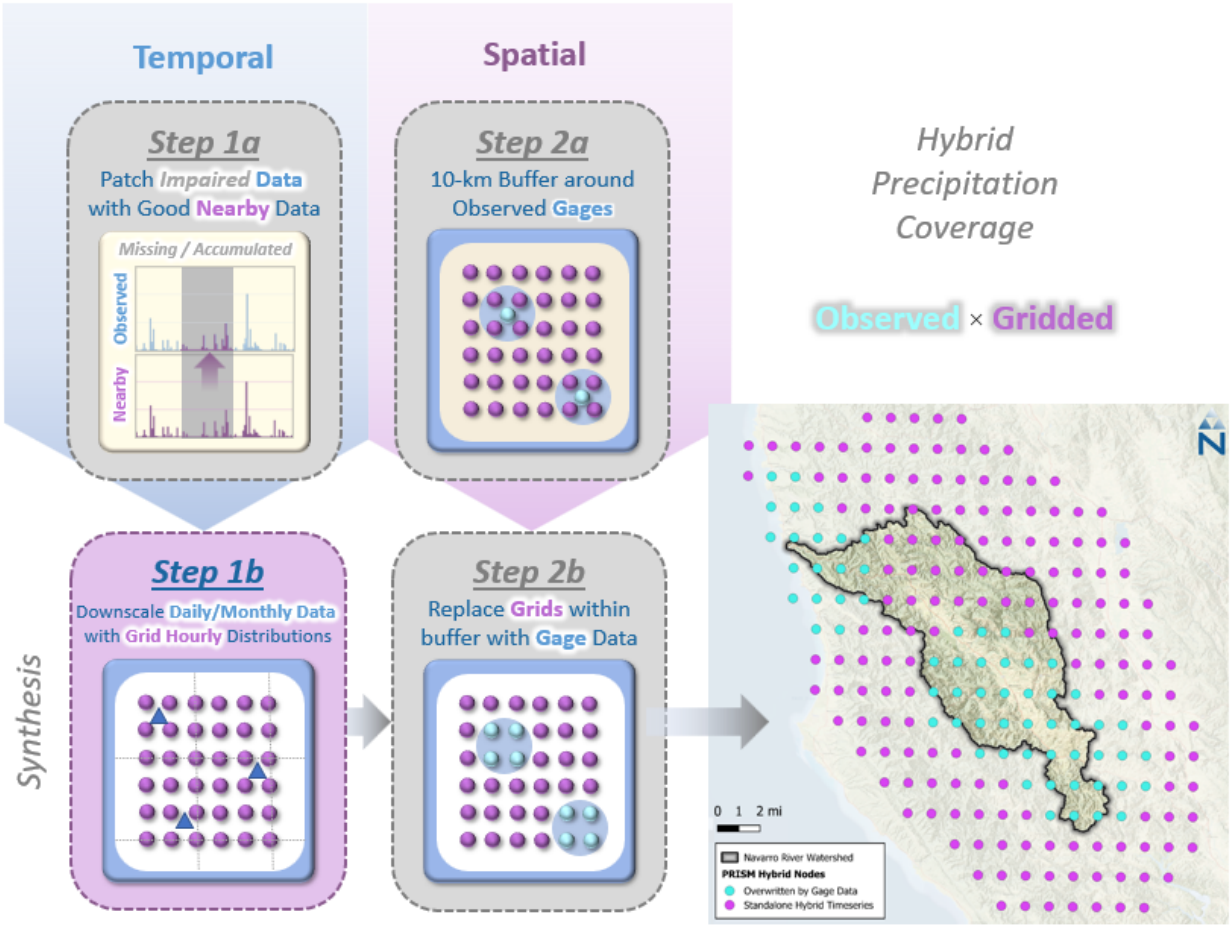

Figure 4-1. Hybrid approach to blend observed precipitation with gridded meteorological products.

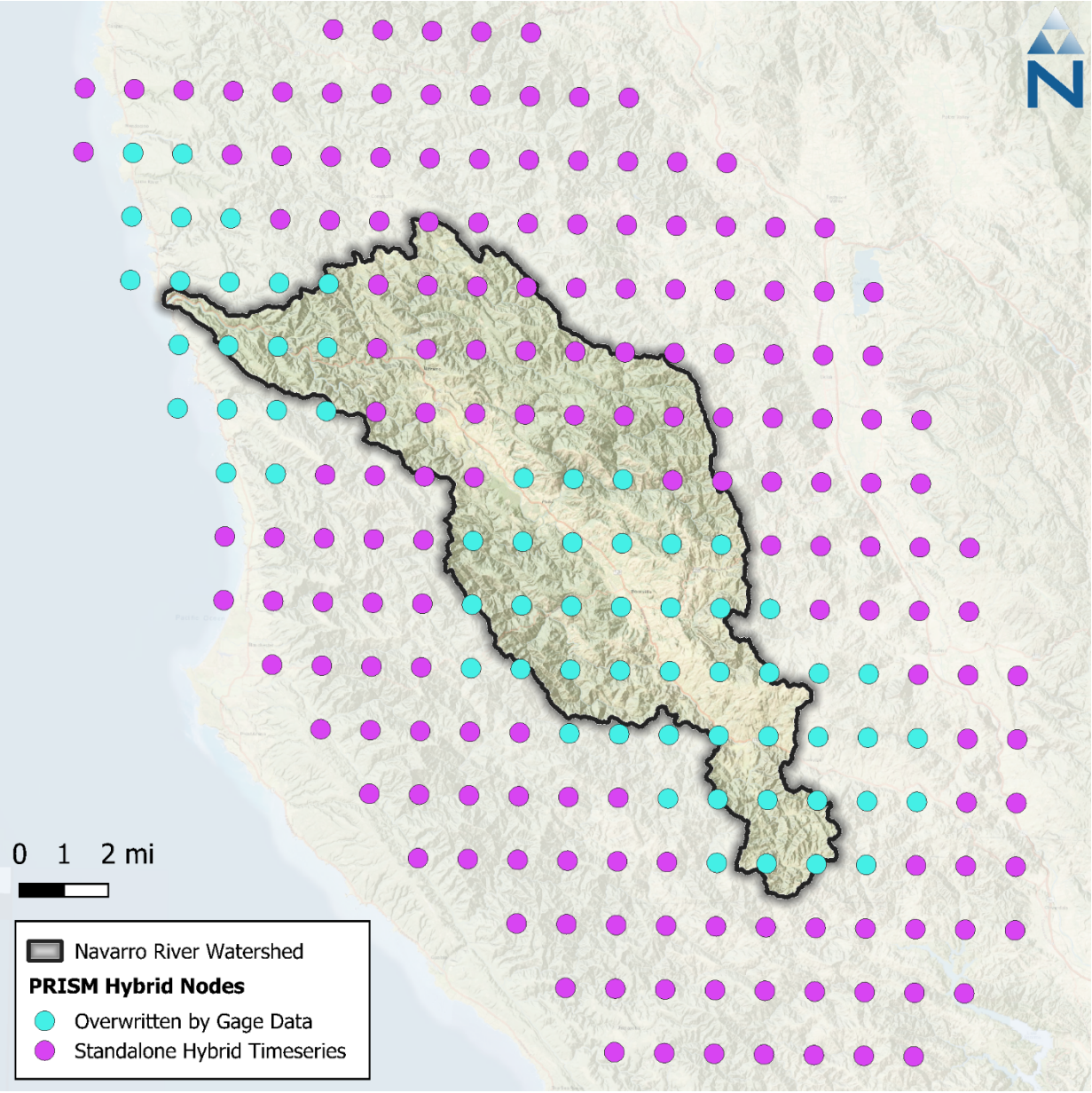

Figure 4-2. Spatial coverage of PRISM nodes by hybrid data source.

4.1.1 Parallel Processing of Observed Data and Gridded Products

Data from 5 observed precipitation gages, summarized in Table 4-1, were processed for use in the hybrid precipitation time series. These stations report daily precipitation totals, which were downscaled to hourly based on the distribution of the nearest NLDAS grid cell, while maintaining observed daily totals. The National Climatic Data Center's (NCDC) Community Collaborative Rain, Hail, and Snow Network (CoCoRaHS) operates three of these gages. The California Data Exchange Center (CDEC) Yorkville station and the Remote Automated Weather Stations (RAWS) Boonville station were also used. The relationship between annual average total precipitation and elevation for these stations is shown in Figure 4-3. The Navarro River work plan had additional precipitation gages listed, however those stations were dropped from further use as duplicates or were outside of the 10km buffer used to create hybrid time series.

Table 4-1. Precipitation stations used to develop hybrid precipitation time series (station locations are shown in Figure 4-4)

Agency	Station ID	Name	Start Date	End Date	Lat.	Long.	Elevation (meters)	Data Coverage (%)[1]
NOAA-CoCoRaHS	GHCND:US1CAMD0042	ALBION 1.1 S, CA US	2/15/2020	Present	39.206	-123.770	60.7	95%
	GHCND:US1CAMD0039	ELK 1.9 NNE, CA US	03/09/2019	Present	39.155	-123.701	367.6	89%
	GHCND:US1CAMD0003	BOONVILLE 2.2 WSW, CA US	1/1/2009	Present	39.006	-123.408	323.4	92%
CDEC	YOR	YORKVILLE	10/1/2003	Present	38.905	-123.231	335.3	100%
RAWS	BNVC1	BOONVILLE	5/1/1990	Present	38.987	-123.348	202.4	99%

[1] NOAA data coverage as reported; CDEC and RAWS estimated based on data flagging and count of time steps.

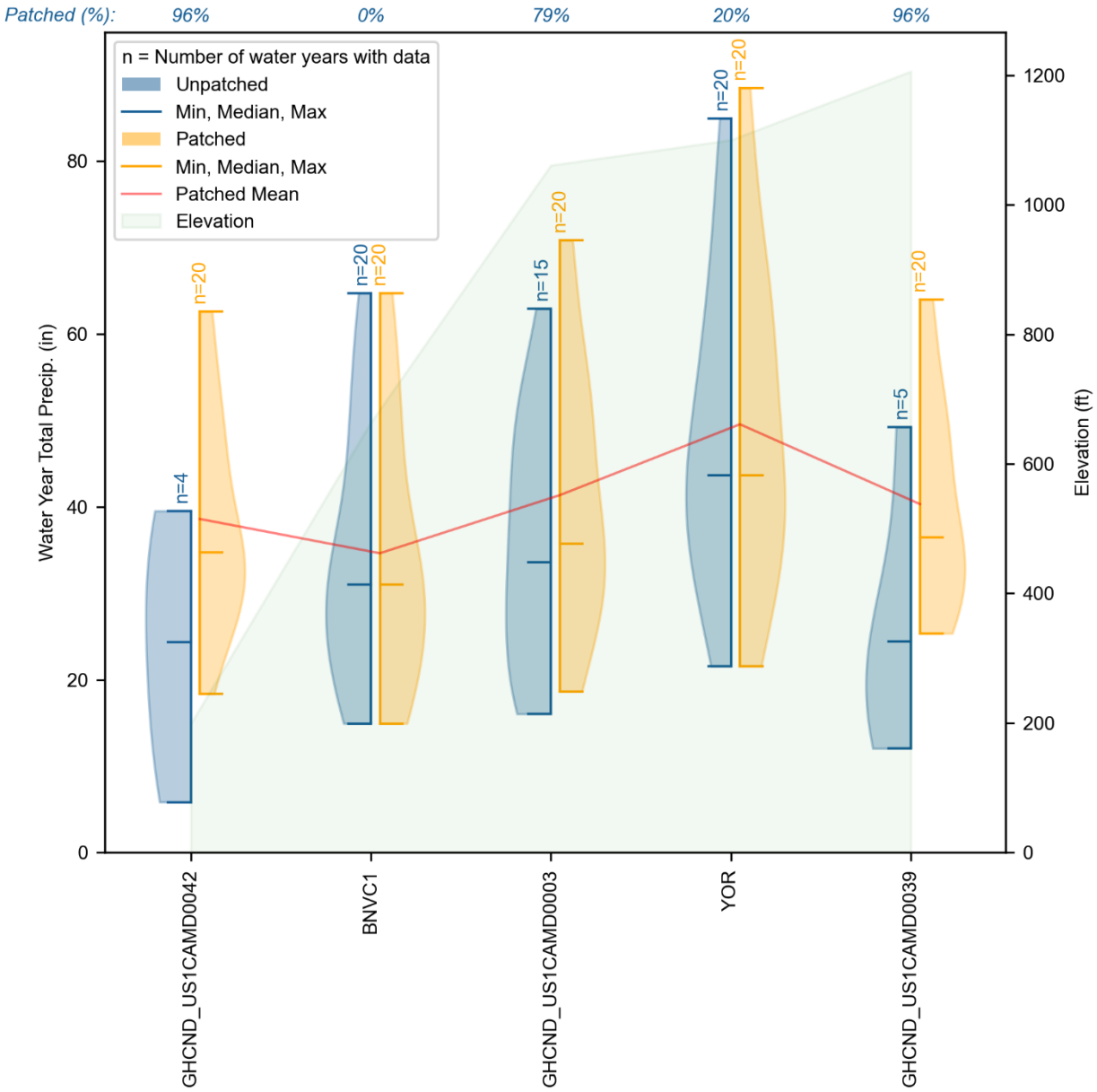

Figure 4-3. Water year precipitation totals and elevation of selected precipitation stations for 2004 - 2023.

The gridded meteorological products were processed in parallel with the observed data and used to patch spatial and temporal gaps in the observed data record. PRISM monthly precipitation time series data are available at a 4-km spatial resolution across the conterminous United States (Daly et al. 1997, 1994; Gibson et al. 2002). PRISM combines point data and spatial datasets (primarily DEMs) via statistical methods to generate estimates of annual, monthly, and event-based precipitation in a gridded format from as early as 1961 (Daly et al. 2000). PRISM has undergone several iterations of refinement, extensive peer review, and performance validation through case study applications.

NLDAS is a quality-controlled meteorological dataset designed specifically to support continuous simulation modeling activities (Cosgrove et al. 2003; Mitchell et al. 2004). NLDAS provides hourly predictions of meteorological data at a 1/8th degree spatial resolution for North America (approximately 8.6-mile intervals), with retrospective simulations beginning in January 1979. For this

model, hourly NLDAS precipitation distributions were mapped to the nearest PRISM grid cell and used to disaggregate the monthly PRISM totals to hourly—the resulting set of gridded precipitation time series reflects monthly PRISM totals that have hourly distributions from the nearest NLDAS grid. Using monthly PRISM totals with hourly NLDAS, as opposed to daily PRISM totals, eliminates the need to estimate distributions for occasional but rare instances where an hourly distribution does not coincide with a daily total.

4.1.2 Synthesis of Observed Data and Gridded Products

Where available, observed precipitation data were preferentially selected over gridded data where data quantity and quality were adequate. Impaired intervals are gaps in the observed record flagged as missing, deleted, or accumulated rainfall. Gridded time series are used to patch impaired intervals as follows. First, a 10-km buffer was created around each of the observed gages that were prescreened for quality. Next, the 10-km gage buffer was intersected with the PRISM grid layer. The time series at any grid falling within the buffer is ultimately overridden by the associated observed gage time series, except for impaired intervals, where the gridded data are retained to patch those temporal impairments. Consequently, most of the observed data at a PRISM grid location will be identical to a neighboring grid within a 10-km buffer of the gage but will have slightly different PRISM time series for impaired intervals.

After the creation of the hybrid precipitation time series, each catchment is assigned a time series based on the Thiessen polygon its centroid falls within. Figure 4-4 illustrates the final assignment of gage-based or LSM-based hybrid time series by catchment. Figure 4-5 shows the distribution of monthly total precipitation across all hybrid time series within the watershed and Figure 4-6 illustrates the spatial distribution of annual average precipitation from the hybrid time series by catchment.

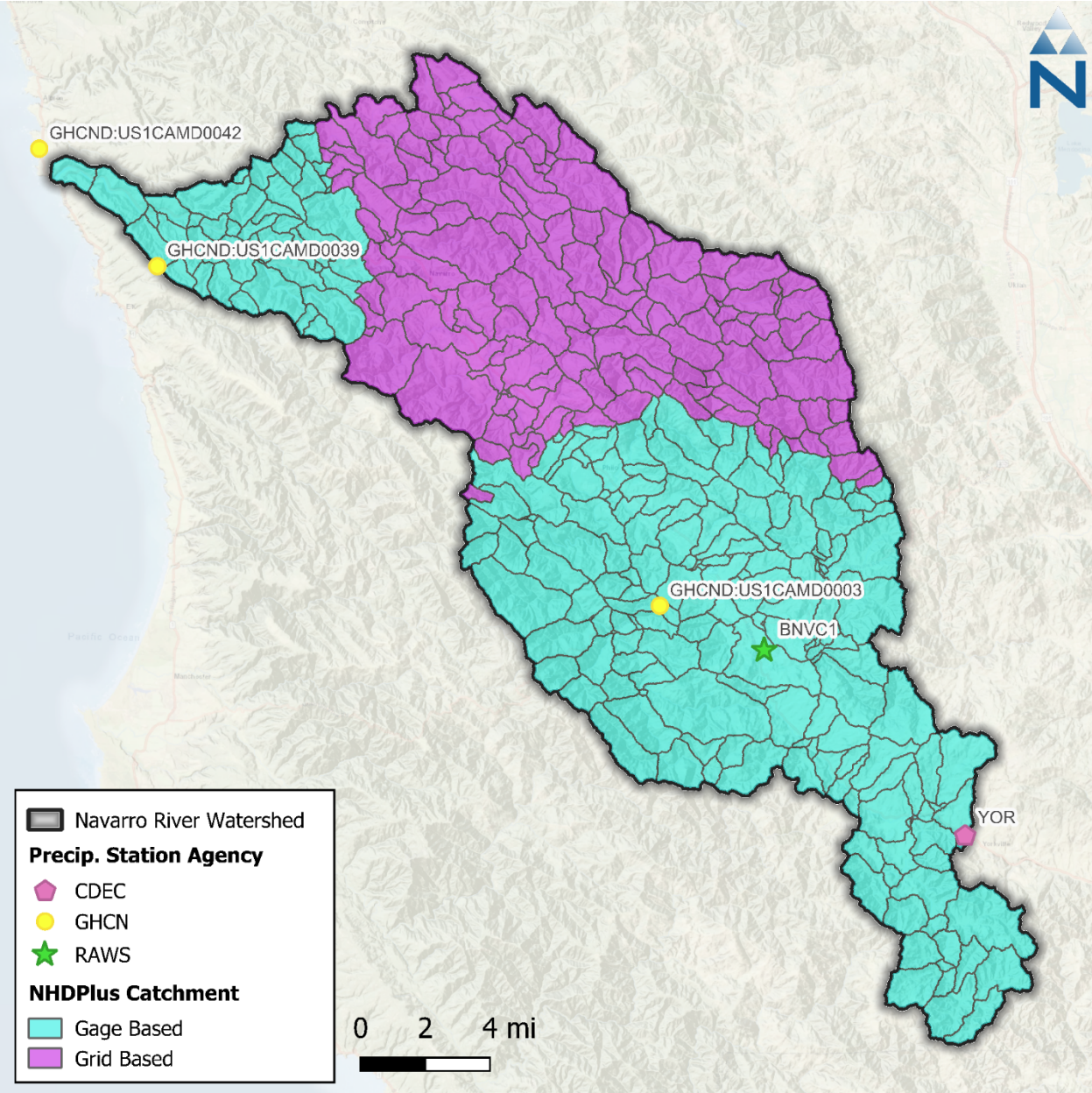

Figure 4-4. Final spatial coverage of precipitation time series by catchment.

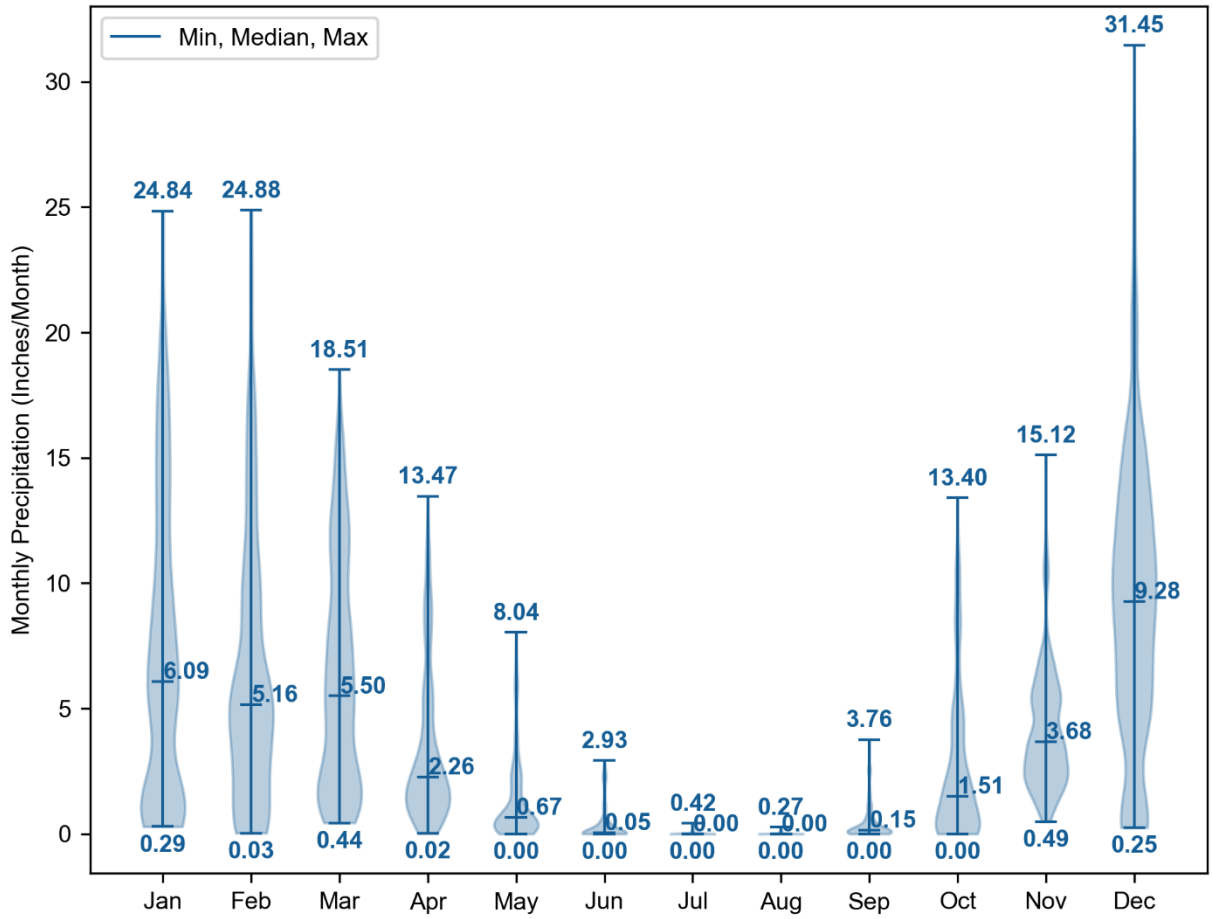

Figure 4-5. Distribution of monthly total precipitation across all hybrid time series within the Navarro River watershed for Water Years 2004-2023.

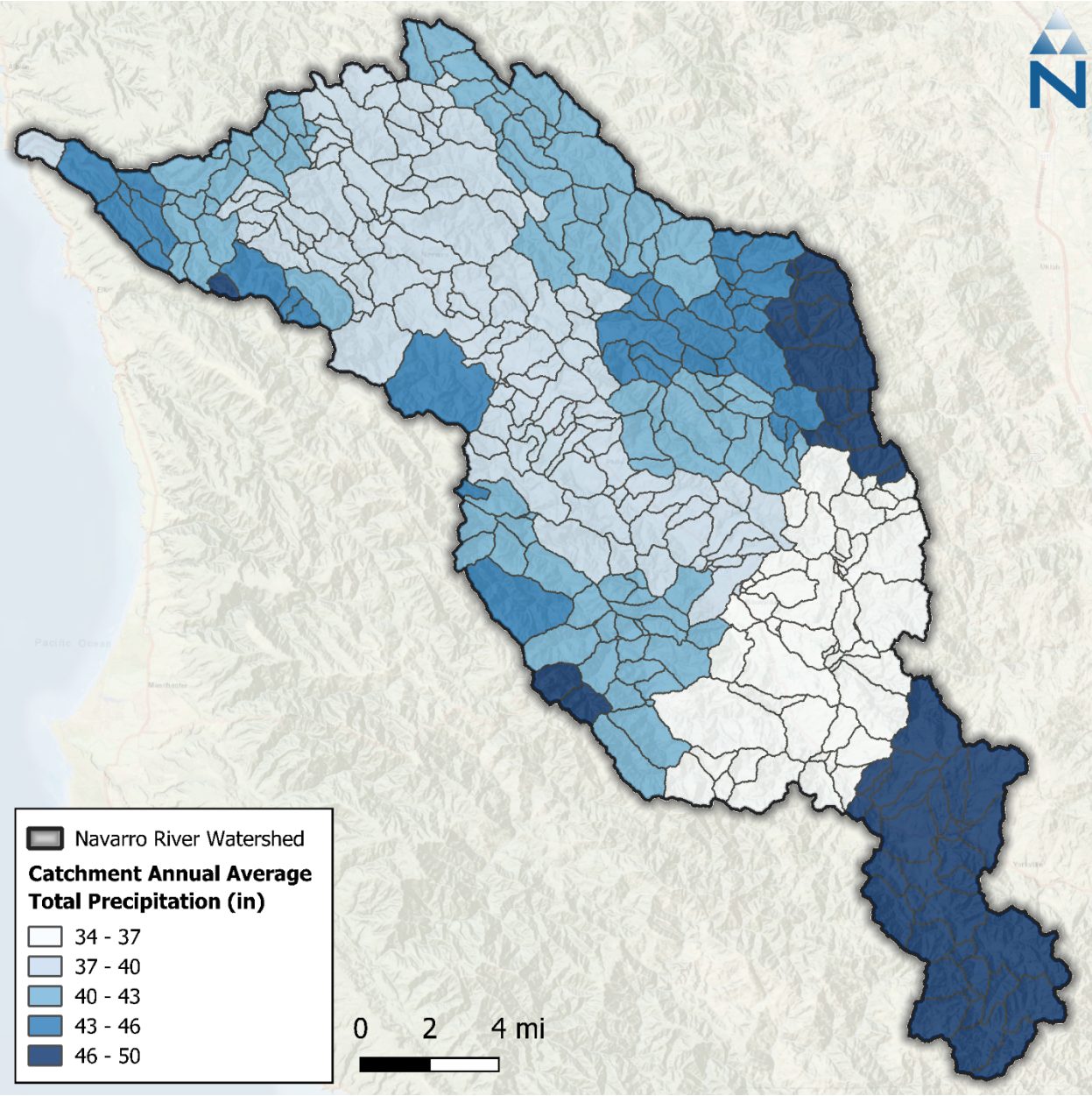

Figure 4-6. Annual average hybrid precipitation totals by catchment from Water Years 2004-2023.

4.2 Potential Evapotranspiration

In addition to precipitation, potential evapotranspiration forcing input time series were created and assigned to each catchment. Daily total reference evapotranspiration (ET_o) from the California Irrigation Management Information System (CIMIS) spatial dataset was downscaled to hourly using the NLDAS hourly solar radiation. CIMIS Spatial expresses daily ET_o estimates calculated at a statewide 2-km spatial resolution using the American Society of Civil Engineers version of the Penman-Monteith equation (ASCE-PM). This product provides a consistent spatial estimate of ET_o that (1) is California-specific, (2) implicitly captures macro-scale spatial variability and orographic influences, (3) is available from 2004 through the present, and (4) is routinely updated. Within each catchment, actual ET is calculated for each Hydrologic Response Unit (HRU) during the model

simulation as a function of parameters representing differences in vegetation (type, height, and density) and soil conditions. Figure 4-7 shows the distribution of monthly total ET_o across all grid points within the watershed. Figure 4-8 shows the spatial distribution of CIMIS annual average total ET_o across the watershed.

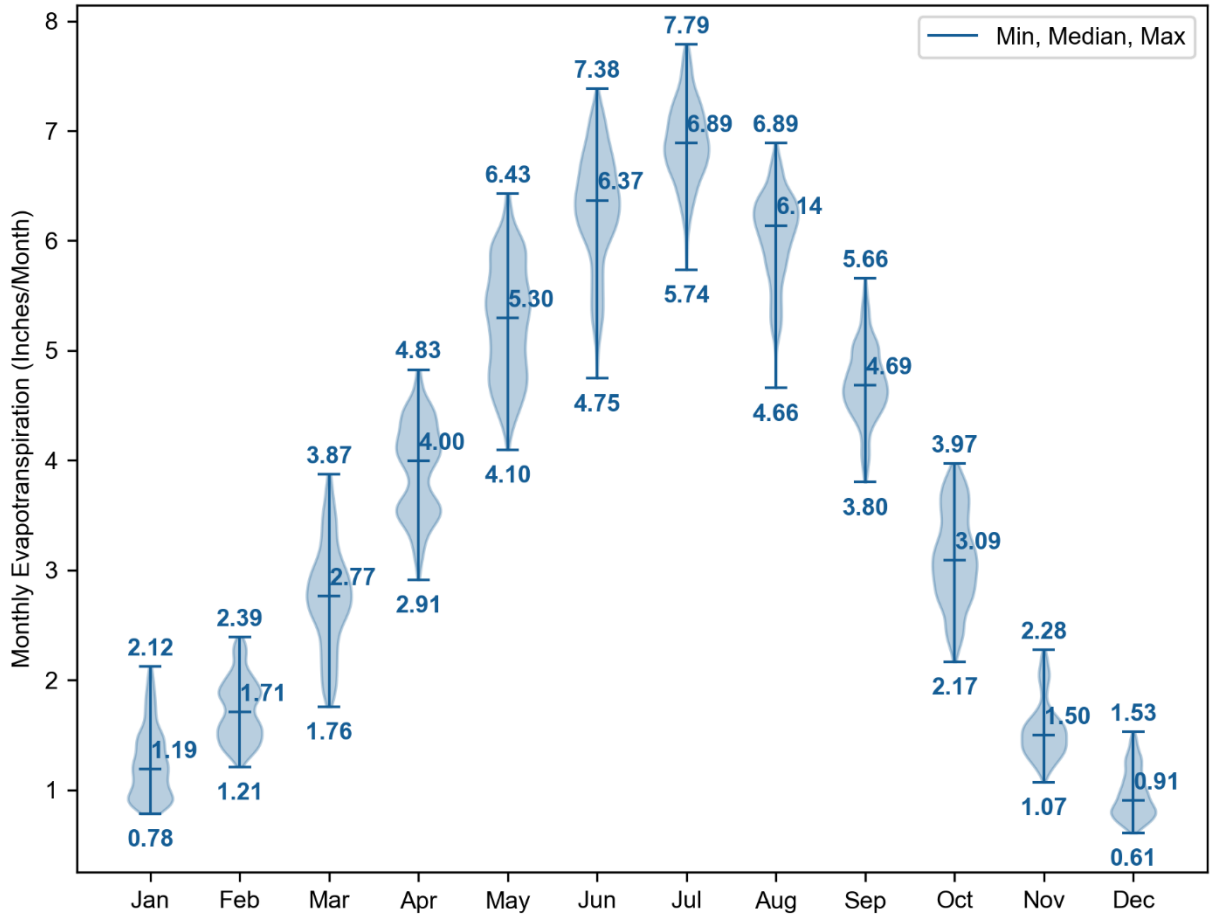

Figure 4-7. Distribution of monthly total ET_o across all CIMIS spatial grid points within the Navarro River watershed for Water Years 2004 to 2023.

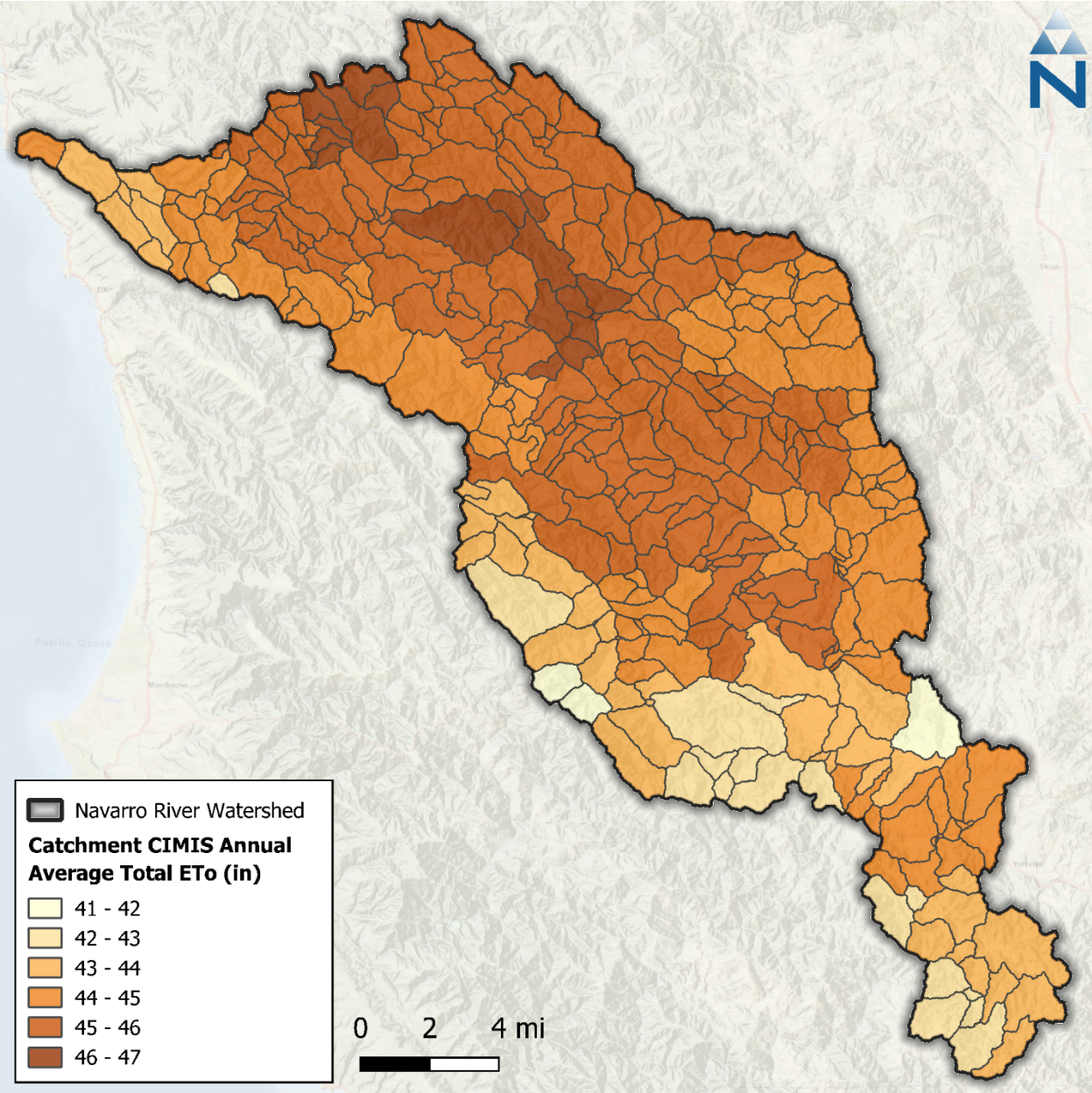

Figure 4-8. CIMIS annual average total ET_o by catchment within the Navarro River watershed.

5 SURFACE WATER WITHDRAWS

Datasets related to water rights, points of diversion (PODs), and irrigation use were identified through the Water Board's eWRIMS database and a University of California Cooperative Extension (UCCE) study assessing agricultural water needs in the Navarro River watershed and the neighboring Russian River watershed (McGourty et al. 2020). These data were used to represent diversions and withdraws in the watershed model. Monthly data from 254 active water rights within the Navarro River watershed from 2017 to 2023 were received from the Board's Supply and Demand Unit staff. Of these, 243 had reported withdrawals; surface water withdrawals from these active water rights occur from the PODs as illustrated in Figure 5-1. By count, water usage is predominately Irrigation (53%) and Domestic (32%) (Figure 5-2). Here, the 'Other' category groups the dust control, stock-watering, and fish and wildlife preservation and enhancement primary uses. By volume, the Irrigation category accounts for more than three-quarters of usage (84%).

For the non-irrigated water demand, the received monthly data in acre-feet are summed by catchment and then converted to a flow rate for withdraw from the appropriate catchment's modeled reach segment. Irrigation demand is similarly converted from monthly volume into a withdraw rate by application number. These water demand data are added to the LSPC model as surface water withdraws from the appropriate reach segments based on the following considerations.

- Diversions were classified based on primary usage (irrigation, municipal, industrial, recreational, etc.) as well as by allocation type (direct and storage).
- During simulations, diverted streamflow was routed out of the system to represent the different uses (i.e. irrigation).
- For instances where PODs in different catchments share the same application/permit number, water demand was proportionally distributed based on the magnitude of upstream drainage area.
- To approximate withdrawals over the entire modeled period, POD time series prior to 2017 were estimated as the monthly average volume based on the 2017-2023 data and extended to the later of the beginning of the modeling period or to the start date of the water right associated with each POD.

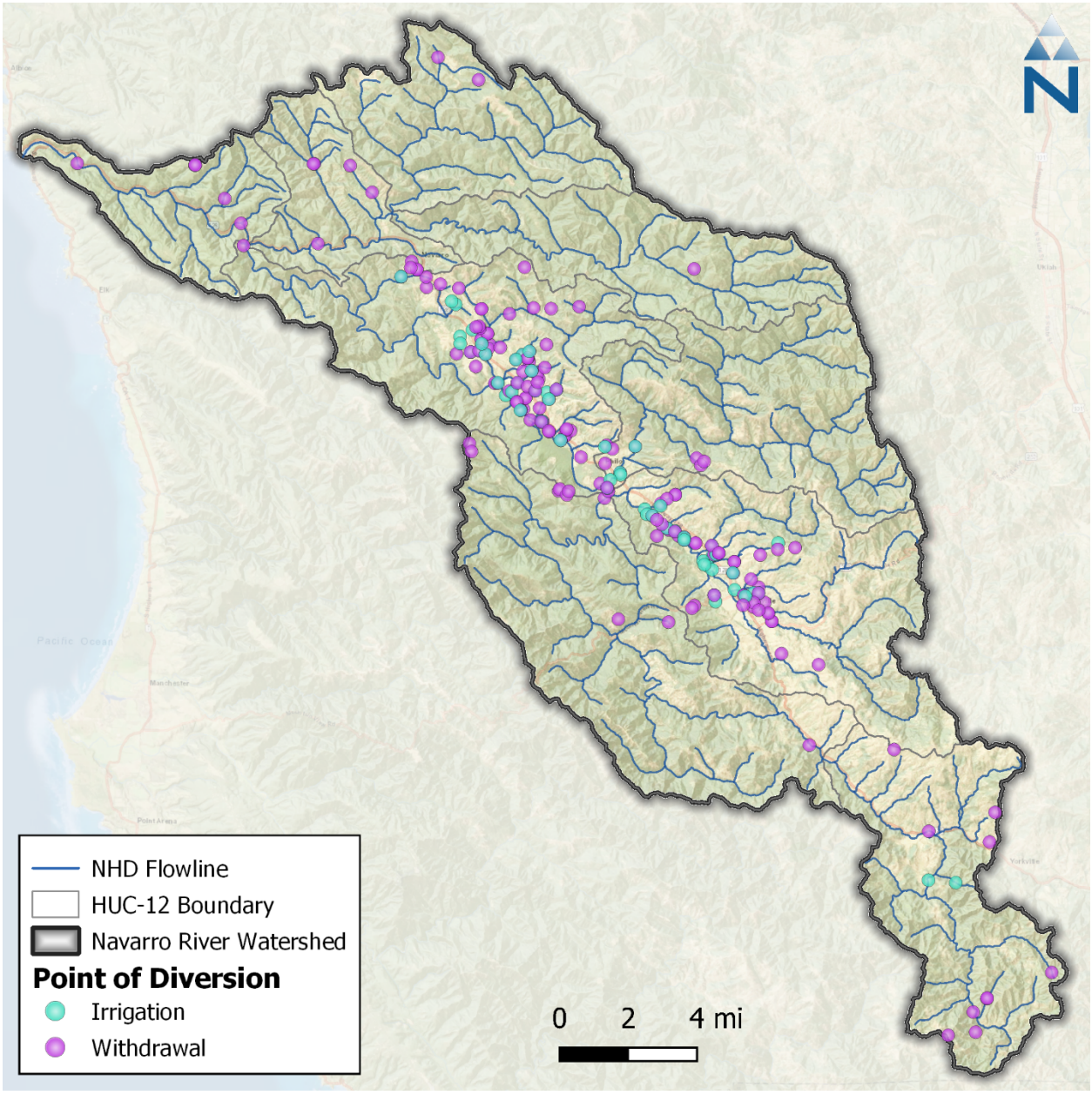

Figure 5-1. Points of diversion within the Navarro River watershed.

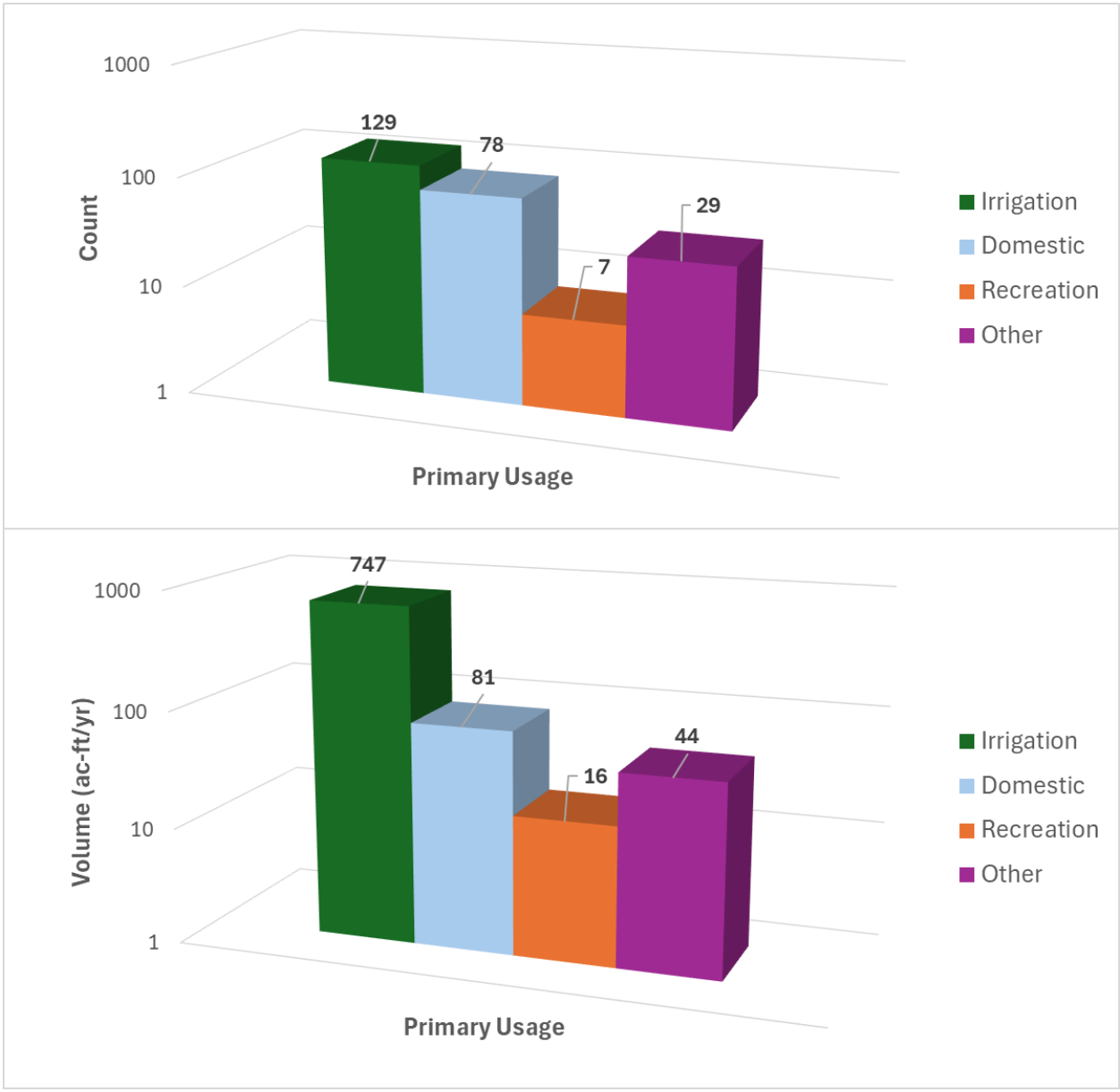

Figure 5-2. Primary water usage for points of diversion within the Navarro River watershed. Note that these are presented on a log scale.

5.1 Irrigation

The LSPC irrigation module is designed to streamline the spatial and temporal representation of water demand, irrigation application, and associated return flows. In practice, irrigation demand is estimated as the deficit of precipitation from the product of a crop-specific evaporative coefficient (ETc) and reference evapotranspiration (PEVT). This LSPC configuration uses a similar approach but instead works backwards to estimate the monthly crop coefficients for agricultural HRUs by using observed irrigation demand and climate data. Those crop coefficients are then used with observed climate data to calculate irrigation application rates during LSPC simulations. The equation used to calculate monthly evaporative crop coefficients for agricultural HRUs is shown as Equation 2:

$$V_{irr} = (PEVT \times ET_c - PREC) \times A_{irr}$$

where (V_{irr}) is the volume of irrigation demand in acre-feet, A_{irr} is the cropland being irrigated in acres, (PEVT) is the reference evapotranspiration depth in feet, ET_c is the crop-specific evaporative coefficient, and (PREC) is the observed precipitation depth in feet. As mentioned above, irrigation demand was inferred from stream diversion records for each catchment. Because the exact location of irrigated vs. non-irrigated parcels was unknown, it was assumed that agricultural land located in catchments immediately draining to reach segments with irrigation PODs were irrigated.

The process for representing irrigation in the Navarro River watershed is summarized by the following steps:

1. Estimate irrigation demand.
2. Define irrigated hydrologic response units.
3. Calculate crop evaporative coefficients.

5.1.1 Estimation of Irrigation Demand

Irrigation demand was inferred from eWRIMS stream diversion data for records between 2017 and 2023. For each LSPC catchment, the total monthly irrigation demand was estimated as the sum of all irrigation-associated stream diversions. As mentioned above, stream diversions were either directly used for the application or routed to a storage facility for later use. Due to data limitations, it was unknown exactly when and how stored streamflow was used for irrigation; however, because direct diversion is higher during the growing season and closely follows PEVT, it was assumed that irrigation of stored water would also follow a similar pattern that scales in proportion to evaporative demand, which is higher during the warmer and drier growing season. Figure 5-3 shows average monthly diversion volumes vs. potential evapotranspiration.

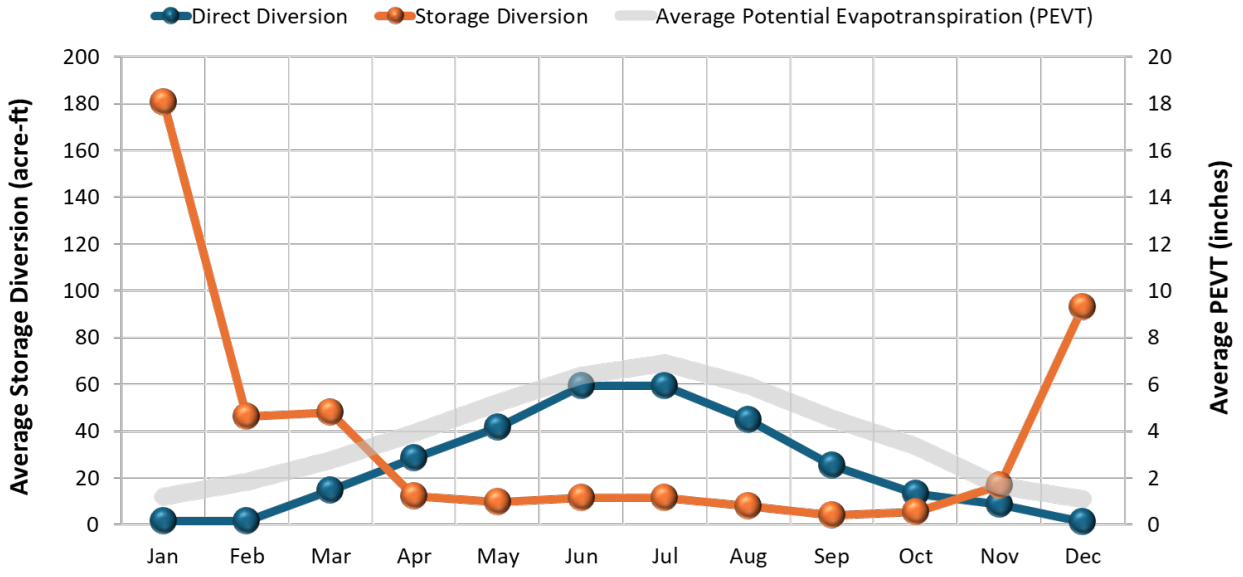

Figure 5-3. Total reported direct and storage diversions vs. average potential evapotranspiration.

5.1.2 Defining Irrigated Hydrologic Response Units

The LSPC model simulates irrigation on a unit-area basis. Agricultural HRUs were partitioned into irrigated and non-irrigated HRU counterparts, as previously described in Section 3.6. Because the exact location of irrigated vs. non-irrigated parcels was unknown, it was assumed that agricultural land located in catchments immediately draining to reach segments with irrigation PODs were irrigated; there were 42 out of the 364 catchments that were irrigated.

As shown in Figure 5-4, the irrigated footprint area is a relatively small portion of the Navarro River model domain. The sum of all croplands, pasture, and grassland areas represents 7.5% of the watershed. Of that area, nearly half (45%) is within the 42 catchments with irrigation. The "Irrigated" area, where the modeled unit-area response is applied, is 916 acres—about 0.5% of the Navarro River watershed. For the unit-area model representation, it was assumed that 50 percent of irrigation water was applied as sprinkler and 50 percent as flood irrigation. Sprinkler irrigation enters the model at the same layer as precipitation, making it subject to interception storage and associated evaporation. Flood irrigation enters the model below interception storage and is only subject to surface ponding and infiltration.

5.1.1 Calculation of Crop Evaporative Coefficients

Crop evaporative coefficients are used to adjust reference evapotranspiration rates to better represent an evaporative demand for a specific vegetation type. In the absence of high-resolution irrigation data, this crop-specific evaporative demand can be used with observed precipitation and PEVT data to predict irrigation demand. For this LSPC model instance, distinct crop types were not represented in hydrologic response units; however, comparing the relative magnitude of direct diversion volumes with potential evapotranspiration forcing data suggested that using a constant coefficient against PEVT would be representative of seasonal irrigation application patterns, as illustrated in Figure 5-3. Storage occurs in the wetter winter/spring months. Direct diversion is higher during the growing season and closely follows PEVT.

The coefficient used in the model was derived by optimizing ET_c in Equation 2 using Microsoft Excel solver to match total irrigation demand volume V_{irr} with the total withdrawal volume for irrigation use. This resulted in a long-term average value of 0.35 for the watershed. Storage diversion and management were not explicitly modeled. By using a constant coefficient, it was assumed that the same total water diverted for irrigation (storage + direct diversion) was eventually irrigated in proportion to potential evapotranspiration.

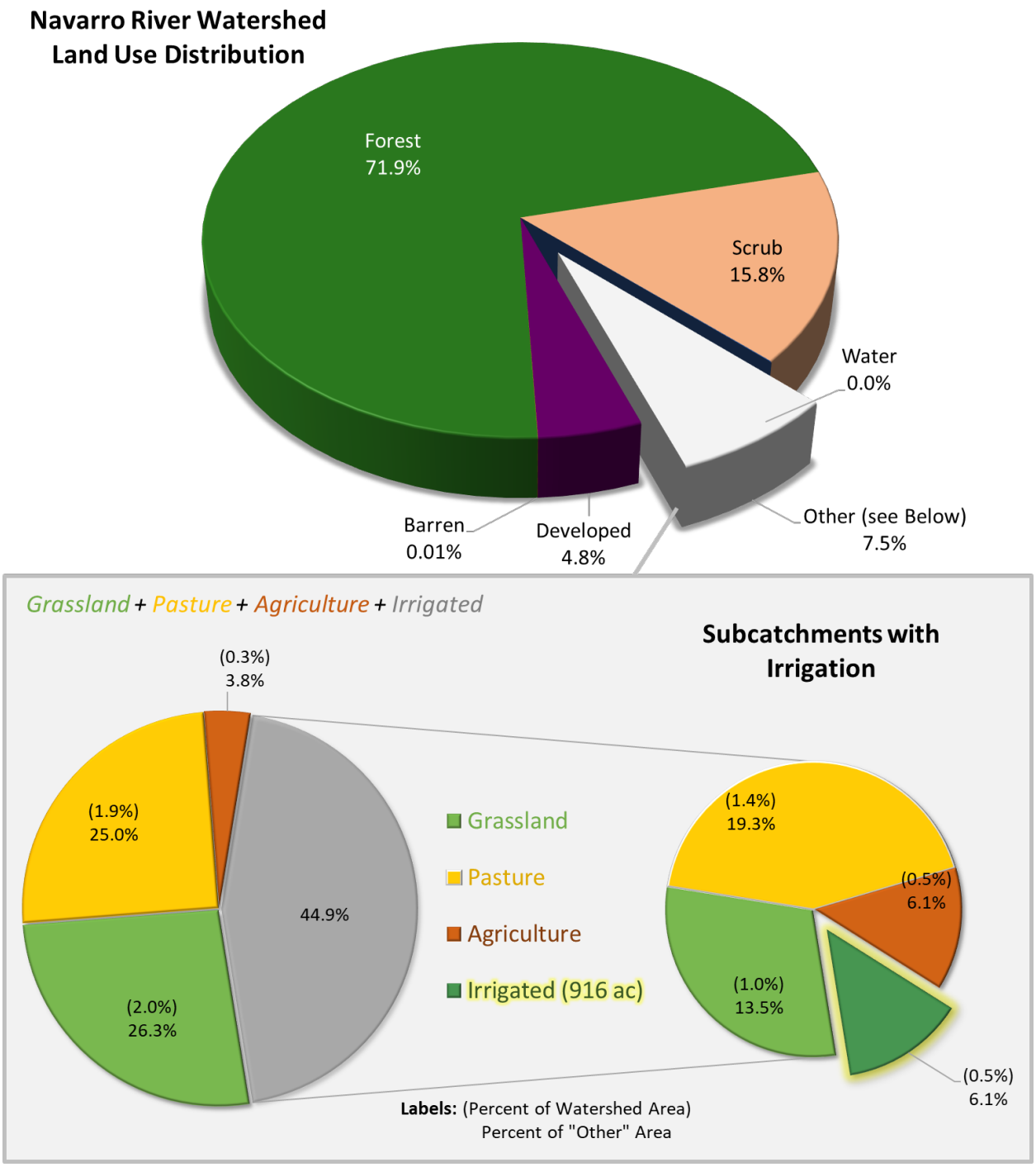

Figure 5-4. Irrigated area as a subset of the Navarro River watershed. Note that for each pie, values in parentheses represent the percentage of total watershed area.

6 MODEL CALIBRATION

The goal of the hydrology model calibration is to adjust model parameters to improve predictive performance based on comparisons to observed data. The desired outcome of the calibration process

is a set of modeling parameters that characterize existing conditions for all processes in LSPC that vary by HRU (as described in Section 3), reach group, and process-based parameters group. The model development approach prioritizes model configuration over calibration by investigating and expressing known physical characteristics of the watershed wherever possible and practical, and only leaving responses that cannot be explained by physical characteristics to calibration of model parameters. The resulting model is parameterized in such a way that variability trends in the observed data are replicated relative to hydrological conditions (e.g. wet and dry streamflow conditions and rainfall magnitude). The resulting calibrated parameters are consistent by HRU with responses varying as a function of HRU distribution and weather variability minimizes spatial biases and reduces the possibility of over tuning during model calibration. A robustly calibrated model can then serve as the starting point for future watershed-specific applications and investigations and management scenarios.

Figure 6-1 shows how the model configuration and calibration components are layered in the model. LSPC makes clear distinctions between inputs that are physical characteristics and process parameters. The term "parameters" refers to the rates and constants used to represent physical processes in the model. All other model inputs previously described such as weather data, HRU distribution, and the length and slope of overland flow for individual HRUs are generally considered physical characteristics of the watershed because they can be directly measured, assigned, or reasonably estimated from available spatial and temporal data sources. Those components are generally set during model configuration and are not varied during model calibration unless new information is received that justifies a systemwide change to those components.

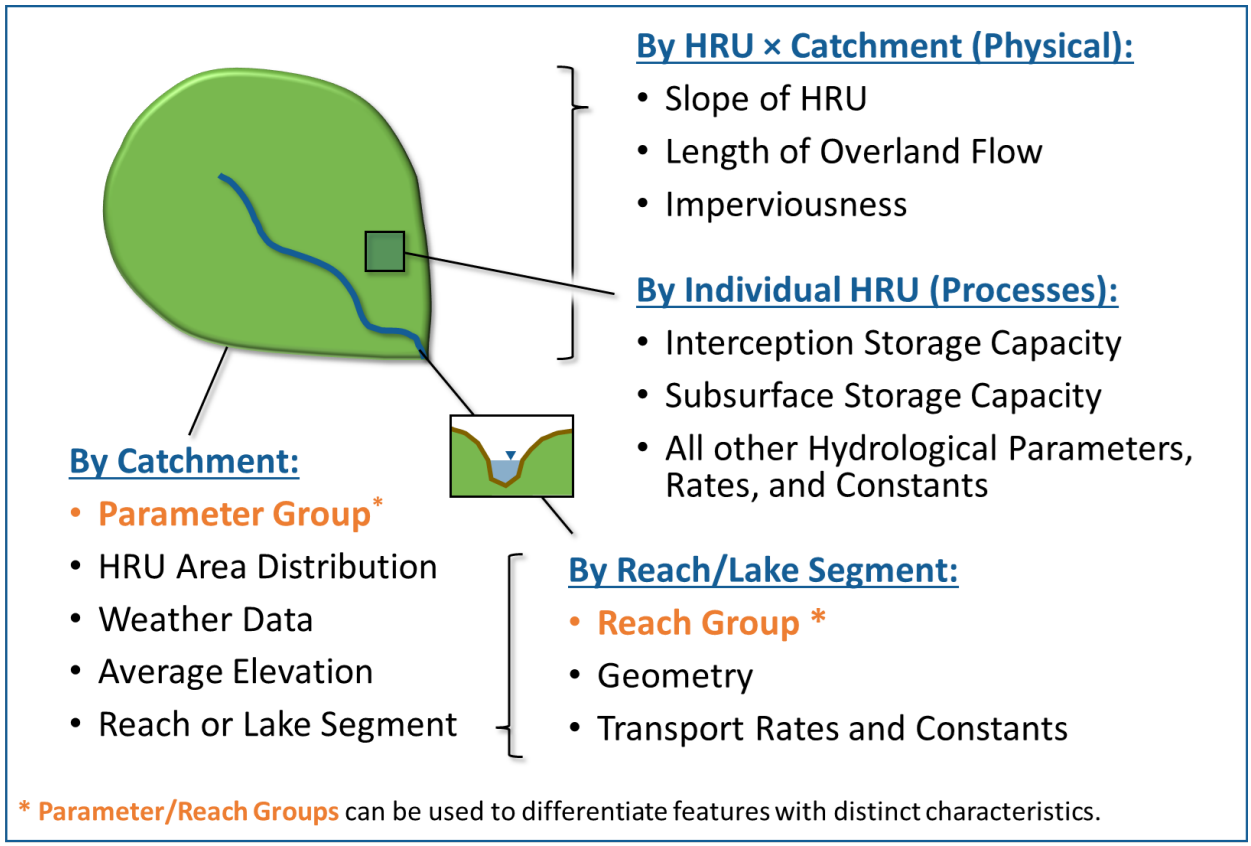

Figure 6-1. LSPC model configuration and calibration components.

Developing modeling parameters begins with specifying one set of parameters systemwide. The Navarro River model comprises 98 possible HRUs per catchment and 114 unique combinations of meteorological boundary conditions (i.e., unique combinations of precipitation time series and

potential evapotranspiration time series). As described in Section 3.4.1, LSUR and SLSUR are uniquely computed by HRU and catchment; therefore, the initial degrees of freedom are already quite broad. Consequently, using one parameter group, the model represents 7,116 unique non-zero area HRU × meteorological responses over the model domain of 364 catchments. Wherever model responses diverge from observed data in ways that the modeling parameters cannot explain, further investigation may warrant introducing a new parameter group or reach group to add more degrees of freedom to the range of model parameters. This methodical calibration sequence can also help to identify areas where additional data collection may be warranted to characterize the physical system better.

Figure 6-2 shows the model calibration sequence, a top-down data approach that began with the extensive model configuration and quality control process previously described in Section 2 through Section 5. The sequence begins with climate-forcing data, followed by edge-of-stream land hydrology and water budget estimates and representation of the stream routing network. This sequencing minimizes the propagation of uncertainty and error by distinguishing physical characteristics of the watershed that can be measured and configured from process-based parameters, which are rates and constants that can be estimated within a reasonable range of variability by HRU.

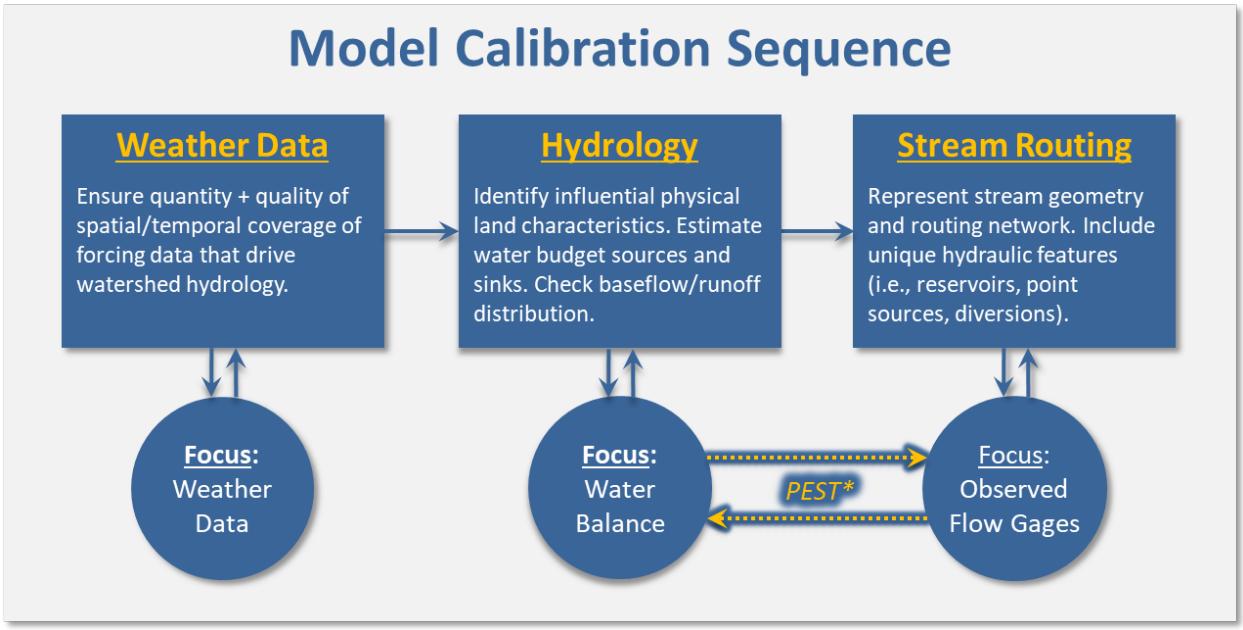

Figure 6-2. Top-down calibration sequence for hydrology model calibration.

Twenty water years of meteorological forcing data between October 2003 and September 2023 were processed to drive the Navarro River watershed model. Consumptive use data were available for the most recent 6 among those 20 years, water years 2018 through 2023; therefore, those 6 years were selected for model calibration. Furthermore, a 2-year subset of those water years, 2022 and 2023, were selected for Parameter Estimation—that process is further described in Section 6.2. As shown in Figure 6-3, the annual precipitation during water year 2022 was approximately equal to the 6-year average, while 2023 was a close second to the wettest year within the 6-year calibration period. A smaller subset was selected because of the computational demand associated with parameter estimation. Finally, the 13 water years prior to the calibration period (water years 2005 through 2017) were selected for independent model validation. Observed streamflow data for the calibration and

validation periods came from the one active USGS streamflow gauge in the watershed located near the mouth of the river (see Figure 6-4 and Table 6-1 for details).

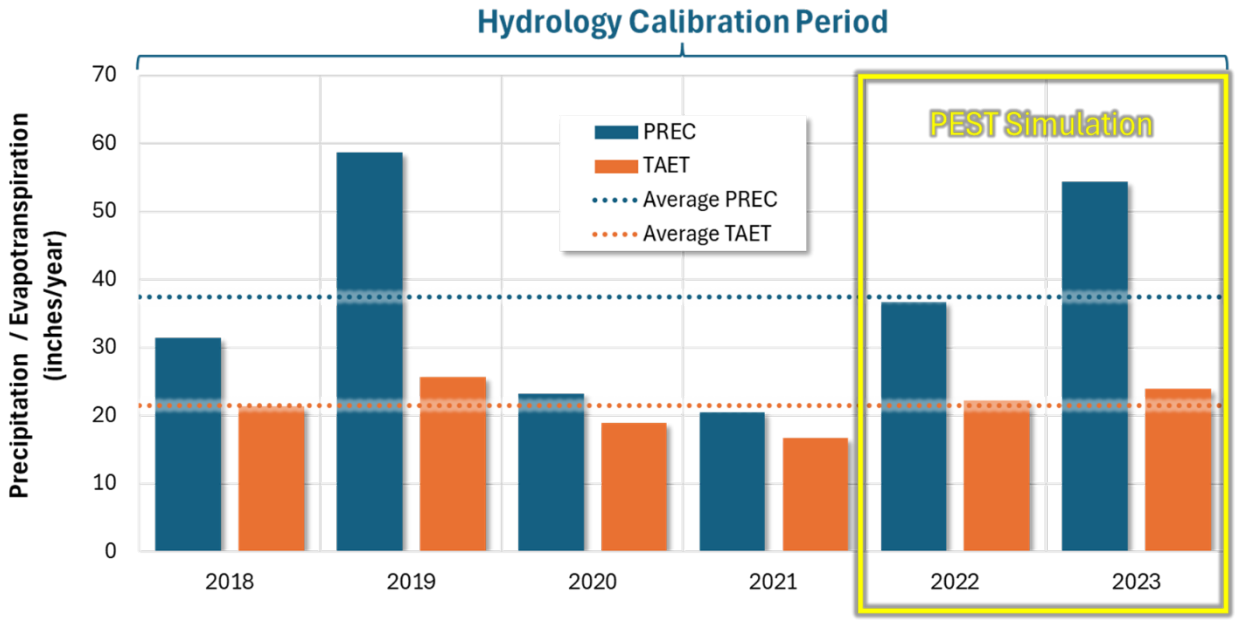

Figure 6-3. Annual average precipitation (PREC) and total evapotranspiration (TAET) between water years 2018 – 2023, along with PEST simulation and hydrology calibration periods.

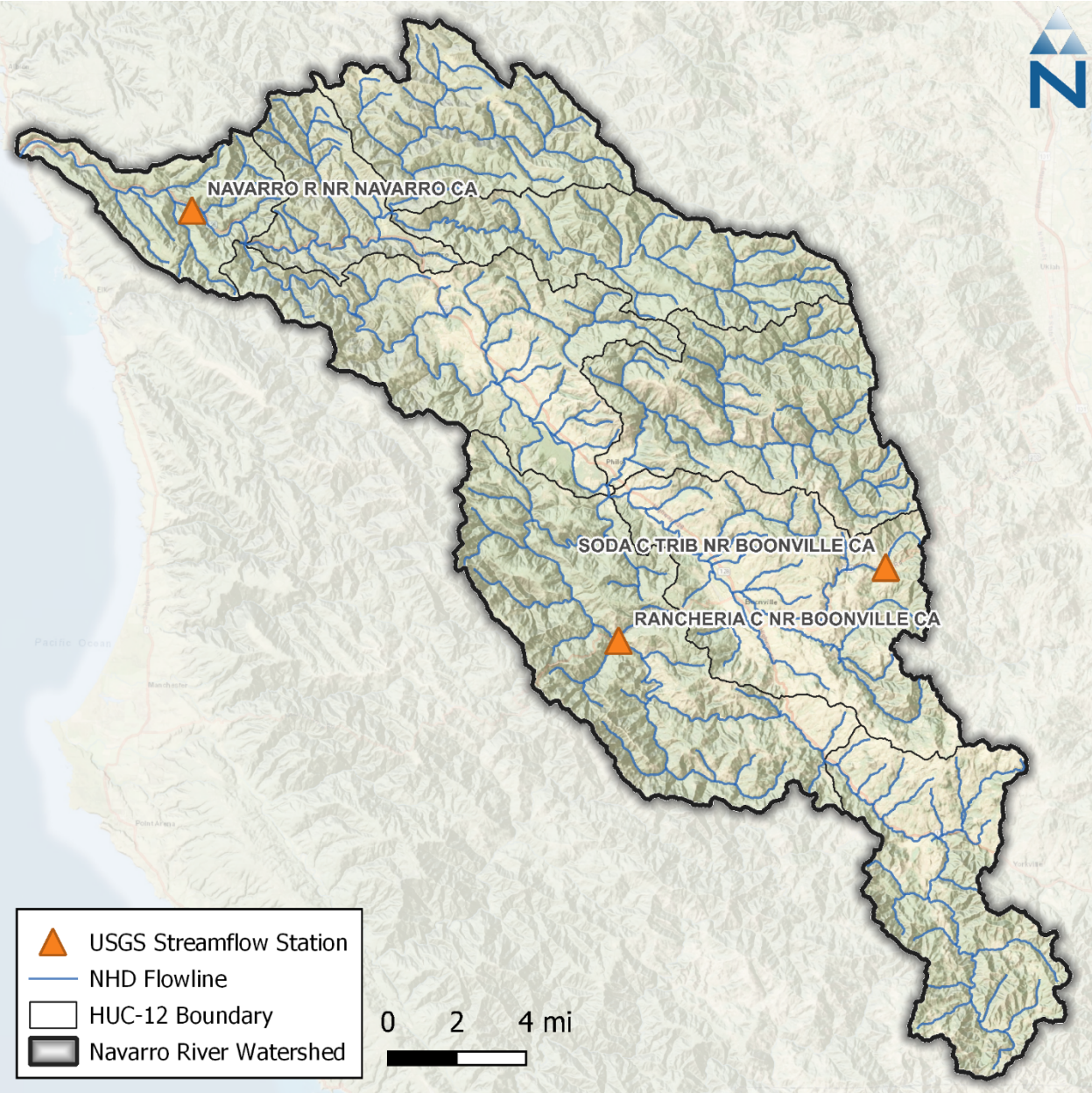

Figure 6-4. USGS streamflow stations in the Navarro River watershed.

Table 6-1. Summary of USGS daily streamflow data

Station Name	Station ID	Drainage Area (mi^2)	Start Date	End Date	Status
NAVARRO R NR NAVARRO CA	11468000	303.0	10/1/1950	Present	Active
RANCHERIA C NR BOONVILLE CA	11467800	65.6	9/1/1959	9/29/1968	Inactive
SODA C TRIB NR BOONVILLE CA	11467850	1.5	10/1/1964	9/29/1968	Inactive

6.1 Calibration Assessment and Metrics

A combination of visual assessments and computed numerical evaluation metrics were used to assess model performance during calibration. Model performance was assessed using graphical comparisons of simulated vs. observed data (e.g., time-series plots, flow duration curves, etc.), quantitative metrics, and qualitative thresholds recommended by Moriasi et al. (2015) and Duda et al. (2012), which are considered highly conservative. Moriasi et al. (2007 and 2015) assign narrative grades for hydrology and water quality modeling to the percent bias (PBIAS), the ratio of the root-mean-square error to the standard deviation of measured data (RSR), and the Nash-Sutcliffe model efficiency (NSE). These metrics are defined as follows:

- The percent bias (PBIAS) quantifies systematic overprediction or underprediction of observations. Positive values of PBIAS reflect a bias towards underestimation, while negative values reflect a bias towards overestimation. Low magnitude values of PBIAS indicate better fit, with a value of 0 being optimal.
- The ratio of the root-mean-square error to the standard deviation of measured data (RSR) provides a measure of error based on the root-mean-square error (RMSE), which indicates error results in the same units as the simulated and observed data but normalized based on the standard deviation of observed data. Values for RSR can be greater than or equal to 0, with a value of 0 indicating perfect fit. Moriasi et al. (2007) provides narrative grades for RSR.
- The Nash-Sutcliffe efficiency (NSE) is a normalized statistic that determines the relative magnitude of the residual variance compared to the measured data variance (Nash and Sutcliffe, 1970). NSE indicates how well the plot of observed versus simulated data fits the 1:1 line. Values for NSE can range between -∞ and 1, with NSE = 1 indicating a perfect fit.

Other metrics were computed and used to assess calibrated model performance, including the Kling-Gupta Efficiency (KGE). This metric can provide additional or complementary information on model performance to the three metrics listed above and is defined as follows:

- The Kling-Gupta Efficiency (KGE) metric is based on the Euclidean Distance between an idealized reference point and a sample's bias, standard deviation, and correlation within a three-dimensional space (Gupta et al. 2009). KGE attempts to address documented shortcomings of NSE, but the two metrics are not directly comparable. A KGE value of 1 indicates perfect fit, with agreement worsening for values less than 1. Knoben et al. (2019) have suggested a KGE value > - 0.41 as a benchmark that indicates a model has more predictive skill than using the mean observed flow. Qualitative thresholds for KGE have been used by Kouchi et al. (2017).

Both simulated time series and observed data were binned into subsets of time to highlight seasonal performance and different flow conditions. Hydrograph separation was also performed to assess stormwater runoff vs. baseflow periods to isolate model performance on stormflows and low flows. Table 6-2 is a summary of performance metrics that will be used to evaluate the hydrology calibration. As shown in the table, "All Conditions" (i.e., annual interval) for R-squared and NSE is the primary condition typically evaluated during model calibration. For sub-annual intervals, the pattern established in the literature for PBIAS/RME when going from "All Conditions" to sub-annual intervals is to shift the qualitative assessment by one category (e.g., use the "good" range for "very good", "satisfactory" for "good", and so on). This pattern was followed for RSR and NSE qualitative assessments of sub-annual intervals.

Table 6-2. Summary of qualitative thresholds for performance metrics used to evaluate hydrology calibration

Performance Metric	Hydrological Condition	Performance Threshold for Hydrology Simulation			
		Very Good	Good	Fair	Poor
Percent Bias (PBIAS)	All Conditions [1]	<5%	5% - 10%	10% - 15%	>15%
	Seasonal Flows [2]	<10%	10% - 15%	15% - 25%	>25%
	Highest 10% of Daily Flow Rates [3]				
	Days Categorized as Storm Flow [4]				
	Days Categorized as Baseflow [4]				
RMSE – Std Dev Ratio (RSR)	All Conditions [1]	≤0.50	0.50 - 0.60	0.60 - 0.70	>0.70
	Seasonal Flows [2]	≤0.40	0.40 - 0.50	0.50 - 0.60	>0.60
Nash-Sutcliffe Efficiency (NSE)	All Conditions [1]	>0.80	0.70 - 0.80	0.50 - 0.70	≤0.50
	Seasonal Flows [2]	>0.70	0.50 - 0.70	0.40 - 0.50	≤0.40
Kling-Gupta Efficiency (KGE)	Monthly Aggregated [5]	≥0.90	0.90 - 0.75	0.75 - 0. 50	<0.50

1. All Flows considers all daily time steps in the model time series.
2. Seasonal Flows consider daily flows during a predefined, seasonal period (e.g., Wet Season and Dry Season). The Wet Season includes the months of October through April. The Dry Season includes the months of May through September.
3. Highest 10% of Flows considers the top 10% of daily flows by magnitude as determined from the observed flow duration curve.
4. Baseflows and Storm flows were determined from analyzing the daily model time series by applying the USGS hydrograph separation approach (Sloto and Crouse 1996).
5. KGE evaluated using thresholds for monthly aggregated time series (Kouchi et al. 2017).

6.2 Parameter Estimation

The model-independent Parameter ESTimation tool (PEST) is a powerful tool used for model parameter estimation, sensitivity analysis, and uncertainty analysis (Doherty 2015). It automates adjusting a specific set of model parameters within a reasonably constrained range of variability, with the objective of minimizing the differences between observed and simulated data. PEST seeks to minimize the sum of Squared Errors (SSE) across all specified observations that can be customized as needed to evaluate complete flow time series or other temporal categorizations such as flow duration intervals, monthly volumes, wet and dry periods, etc. A supervised PEST simulation helps to ensure that recommended outcomes are realistic and representative of the natural system being modeled. PEST is versatile and can be integrated with a wide range of environmental and hydrological models, including LSPC.

Sections 2 through 5 above describe model configuration and quality control methods used to represent physical characteristics of the watershed that are either directly measurable or can be reasonably estimated from available spatial or temporal data. On the other hand, parameters associated with subsurface geology represent one of the areas of uncertainty in the model where optimization of model parameters can improve performance. PEST was used in conjunction with model parameterization guidance documentation (BASINS Technical Note 6 [EPA 2000]) to vary six parameters associated with subsurface geology: the infiltration index parameter (INFILT), the lower zone nominal storage parameter (LZSN), the upper zone nominal storage parameter (UZSN), the non-linear groundwater recession flow parameter (KVARY), the active groundwater recession coefficient (AGWRC), and the interflow recession coefficient (IRC).

The infiltration index parameter (INFILT) is one of the parameters optimized by PEST. Within a given hydrological soil group, TN6 guidance suggests that INFILT typically varies within minimum and maximum values shown in Table 6-3. Some model parameters are codependent. For example, TN6 recommends that the upper zone nominal storage parameter (UZSN) should first be estimated as a percentage of the lower zone nominal storage parameter (LZSN), taking into consideration other physical characteristics such as slope, vegetation cover, and depression storage, and then calibrated. Table 6-4 shows recommended initial values for UZSN as a percentage of LZSN and other physical characteristics. The non-linear groundwater recession coefficient (KVARY) "is used when the observed groundwater recession demonstrates a seasonal variability with a faster recession (i.e., higher slope and lower AGWRC values) during wet periods, and the opposite during dry periods" according to TN6. The active groundwater recession coefficient (AGWRC), the ratio of current groundwater discharge to that of the previous day, was the fourth parameter optimized by PEST. TN6 notes that "the overall watershed recession rate is a complex function of watershed conditions, including climate, topography, soils, and land use" that can be estimated from observed time series, and then adjusted during calibration (EPA 2000). Interflow recession coefficient (IRC), the ratio of the current daily interflow discharge to the interflow discharge on the previous day, affects the rate that interflow is discharged from storage and, therefore, the shape of the hydrograph receding limb after storm events. Model guidance and previous experience suggest that these parameters are both uncertain and very sensitive; therefore, using PEST to explore their impact and optimize performance is worthwhile and beneficial.

Table 6-3. Typical ranges by hydrological soil group for the infiltration index model parameter, INFILT

Hydrological Soil Group	INFILT Typical Ranges (in./hr)		Runoff Potential
	Low	High	
A	0.40	1.00	Low
B	0.10	0.40	Moderate
C	0.05	0.10	Moderate to High
D	0.01	0.05	High

Source: BASINS Technical Note 6 (EPA 2000)

Table 6-4. Recommended initial values for upper zone nominal storage (UZSN) as a percentage of lower zone nominal storage (LZSN) and other physical characteristics

Slope	Vegetation Cover	Depression Storage	UZSN (% of LZSN)
Very Mild	Heavy/Forest	High	14%
Moderate	Moderate	Moderate	8%
Steep	Moderate	Moderate	6%

Source: BASINS Technical Note 6 (EPA 2000)

PEST could have optimized model parameters at the HRU level (up to 85 possible degrees of freedom per parameter for previous HRUs); however, to better manage the search space, those degrees of freedom were constrained to 12 combinations of hydrological soil group (4 types) × slope (3 categories). Figure 6-5 is a schematic of HRU-level LSPC hydrology parameters with the six PEST-optimized parameters and process pathways highlighted. Table 6-5 shows the minimum and maximum parameter value ranges used to constrain PEST optimization by hydrological soil group and slope. Table 6-6 shows the initial and final PEST-optimized estimates for subsurface process parameters, summarized by hydrological soil group and slope—the data bars show the relative magnitude of the initial and estimated parameter value within the PEST min/max range (a full cell indicates the maximum value while an empty cell indicates the minimum value).

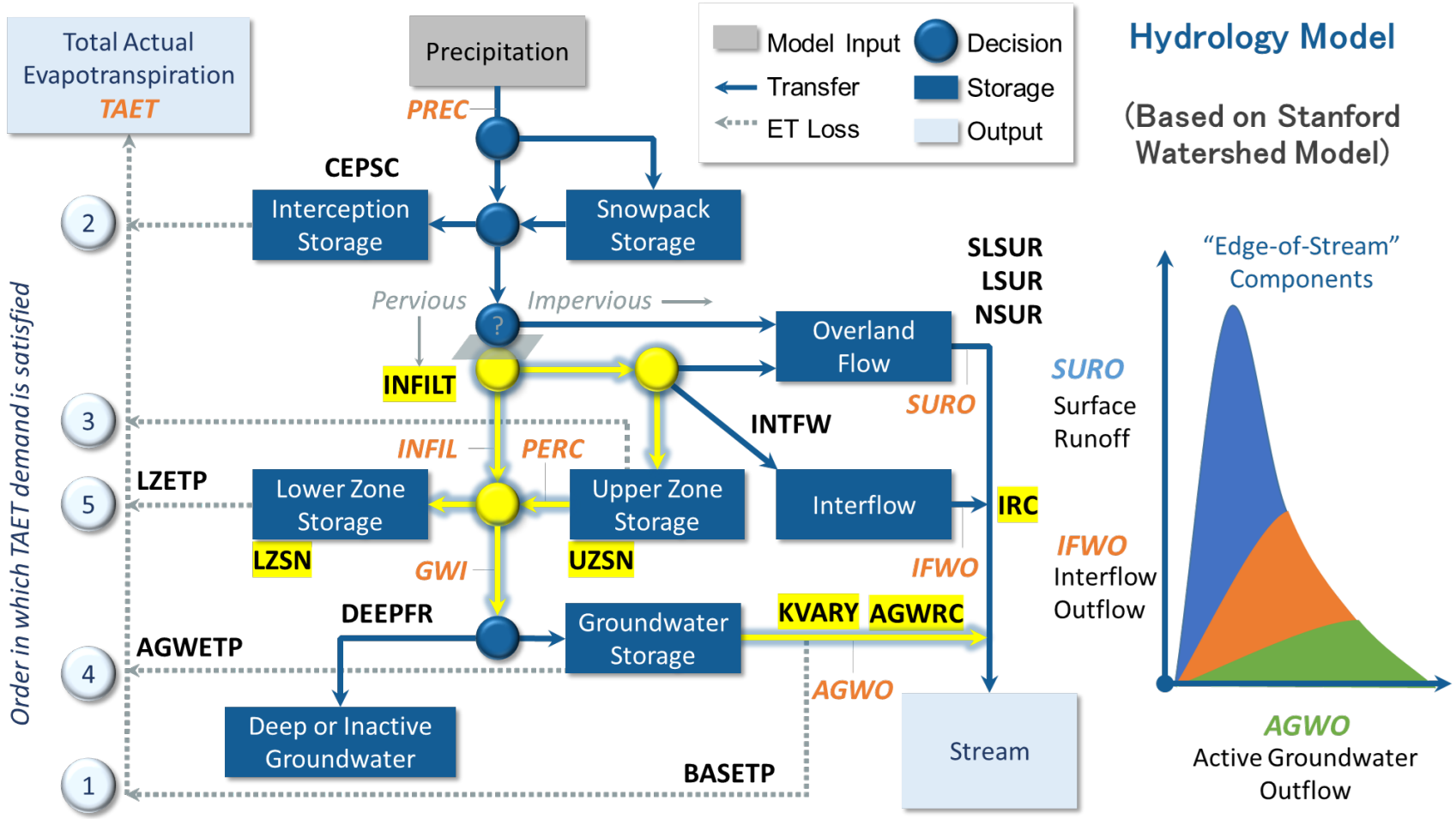

PEST: LSPC parameters and process optimized by Parameter Estimation (PEST) during hydrology calibration.

Figure 6-5. HRU-level LSPC hydrology parameters with PEST-optimized parameters and process pathways highlighted.

Table 6-5. Minimum and maximum parameter value ranges used to constrain PEST optimization, by hydrological soil group and slope

Hydrological Soil Group	Slope	Area (ac)	Area (%)	LZSN		INFILT		KVARY		AGWRC		UZSN (% LZSN)		IRC	
				Min	Max	Min	Max	Min	Max	Min	Max	Min	Max	Min	Max
A	Low	573.1	0.3%	2	15	0.4	1	0	3	0.85	0.999	1	21	0.3	0.85
A	Med	446.7	0.2%	2	15	0.4	1	0	3	0.85	0.999	1	21	0.3	0.85
A	High	549.2	0.3%	2	15	0.4	1	0	3	0.85	0.999	1	21	0.3	0.85
B	Low	2,087.8	1.0%	2	15	0.1	0.4	0	3	0.85	0.999	1	21	0.3	0.85
B	Med	8,690.7	4.3%	2	15	0.1	0.4	0	3	0.85	0.999	1	21	0.3	0.85
B	High	92,341.2	45.9%	2	15	0.1	0.4	0	3	0.85	0.999	1	21	0.3	0.85
C	Low	2,742.7	1.4%	2	15	0.05	0.1	0	3	0.85	0.999	1	21	0.3	0.85
C	Med	8,595.0	4.3%	2	15	0.05	0.1	0	3	0.85	0.999	1	21	0.3	0.85
C	High	60,991.5	30.3%	2	15	0.05	0.1	0	3	0.85	0.999	1	21	0.3	0.85
D	Low	876.7	0.4%	2	15	0.001	0.05	0	3	0.85	0.999	1	21	0.3	0.85
D	Med	2,300.6	1.1%	2	15	0.001	0.05	0	3	0.85	0.999	1	21	0.3	0.85
D	High	20,953.2	10.4%	2	15	0.001	0.05	0	3	0.85	0.999	1	21	0.3	0.85

Table 6-6. Initial and final PEST optimized estimates for subsurface process parameters, summarized by hydrological soil group and slope

HSG	Slope	Area (ac)	Area (%)	LZSN		INFILT		KVARY		AGWRC		UZSN (% LZSN)		IRC	
				Initial	Estimated	Initial	Estimated	Initial	Estimated	Initial	Estimated	Initial	Estimated	Initial	Estimated
A	Low	573.1	0.30%	10.00	10.18	0.75	0.400	1.00	0.21	0.95	0.850	14.00	14.26	0.70	0.65
A	Med	446.7	0.20%	10.00	10.18	0.75	0.400	1.00	0.21	0.95	0.850	8.00	8.15	0.70	0.65
A	High	549.2	0.30%	10.00	10.18	0.75	0.400	1.00	0.21	0.95	0.850	6.00	6.11	0.70	0.65
B	Low	2,087.8	1.00%	10.00	12.50	0.25	0.100	1.00	2.50	0.95	0.950	14.00	17.50	0.70	0.58
B	Med	8,690.7	4.30%	10.00	12.50	0.25	0.100	1.00	2.50	0.95	0.950	8.00	10.00	0.70	0.58
B	High	92,341.2	45.90%	10.00	12.50	0.25	0.100	1.00	2.50	0.95	0.950	6.00	7.50	0.70	0.58
C	Low	2,742.7	1.40%	10.00	15.00	0.08	0.050	1.00	0.00	0.95	0.973	14.00	21.00	0.70	0.57
C	Med	8,595.0	4.30%	10.00	15.00	0.08	0.050	1.00	0.00	0.95	0.973	8.00	12.00	0.70	0.57
C	High	60,991.5	30.30%	10.00	15.00	0.08	0.050	1.00	0.00	0.95	0.973	6.00	9.00	0.70	0.57
D	Low	876.7	0.40%	10.00	15.00	0.03	0.007	1.00	2.85	0.95	0.850	14.00	21.00	0.70	0.35
D	Med	2,300.6	1.10%	10.00	15.00	0.03	0.007	1.00	2.85	0.95	0.850	8.00	12.00	0.70	0.35
D	High	20,953.2	10.40%	10.00	15.00	0.03	0.007	1.00	2.85	0.95	0.850	6.00	9.00	0.70	0.35

Data Bars Show the relative magnitude of the parameter values within the PEST min/max ranges (See Table 6-5).

6.3 Calibration Results

Using the PEST estimated parameters, the model was run for water years 2018 through 2023 and calibration performance was evaluated. Note that all results presented below exclude observed flows < 1 cfs, where there may be more uncertainty in gage readings. As shown in Table 6-7, performance across the calibration period was "Very Good" for PBIAS with simulated flow volumes slightly overpredicted by 2%. Wet season and dry season PBIAS were "Very Good" with 1% and 10% overprediction, respectively. RSR and NSE performance was "Very Good" across the entire calibration period and seasons. KGE (calculated with monthly flow values) was "Very Good" across the entire calibration period and the wet season and nearly in the "Very Good" range for the dry season (0.898). These metric values indicate the model is performing well at capturing the observed volume (PBIAS) and trends in wet and dry season flow (RSR, NSE, KGE).

Examination of daily and normalized monthly streamflow (Figure 6-6 and Figure 6-7, respectively) shows that, as indicated by the metrics, the most extreme peaks are slightly underestimated, but general rising/falling patterns in the hydrographs are well captured. Figure 6-8 and Figure 6-9 present the interquartile ranges and averages, respectively, of monthly normalized flow—both show a high degree of correspondence between observed and simulated values. The flow duration curve (FDC) shown in Figure 6-10 indicates that observed flow regime trends are generally well matched by the model. Below the 26th percentile, modeled flows are lower than observed; it should be noted that modeled and observed FDCs are calculated independently and flows of the same percentile do not necessarily occur at the same time.

Table 6-7. Summary of daily calibration performance metrics

Hydrology Monitoring Locations	Performance Metrics (10/01/2017 - 09/30/2023)														
	PBIAS						RSR			NSE			KGE[1]		
	All	Wet Season	Dry Season	>10th %ile Flows	Storm Flows	Baseflow	All	Wet Season	Dry Season	All	Wet Season	Dry Season	All	Wet Season	Dry Season
NAVARRO R NR NAVARRO CA	-2%	-1%	-10%	4%	-1%	-3%	0.19	0.20	0.26	0.96	0.96	0.93	0.96	0.96	0.90

[1] Monthly, as specified in Table 6-2.

Very Good | Good | Fair | Poor

\- Overpredicts | + Underpredicts

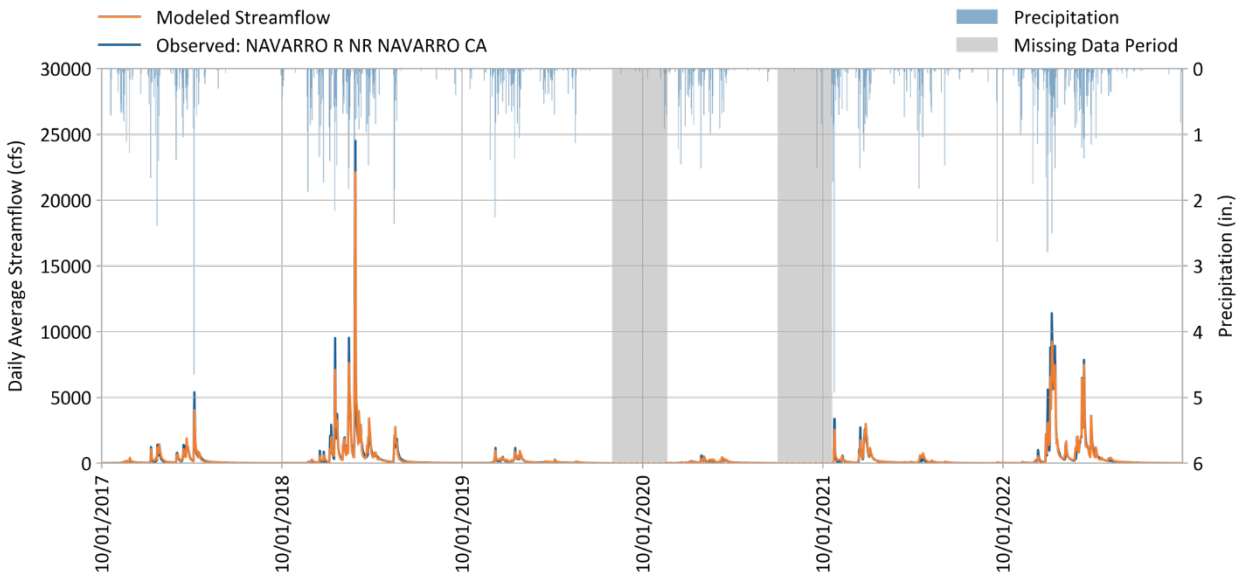

Figure 6-6. Daily simulated vs. observed streamflow for NAVARRO R NR NAVARRO CA (11468000).

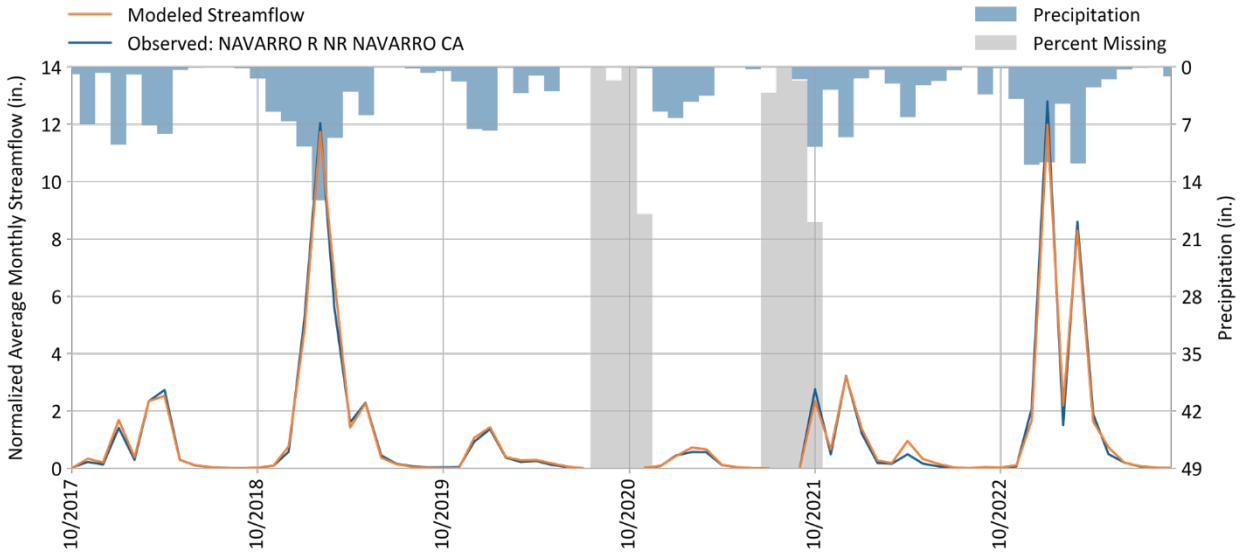

Figure 6-7. Monthly simulated vs. observed streamflow for NAVARRO R NR NAVARRO CA (11468000).

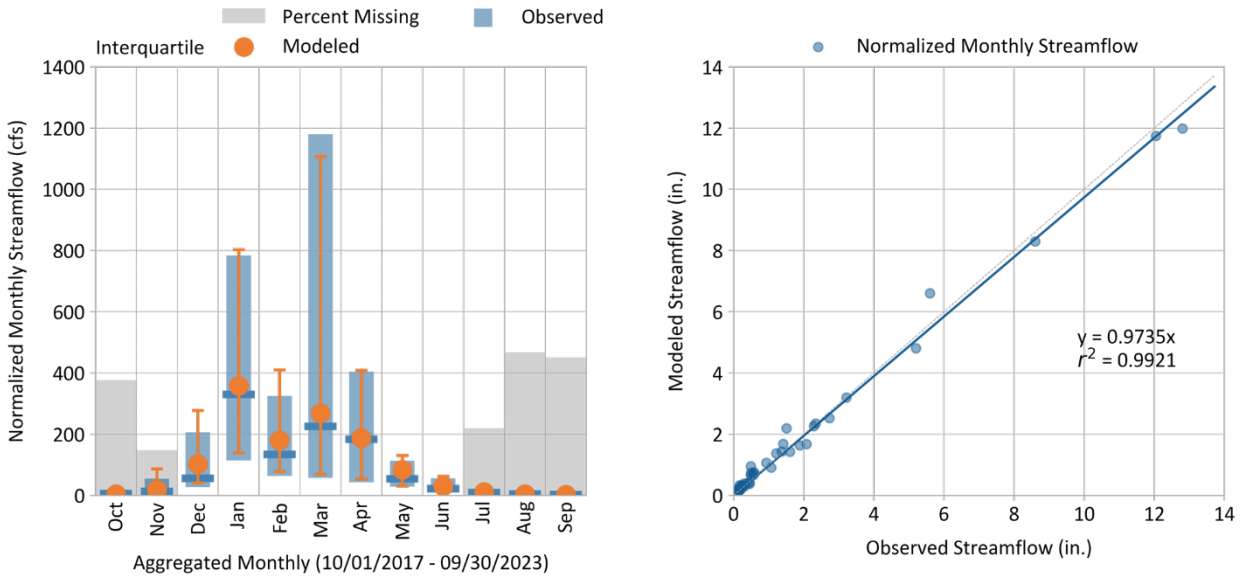

Figure 6-8. Monthly simulated vs. observed streamflow for NAVARRO R NR NAVARRO CA (11468000).

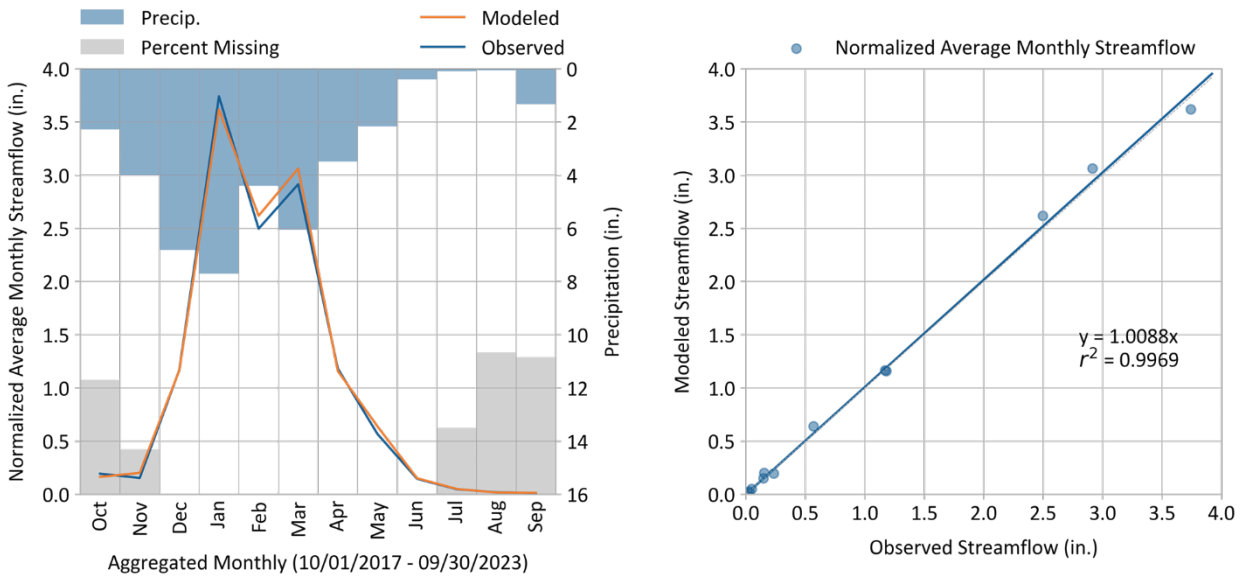

Figure 6-9. Average Monthly simulated vs. observed streamflow for NAVARRO R NR NAVARRO CA (11468000).

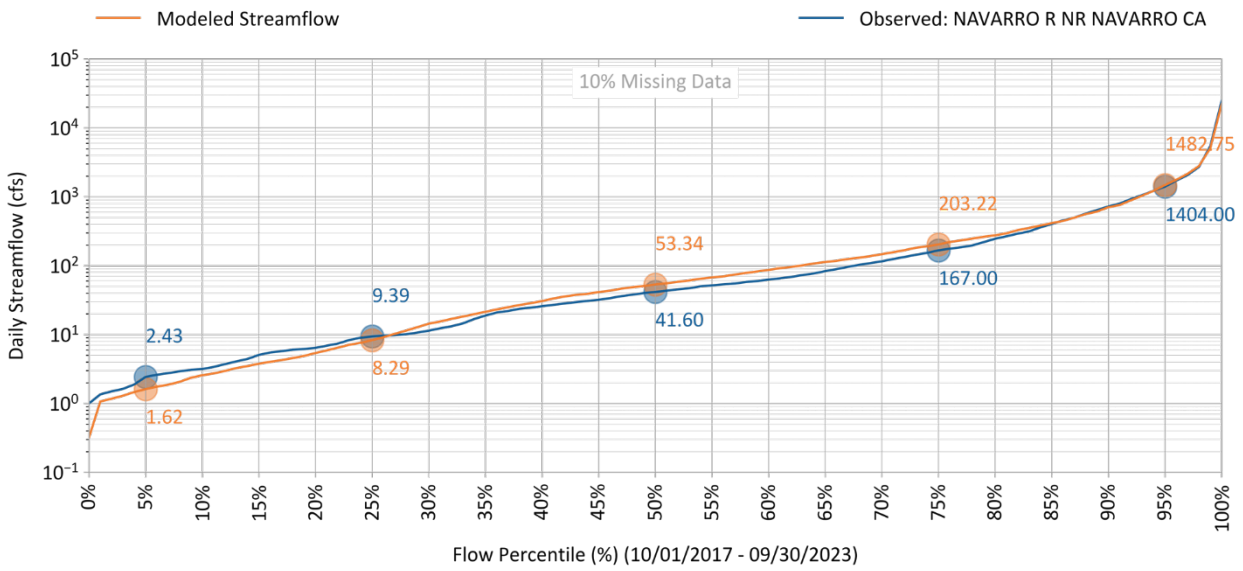

Figure 6-10. Simulated vs. observed flow duration curve for NAVARRO R NR NAVARRO CA (11468000).

PBIAS, NSE, and RSR performance values by season and flow regime are shown in Table 6-8, Table 6-9, and Table 6-10, respectively. The "Days Categorized as Baseflow" metric, which is derived from hydrograph separation, consistently shows "Very Good" model performance across all conditions and all metrics. Using hydrograph separation to classify baseflow and stormflow provides a more reliable method for assessing low-flow model performance than using the lowest 50% of flows, a metric widely used in hydrology model calibration as a convenient indicator of low-flow model performance. There are several key reasons for this:

1. **Improved Representation of Low-Flow Conditions:** The lowest 50% of flows include not only baseflow but also portions of stormflow as the hydrograph rises and falls. This can mask the true low-flow or baseflow behavior of the system, as the transitions from baseflow to stormflow can have very different physical and hydrological drivers. By using hydrograph separation, baseflow, which is primarily driven by groundwater contributions, can be isolated from storm flows, which are influenced by rainfall (Smakhtin 2001). This provides a clearer, more consistent metric for assessing low-flow conditions during model calibration and performance evaluation.
2. **Reduction in Variability of Metrics:** Because the rising and falling limbs of the hydrograph are affected by factors such as precipitation intensity, antecedent moisture conditions, and catchment characteristics, including portions of these limbs in the low-flow metric can lead to high variability in model performance metrics. This variability can obscure the modeler's ability to accurately assess low-flow performance. Hydrograph separation, on the other hand, offers a cleaner classification, resulting in lower variability and a more stable and reliable assessment of baseflow model performance.
3. **Better Calibration for Baseflow-Driven Processes:** In many hydrological studies, low flows are important for understanding groundwater-surface water interactions, sustaining streamflow during dry periods, and supporting aquatic habitats. Hydrograph separation allows for the explicit calibration of baseflow processes, providing a better assessment of groundwater dynamics and groundwater-fed contributions to the stream network. Without separating baseflow and stormflow, calibration based on the lowest 50% of flows may inadvertently skew model performance statistics by over-emphasizing short-term stormflow events and recession behavior, rather than the sustained low flow processes crucial to many hydrological applications.

4. **Alignment with Process-Based Hydrology:** Hydrograph separation aligns with a process-based understanding of hydrology, where distinct processes govern baseflow and stormflow. This approach respects the inherent differences in generation mechanisms: baseflow is usually a slower, more consistent groundwater-driven process, while stormflow is a quicker response to precipitation events. This distinction is essential for accurately simulating hydrological systems and ensuring model results that are realistic and representative of different flow conditions. Models that capture these distinct flow components are better suited for making predictions about changes in land use, climate, or other factors affecting baseflow and stormflow differently.
5. **Widely Accepted in Hydrological Modeling:** Hydrograph separation techniques are well-established and widely used in hydrological research and practice, offering a consistent framework for distinguishing between baseflow and stormflow (Arnold et al. 1995; Nathan and McMahon 1990). Techniques like those used in the United States Geological Survey (USGS) Hydrograph SEParation (HySEP) methodology provide different options for empirically parsing baseflow time series from storm flows (Sloto and Crouse 1996). The sliding interval method was used to separate both observed and simulated hydrographs at a daily timestep. Figure 6-11 and Figure 6-12 show simulated vs. observed sliding-interval hydrograph separation for water year 2018 wet and dry seasons, respectively. This provides a consistent approach for the rollup and comparison of hydrograph components. This method is robust because they can be directly applicable to time series data as a function of the upstream drainage area. It also performs well on natural hydrological watersheds like the Navarro River.

In the Navarro River watershed, 15% of days within the lowest 50% of flows are in the wet season. The lowest 50% of flows also includes rainfall days: up to 3 inches of daily total rainfall during the wet season and up to 2.3 inches of daily total rainfall during the dry season at the catchment with the USGS gauge. The current calibrated model slightly underpredicts streamflow during low flow conditions, as indicated by the FDC (Figure 6-10), which is conservative for management scenarios focused on maintaining minimal flows.

Table 6-8. Simulated vs. observed daily streamflow PBIAS at NAVARRO R NR NAVARRO CA (11468000)

Calibration Metrics *(10/01/2017 - 09/30/2023)*	Percent Bias (PBIAS)		
	All Seasons	Wet Season	Dry Season
All Conditions	-1.7%	-1.2%	-10.0%
Highest 10% of Daily Flow Rates	3.7%	3.9%	-2.3%
Days Categorized as Storm Flow	-0.7%	0.0%	-24.6%
Days Categorized as Baseflow	-3.2%	-3.0%	-4.8%

Table 6-9. Simulated vs. observed daily streamflow NSE at NAVARRO R NR NAVARRO CA (11468000)

Calibration Metrics *(10/01/2017 - 09/30/2023)*	Nash-Sutcliffe Efficiency (NSE)		
	All Seasons	Wet Season	Dry Season
All Conditions	0.96	0.96	0.93
Highest 10% of Daily Flow Rates	0.94	0.94	0.49
Days Categorized as Storm Flow	0.96	0.96	0.94
Days Categorized as Baseflow	0.96	0.96	0.92

Table 6-10. Simulated vs. observed daily streamflow RSR at NAVARRO R NR NAVARRO CA (11468000)

Calibration Metrics *(10/01/2017 - 09/30/2023)*	RMSE-Std-Dev. Ratio (RSR)		
	All Seasons	Wet Season	Dry Season
All Conditions	0.19	0.2	0.26
Highest 10% of Daily Flow Rates	0.24	0.24	0.71
Days Categorized as Storm Flow	0.2	0.2	0.24
Days Categorized as Baseflow	0.19	0.19	0.29

Very Good Good Fair Poor
\- Overpredicts + Underpredicts

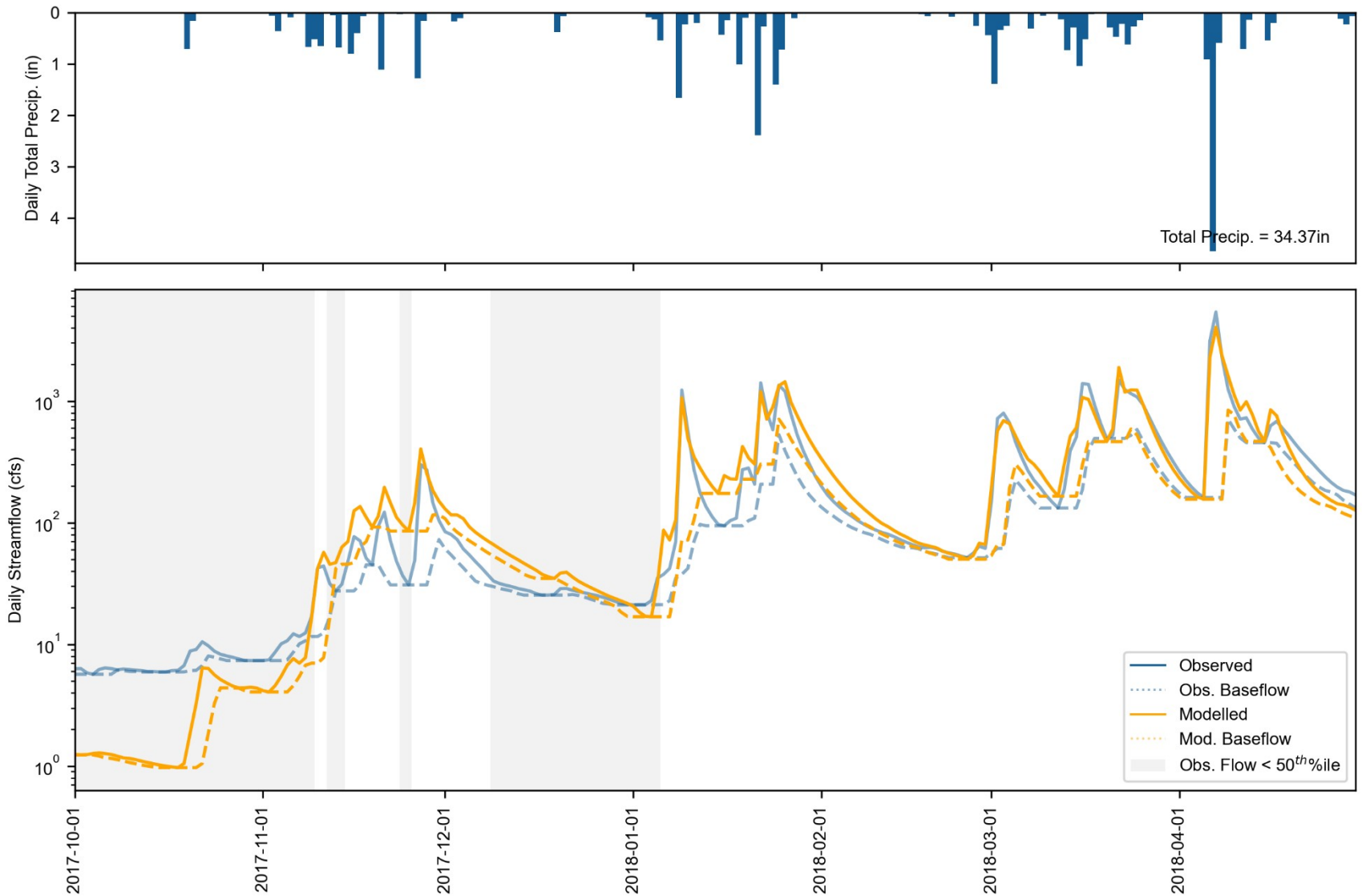

Figure 6-11. Water Year 2018 Wet season daily total precipitation (top) and streamflow (bottom) at NAVARRO R NR NAVARRO CA (11468000). Observed and simulated baseflow are calculated with HYSEP; grey shading indicates observed flow is less than the 50th percentile.

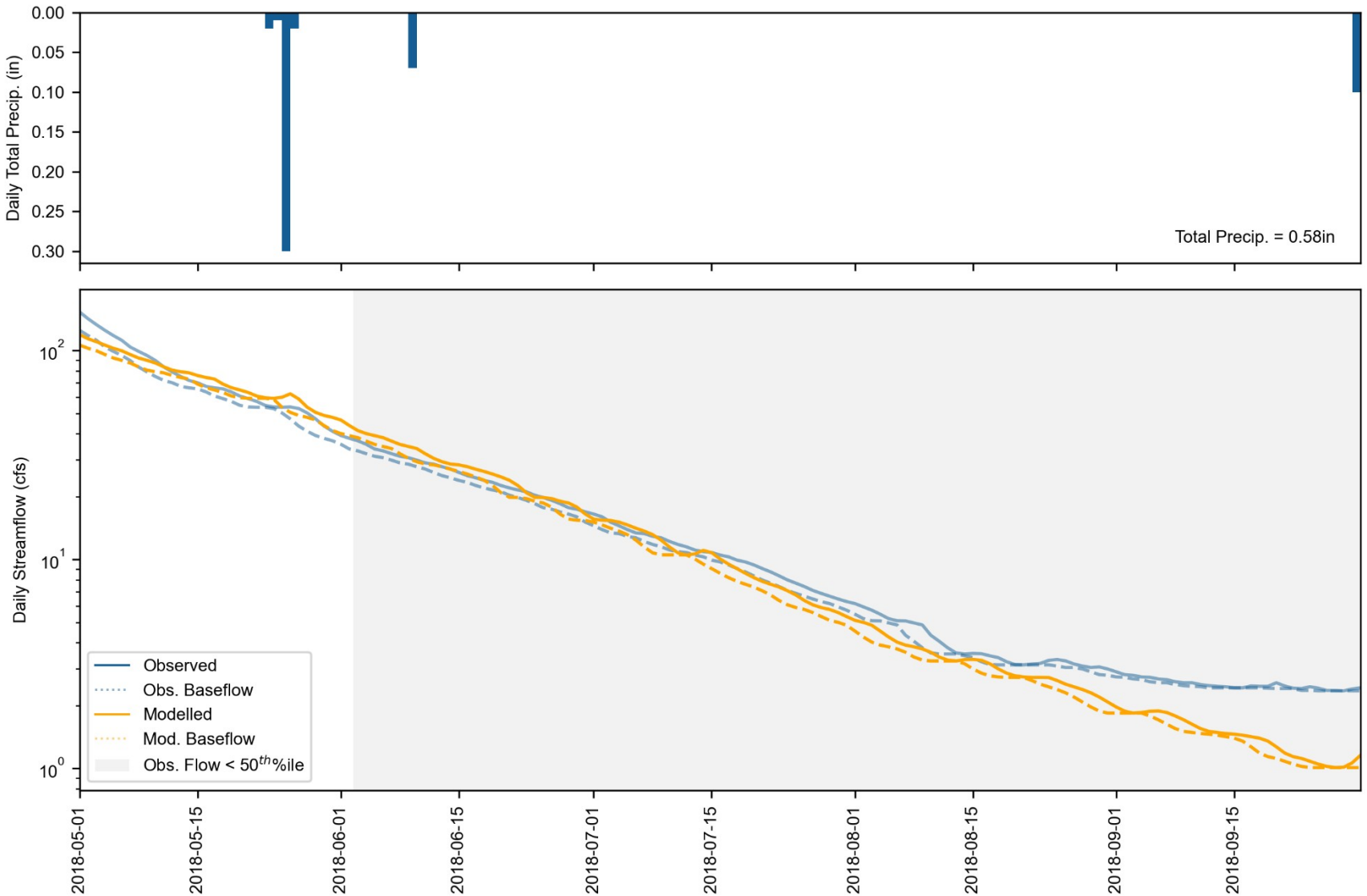

Figure 6-12. Water Year 2018 Dry season daily total precipitation (top) and streamflow (bottom) at NAVARRO R NR NAVARRO CA (11468000). Observed and simulated baseflow are calculated with HYSEP; grey shading indicates observed flow is less than the 50th percentile.

7 MODEL VALIDATION

The model was calibrated for water years 2018-2023 (6 years) and validated for water years 2004-2017 (previous 13 years). First, a water budget analysis was conducted for the period 2018-2023 because reported diversion estimates were only available for that period. Next, the irrigation water budget was confirmed by normalizing associated inputs and outputs by total irrigated area. This validation check was to confirm that applied irrigation water and withdraws as represented using the coefficients, rates, and methods described in Section 5.1 produced a reasonable and representative average monthly distribution relative to the precipitation and evapotranspiration meteorological forcing data. Irrigation was simulated for the full period from 2004-2023. This section presents results for the water budget analysis (Section 7.1), the validation period performance at the USGS gauge (Section 7.2), and an evaluation of model performance at additional stations for dry season flows (Section 7.3).

7.1 Water Budget

A water budget analysis was conducted to validate a match between the sum of model inputs and outputs. Water inputs include precipitation (both to land segments and water body surfaces) and applied irrigation water. Water outputs include terminal outflow at the most downstream outlet of the Navarro River, total actual evapotranspiration (from land segments + direct evaporation from water bodies), and total withdraws (i.e., irrigation and non-irrigation diversion). The water budget was calculated from October 2017 through September 2023, the period for which withdraw information was available. The water budget validation showed a close match between all model inputs and outputs—there is a 0.09% difference between inflow and outflow, which represents net volume to/from system storage over the 6-year simulation period; this is an expected difference for water balances at the watershed scale. Figure 7-1 shows the simulated water balance expressed as total volumes and area-normalized annual average depths for water years 2018-2023 at the Navarro River gage. Figure 7-2 shows monthly average area-normalized simulated water balance components for the same period. In both figures, intermediate values for edge-of-stream outflows prior to stream routing (i.e., surface runoff + interflow outflow + active groundwater outflow) and inflow to active groundwater storage are presented to illustrate the relative scale of those components. The monthly summary also illustrates the expected system lag of approximately 5 months between peak rainfall (Dec-Jan) and peak evapotranspiration (Apr-May).

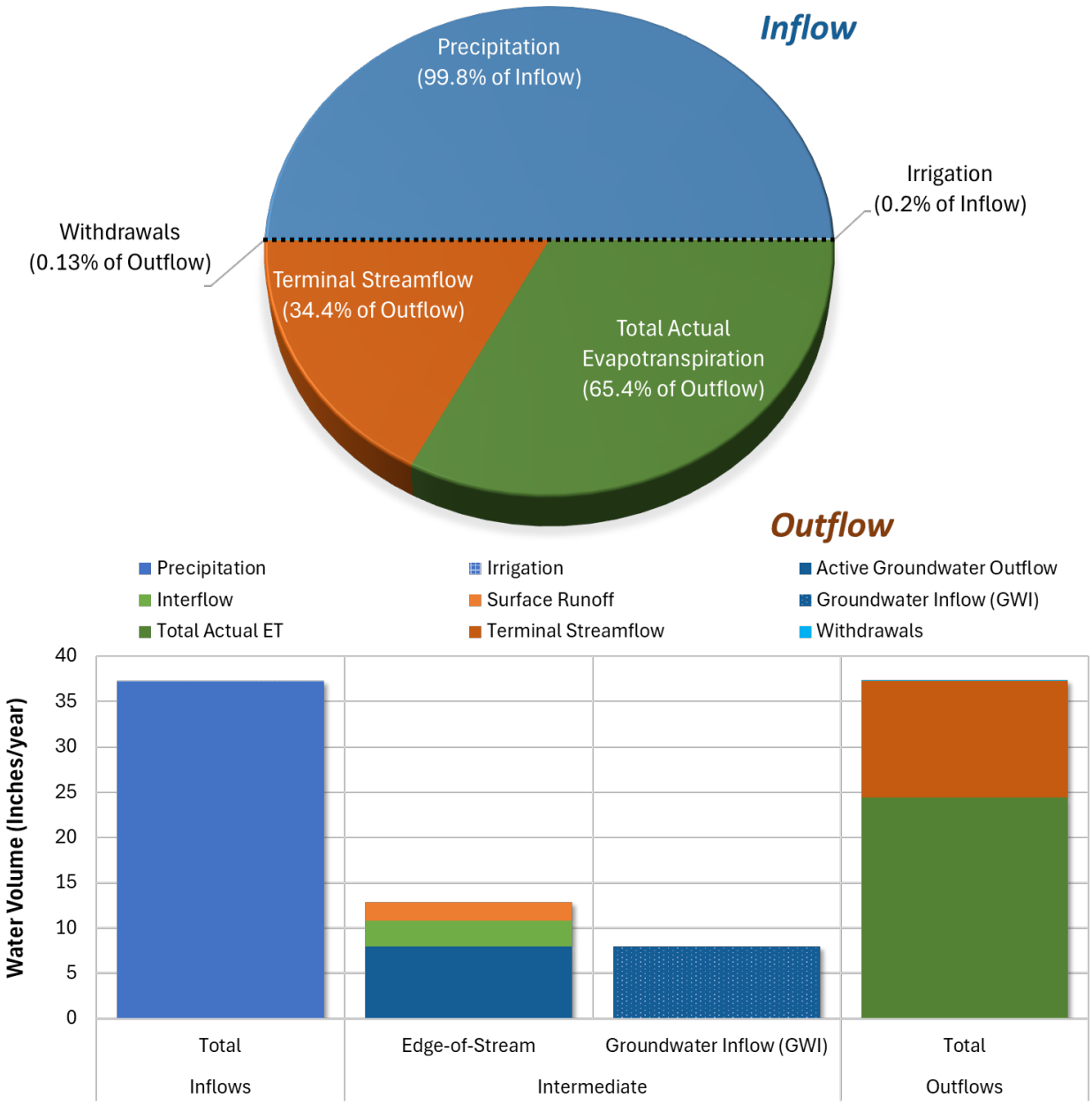

Figure 7-1. Simulated water balance expressed as total volumes and area-normalized annual average depths for the calibration period (water years 2018-2023) at the NAVARRO R NR NAVARRO CA (11468000) gauge.

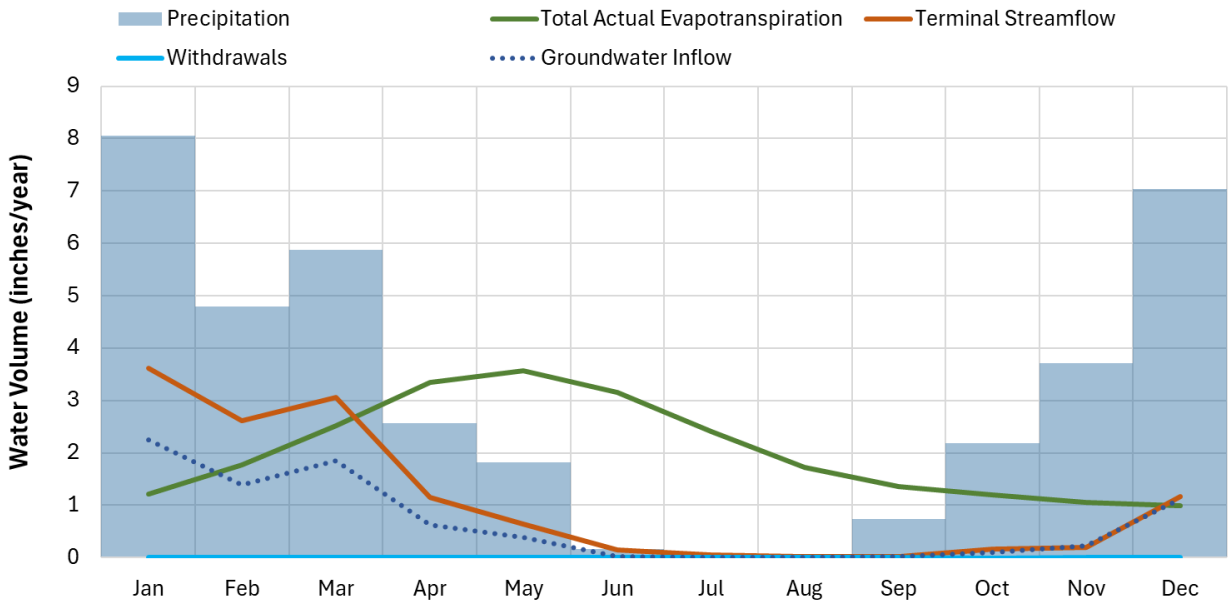

Figure 7-2. Monthly average area-normalized simulated water balance components for water years 2018-2023 at the NAVARRO R NR NAVARRO CA (11468000) gauge. Note that withdrawals are a minor portion of the water balance and are discussed in detail in Section 5.

The water budget for applied irrigation volume was also summarized from calibrated model outputs. On average, a total of 1,099 acre-feet of irrigation water per year was applied on 916 acres of land in the Navarro model. Irrigation volume was temporally distributed as 35% of potential evapotranspiration so that more irrigation occurred during the drier months, as shown in Figure 7-3. The total reported volume of surface water withdrawn either for direct irrigation or to storage represents about 71% of the total volume of irrigation water applied—the remainder of irrigation water applied was assumed to be sourced from groundwater.

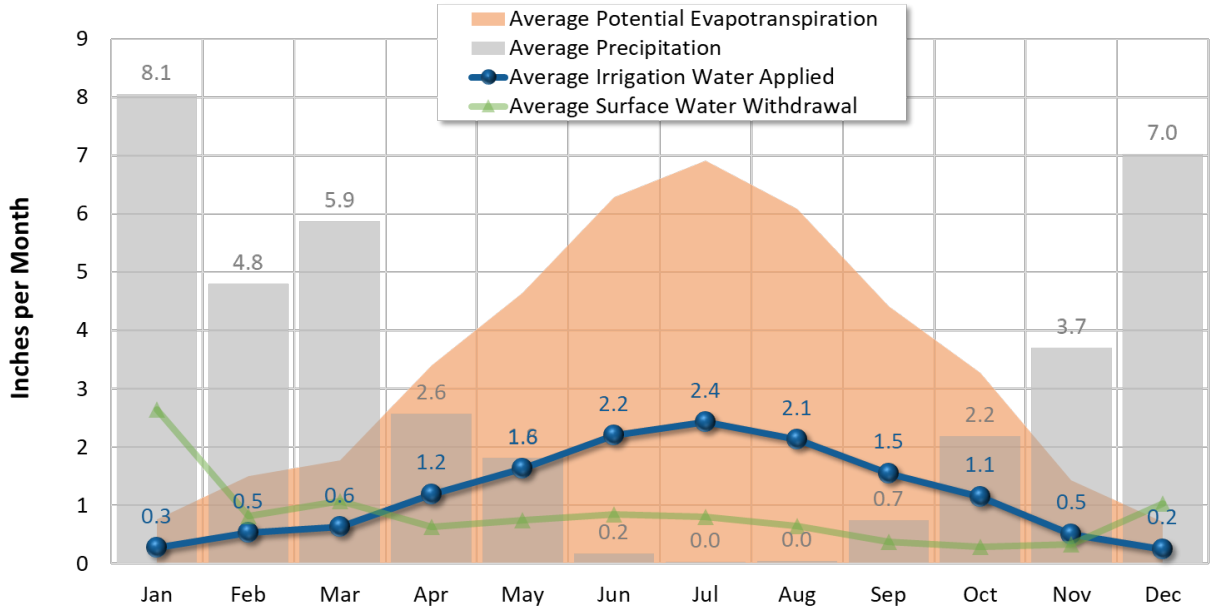

Figure 7-3. Monthly average area-normalized irrigation water balance for irrigated HRUs in the Navarro River watershed (average precipitation in the watershed is also plotted for reference).

7.1.1 ET Comparison

Because the Navarro River watershed only has one streamflow gage for estimating water balance components, evapotranspiration data from OpenET was considered as an alternate source of "observed" evapotranspiration data for validating the simulated spatial distribution and variability of a key predicted model component of the water budget upstream of the streamflow gage. The OpenET project is an operational system for generating and distributing ET data at a field scale using an ensemble of six well-established satellite-based approaches for mapping ET (Melton et al. 2022). Within California, OpenET has data beginning in 2018 and uses CIMIS meteorological datasets to compute reference ET and actual ET. OpenET has undergone extensive intercomparison and accuracy assessment conducted using ground measurements of ET; for agricultural areas, results of these assessments demonstrate strong agreement between the satellite-driven ET models and observed flux tower ET data. However, for natural land covers like forests, scrub, and grasslands, which are the dominate land cover types in the Navarro River watershed (Table 7-1), the OpenET ensemble is known to be biased towards overprediction (OpenET 2021). OpenET data were used in an exploratory comparison with simulated total actual ET (TAET) and the CIMIS reference ET at the HUC-12 scale and were not used for calibration because of the known biases. In highly agricultural watersheds, OpenET could prove to be a valuable data point for model calibration and validation, however in the Navarro River watershed, OpenET closely resembles CIMIS reference ET.

For the Navarro River watershed, monthly total OpenET, CIMIS reference ET, and LSPC TAET by HUC-12 and watershed-wide were compared for the period with available OpenET data (February 2016 – September 2022). As seen in Figure 7-4, OpenET is similar in magnitude and timing to the CIMIS reference ET and both data sets are high, as expected for reference ET. When estimated as annual average observed precipitation minus annual average observed streamflow, actual ET (and a storage component) is approximately 61% of the outflow portion of the water budget. This is close to the simulated value of 64% from the calibration period (see Section 7.1) and 65% for the OpenET period.

At the HUC-12 scale, ET datasets were mapped as the ratio of annual average totals for: (1) TAET:OpenET, (2) OpenET:PEVT (CIMIS reference ET), (3) PREC:OpenET. These comparisons are shown in Figure 7-5 to Figure 7-7, respectively. These maps show that TAET is between 56% to 69% of OpenET (Figure 7-5), OpenET is between 78% and 98% of CIMIS reference ET (Figure 7-6), and OpenET ranges from 83% to 119% of total annual precipitation (Figure 7-7)—note the inverted phase shift between the two (Figure 7-4).

Table 7-1. Summary of HRU area grouped by land cover for HUC-12s within the Navarro River watershed

HUC-12		HRU Land Cover Area (%)									
Name	Area (ac)	Developed Impervious	Developed Pervious	Barren	Forest	Scrub	Grassland	Pasture	Agriculture	Irrigation	Water
Upper Rancheria Creek	23,821.7	0.05%	4.44%	0.00%	53.51%	33.16%	4.01%	4.44%	0.30%	0.05%	0.03%
Lower Rancheria Creek	35,348.4	0.03%	4.06%	0.03%	80.32%	12.86%	1.42%	1.21%	0.03%	0.02%	0.03%
Anderson Creek	29,412.5	0.18%	4.33%	0.00%	41.19%	35.53%	6.90%	9.07%	1.82%	0.93%	0.04%
Indian Creek	25,252.4	0.03%	3.74%	0.01%	76.14%	15.53%	2.14%	1.99%	0.24%	0.18%	0.01%
North Branch N.F. Navarro River	18,190.0	0.01%	5.23%	--	89.77%	2.42%	1.43%	1.13%	0.01%	--	--
South Branch N.F. Navarro River	18,790.5	0.00%	5.30%	0.00%	89.82%	4.25%	0.51%	0.09%	0.01%	--	--
North Fork Navarro River	10,498.6	0.02%	7.11%	--	79.94%	11.47%	0.86%	0.57%	0.03%	--	--
Upper Navarro River	28,660.8	0.07%	4.55%	0.02%	72.32%	7.81%	4.63%	5.78%	2.77%	2.02%	0.05%
Lower Navarro River	11,393.5	0.06%	6.83%	0.01%	87.84%	2.24%	1.81%	0.73%	0.06%	--	0.41%
Total	**201,368**	**0.1%**	**4.7%**	**0.0%**	**71.9%**	**15.8%**	**3.0%**	**3.3%**	**0.7%**	**0.5%**	**0.0%**

Color Gradient: Lowest | Low | Med | High | Highest

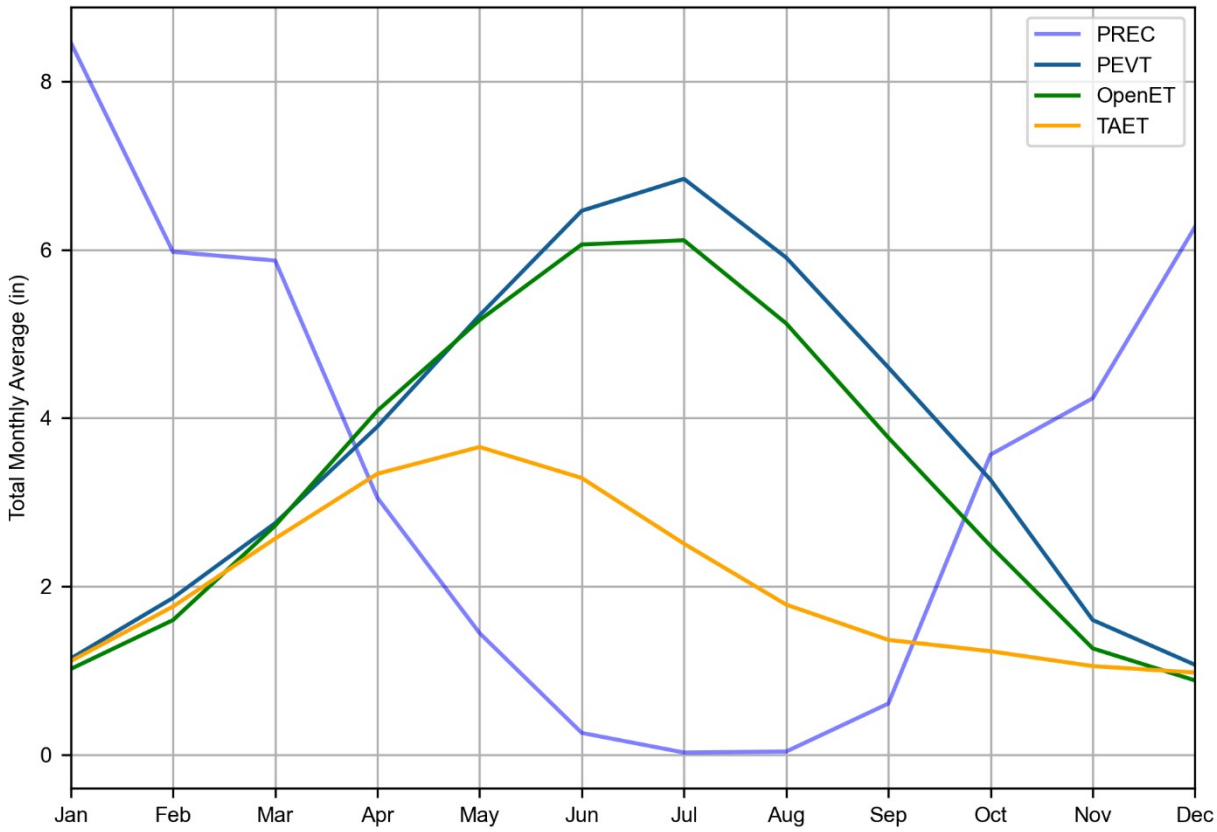

Figure 7-4. Comparison of average monthly totals from February 2016 – September 2022 for rainfall (PREC), potential ET (PEVT), OpenET, and simulated total actual ET (TAET) for the Navarro River watershed.

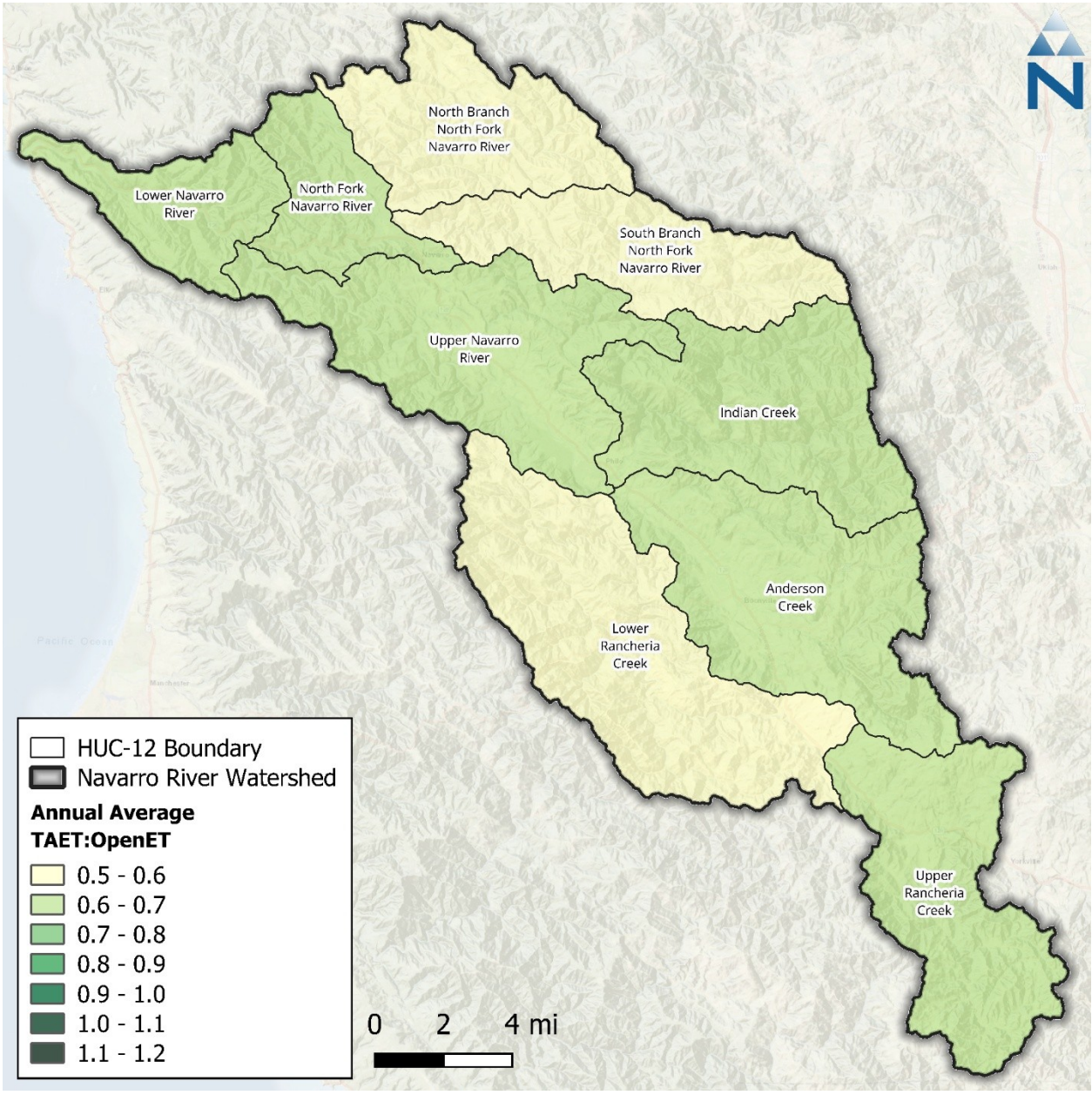

Figure 7-5. Ratio of annual average simulated total actual ET (TAET) to OpenET by HUC-12 within the Navarro River watershed.

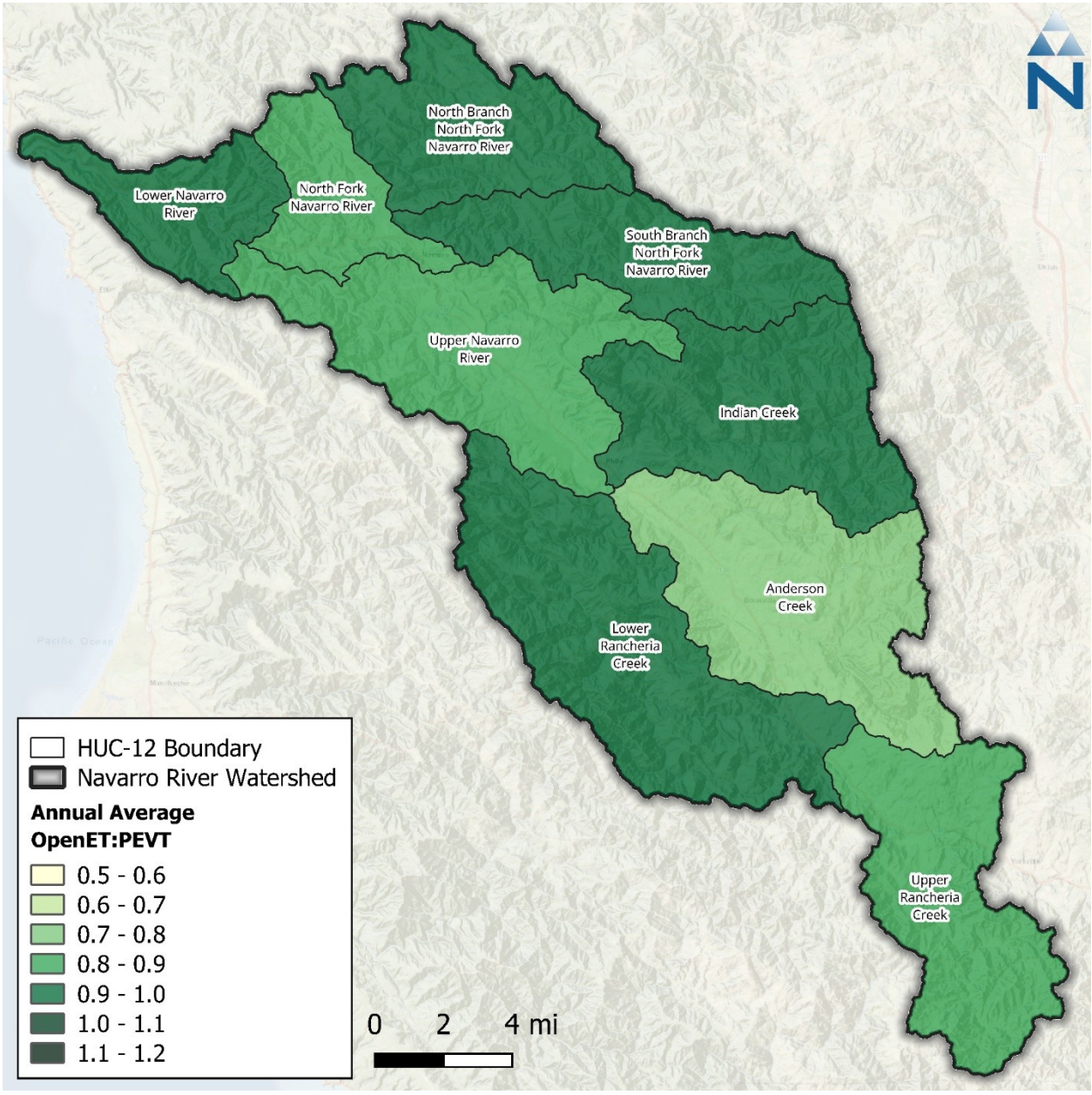

Figure 7-6. Ratio of annual average OpenET to CIMIS reference ET (PEVT) by HUC-12 within the Navarro River watershed.

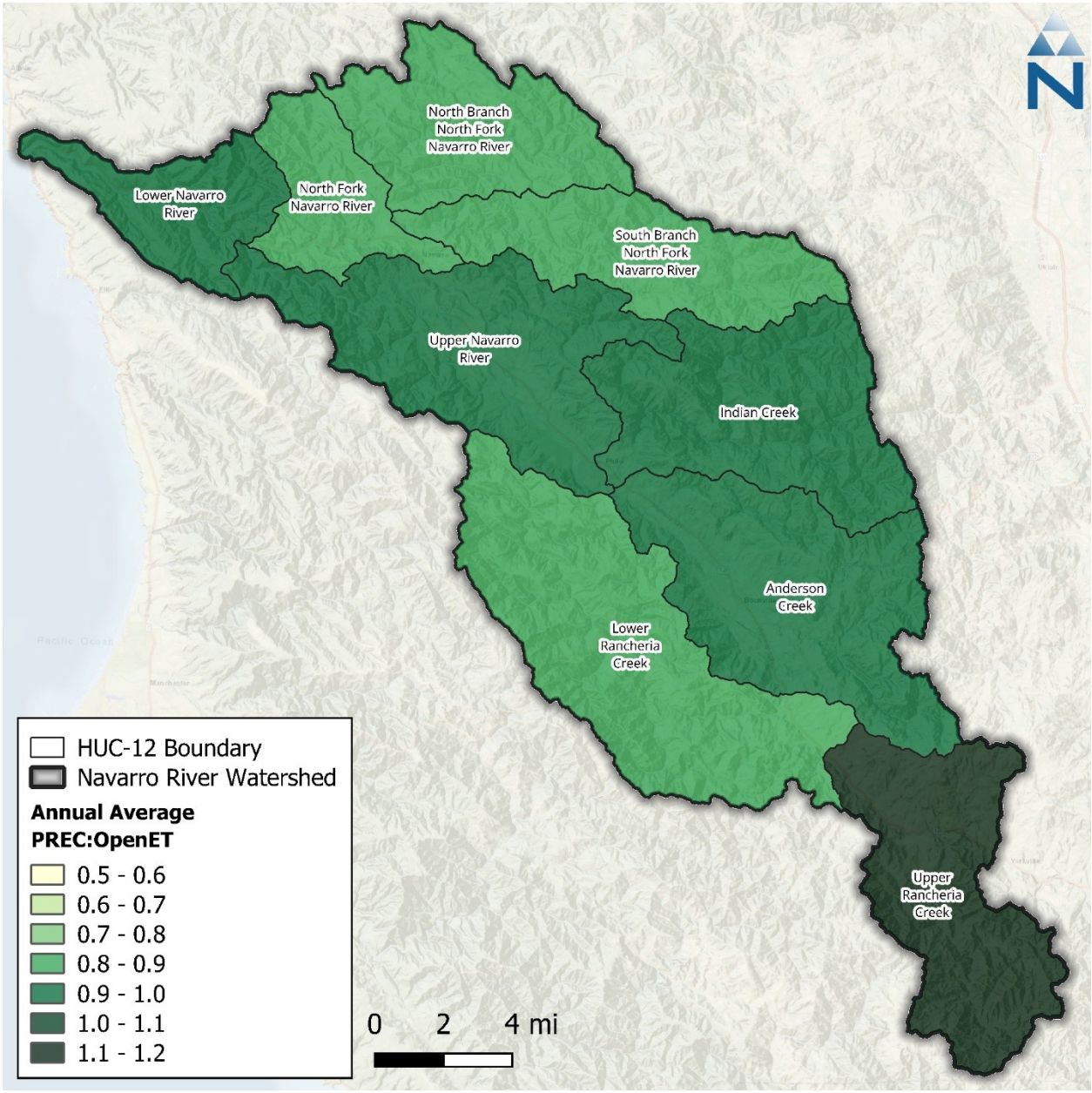

Figure 7-7. Ratio of annual average precipitation (PREC) to OpenET by HUC-12 within the Navarro River watershed.

7.2 Hydrology

Across the validation period (water years 2005 to 2017) hydrologic performance was similar to the calibration period. Note that all results below exclude observed average daily flows < 1 cfs, where there may be more uncertainty in gage readings. Over the long-term simulation, PBIAS is "Good" and slightly underpredicted (Table 7-2); seasonal PBIAS values were "Very Good". All calibration statistics so far, including those in Table 7-2, were computed using daily average time series and included higher resolution flow-regime metrics like the highest 10% of flows, storm flows, and baseflow. Table 7-3 is a summary of model calibration vs. validation performance metrics computed using monthly time series, as recommended by Moriasi et al. (2015). As expected, PBIAS is not impacted by the time step change, however, RSR and NSE both show notable improvement in performance compared to using daily average time series.

Table 7-2. Summary of daily validation performance metrics

Hydrology Monitoring Locations	Performance Metrics (10/01/2004 - 09/30/2017)														
	PBIAS						RSR			NSE			KGE[1]		
	All	Wet Season	Dry Season	>10th %ile Flows	Storm Flows	Baseflow	All	Wet Season	Dry Season	All	Wet Season	Dry Season	All	Wet Season	Dry Season
NAVARRO R NR NAVARRO CA	7%	8%	-5%	11%	8%	7%	0.34	0.35	0.40	0.88	0.88	0.84	0.87	0.86	0.92

[1] Monthly, as specified in Table 6-2.

Very Good | Good | Fair | Poor
- Overpredicts | + Underpredicts

Table 7-3. Summary of calibration and validation performance metrics using monthly averages

Calibration Metrics for Monthly Flow	Calibration: 10/01/2017 - 09/30/2023			Validation: 10/01/2004 - 09/30/2017		
	All	Wet Season	Dry Season	All	Wet Season	Dry Season
Count:	69	41	28	154	91	63
PBIAS	-1.4%	-0.9%	-9.8%	7.4%	7.9%	-5.2%
RSR	0.09	0.1	0.14	0.17	0.18	0.26
NSE	0.99	0.99	0.98	0.97	0.97	0.93
KGE	0.96	0.96	0.9	0.87	0.86	0.92

1: RSR is the ratio of the root-mean-square error to the standard deviation of observations

Very Good | Good | Fair | Poor
- Overpredicts | + Underpredicts

As with the calibration period, flow time series plots, monthly aggregate figures, and FDC were also created for the validation period, and are shown in Figure 7-8 to Figure 7-12. PBIAS, NSE, and RSR performance values by season and flow regime are shown in Table 6-8, Table 6-9, and Table 6-10, respectively. In general, performance metrics were similar between calibration and validation periods, which is likely an artifact of having the longer 13-year averaging period for computing validation metrics, compared to 6 years for the calibration period. The only metric that became "Poor" for the validation period was the highest 10% of flows during the "Dry Season." It should be noted that the dry season represents 15% of total annual flows; therefore, the highest 10% of flows within the dry season subset is a relatively small volume; therefore, small differences in flow may produce an exaggerated PBIAS error statistic.

Another notable event during the validation period was the atmospheric river event that occurred between December 2005 and January 2006, which brought heavy rainfall and high runoff to the Navarro River watershed and nearby coastal watersheds. The Navarro River USGS gage recorded an average daily streamflow of 44,400 cfs for December 31, 2005, as shown in Figure 7-13. Although the model also had the highest simulated streamflow on that day, it was not able replicate that extremely intense runoff event at that gage. Nevertheless, on average, the performance assessments demonstrate that the model performs very well across both wet and dry conditions and is a robust predictor of hydrological conditions in the Navarro River and the transition periods between both individual storms and wet/dry seasons.

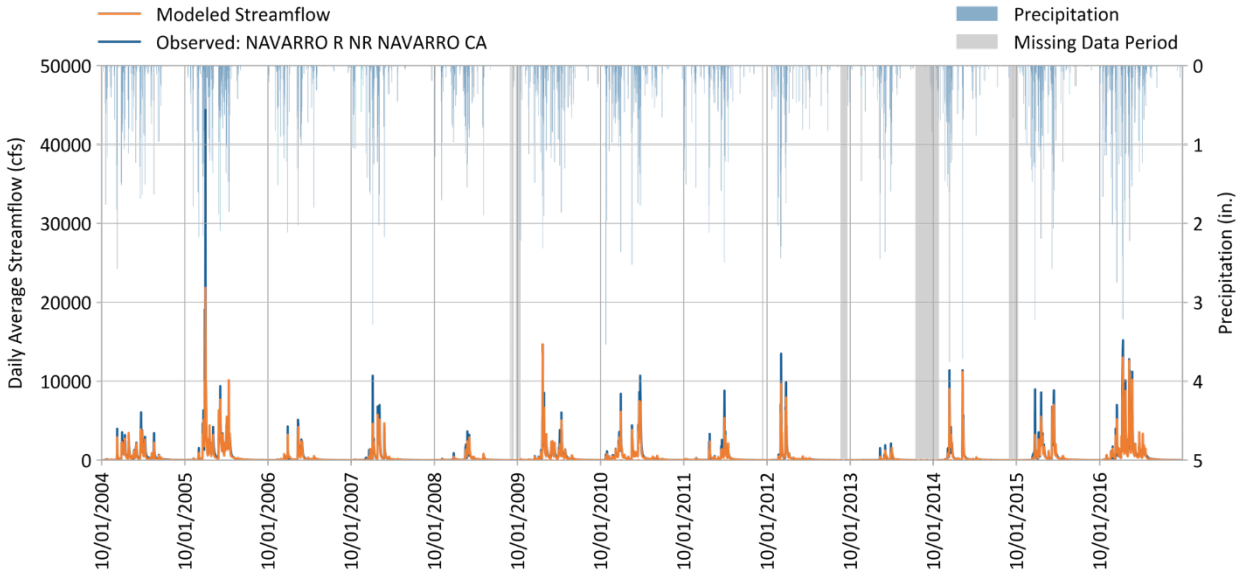

Figure 7-8. Daily simulated vs. observed streamflow for NAVARRO R NR NAVARRO CA (11468000).

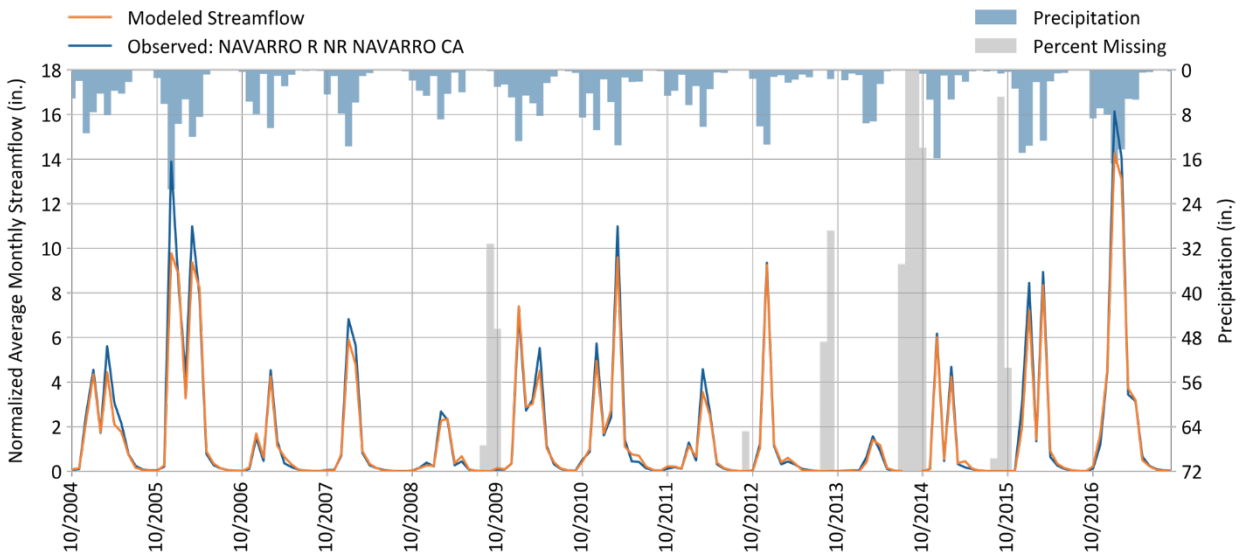

Figure 7-9. Monthly simulated vs. observed streamflow for NAVARRO R NR NAVARRO CA (11468000).

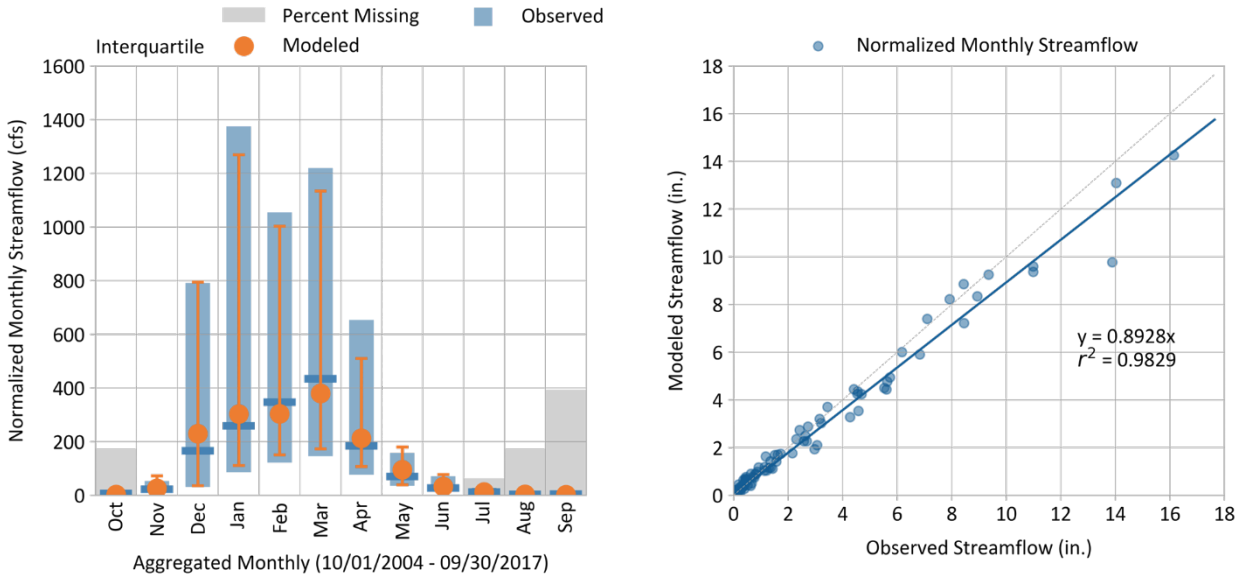

Figure 7-10. Monthly simulated vs. observed streamflow for NAVARRO R NR NAVARRO CA (11468000).

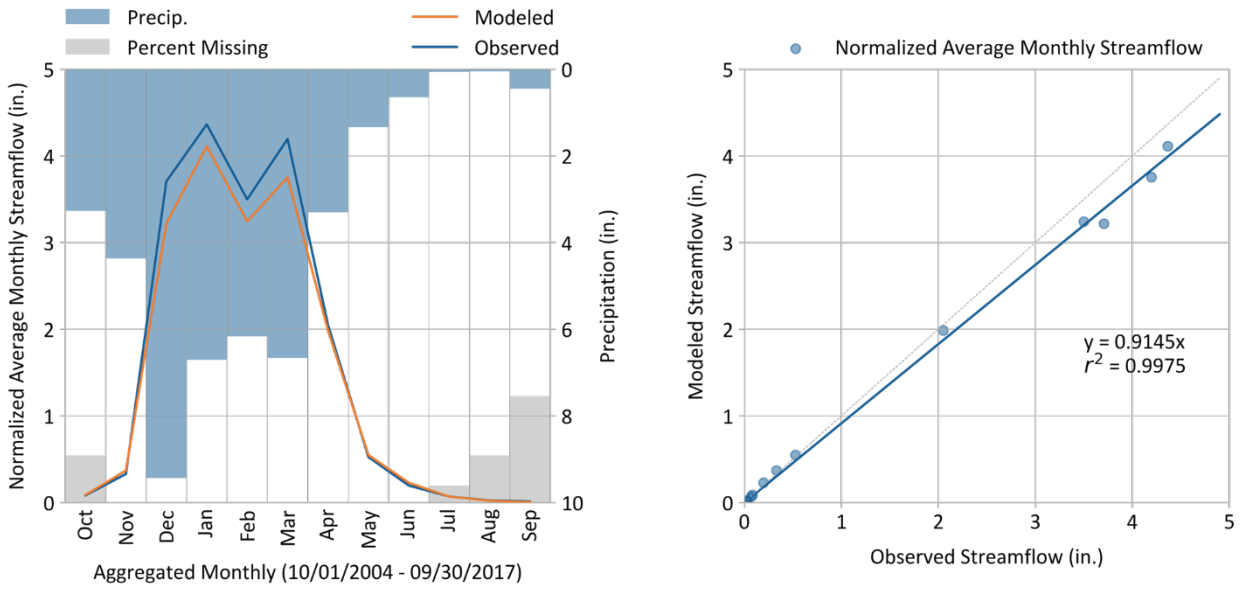

Figure 7-11. Average monthly simulated vs. observed streamflow for NAVARRO R NR NAVARRO CA (11468000).

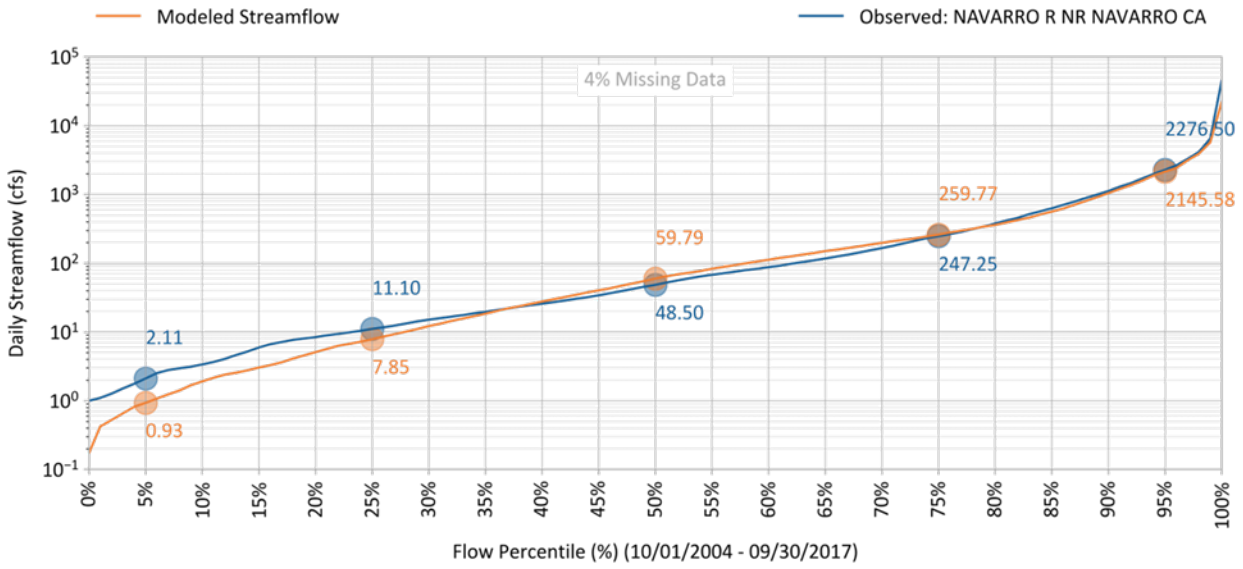

Figure 7-12. Simulated vs. observed flow duration curve for NAVARRO R NR NAVARRO CA (11468000).

Table 7-4. Simulated vs. observed daily streamflow PBIAS at NAVARRO R NR NAVARRO CA (11468000)

Validation Metrics *(10/01/2004 - 09/30/2017)*	Percent Bias (PBIAS)		
	All Seasons	Wet Season	Dry Season
All Conditions	7.4%	8.0%	-5.2%
Highest 10% of Daily Flow Rates	11.3%	11.1%	30.1%
Days Categorized as Storm Flow	7.7%	8.1%	-10.0%
Days Categorized as Baseflow	6.8%	7.7%	-3.1%

Table 7-5. Simulated vs. observed daily streamflow NSE at NAVARRO R NR NAVARRO CA (11468000)

Validation Metrics *(10/01/2004 - 09/30/2017)*	Nash-Sutcliffe Efficiency (NSE)		
	All Seasons	Wet Season	Dry Season
All Conditions	0.88	0.88	0.84
Highest 10% of Daily Flow Rates	0.78	0.78	0.27
Days Categorized as Storm Flow	0.87	0.86	0.85
Days Categorized as Baseflow	0.95	0.94	0.8

Table 7-6. Simulated vs. observed daily streamflow RSR at NAVARRO R NR NAVARRO CA (11468000)

Validation Metrics *(10/01/2004 - 09/30/2017)*	RMSE-Std-Dev. Ratio (RSR)		
	All Seasons	Wet Season	Dry Season
All Conditions	0.34	0.35	0.4
Highest 10% of Daily Flow Rates	0.46	0.46	0.85
Days Categorized as Storm Flow	0.37	0.37	0.39
Days Categorized as Baseflow	0.23	0.24	0.45

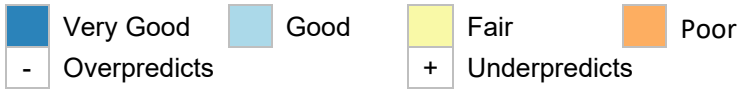

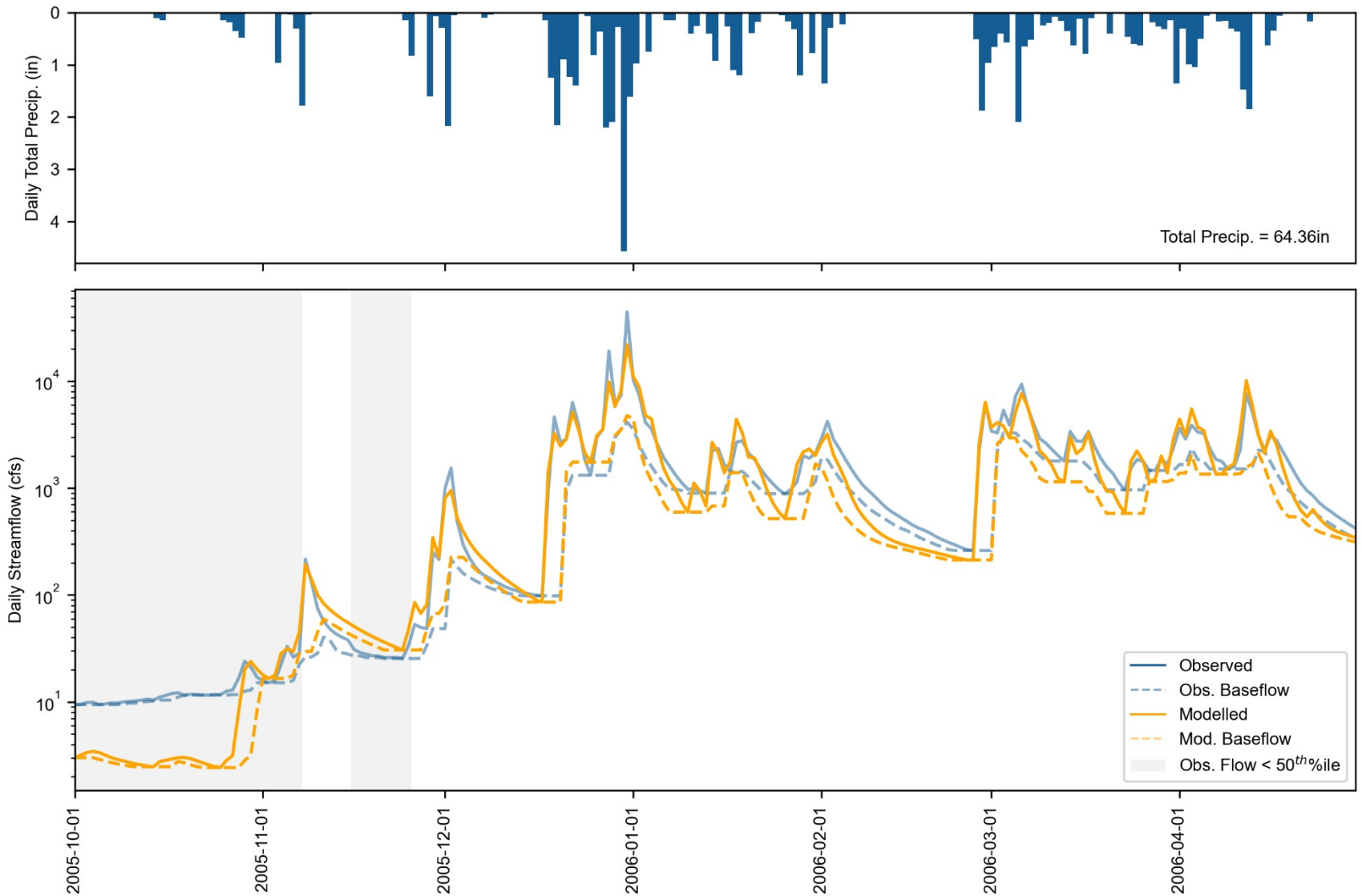

Figure 7-13. Water Year 2006 Wet season daily total precipitation (top) and streamflow (bottom) at NAVARRO R NR NAVARRO CA (11468000. Observed and simulated baseflow are calculated with HYSEP; grey shading indicates observed flow is less than the 50th percentile.

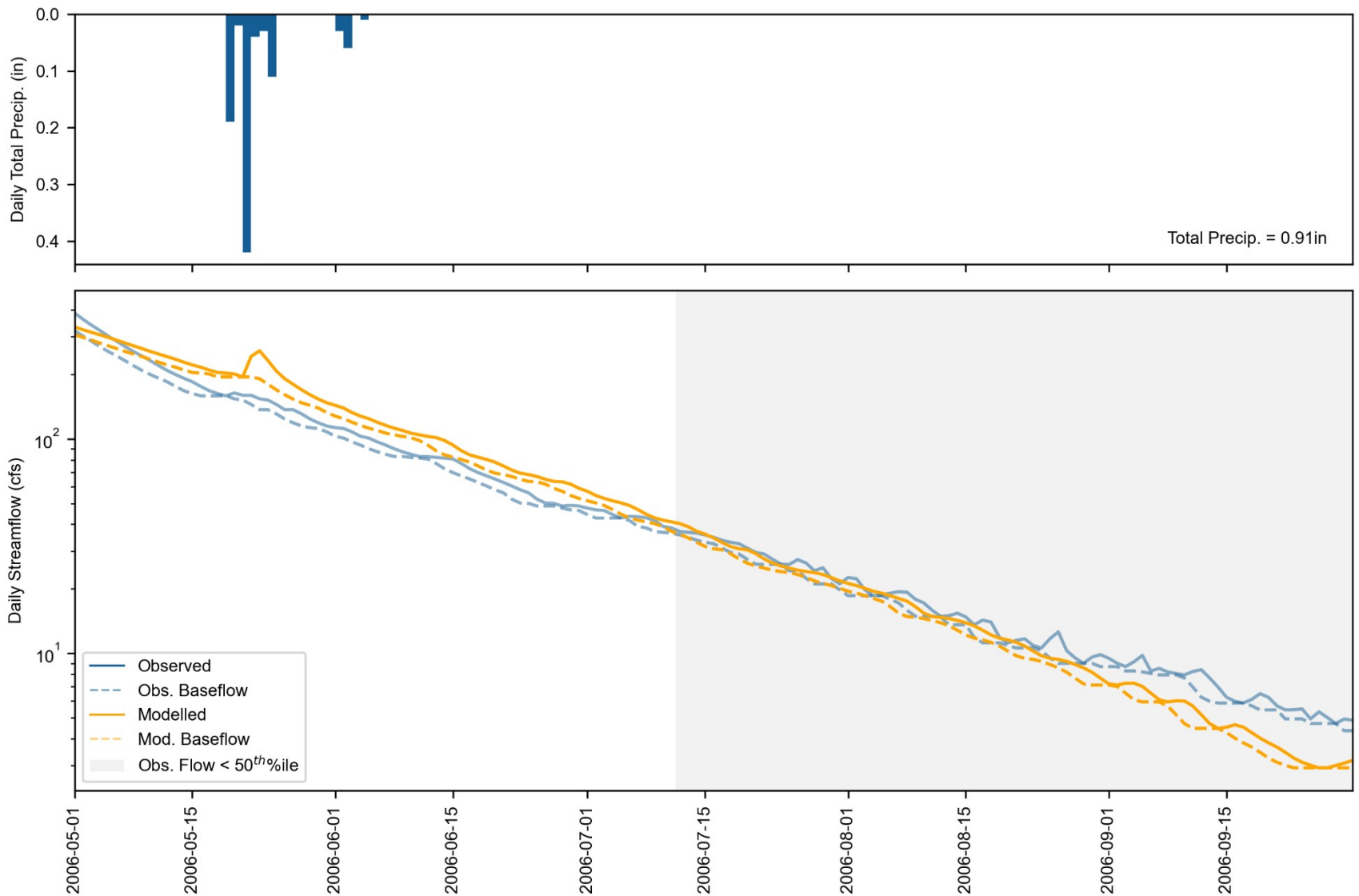

Figure 7-14. Water Year 2006 Dry season daily total precipitation (top) and streamflow (bottom) at NAVARRO R NR NAVARRO CA (11468000. Observed and simulated baseflow are calculated with HYSEP; grey shading indicates observed flow is less than the 50th percentile.

7.3 Low Flow Stream Gauges

Since 2019, the North Coast Regional Water Quality Control Board (NCRWQCB) has been monitoring dry season streamflow for 4 tributaries of the Navarro River, as shown in Figure 7-15. Flows at these locations are collected using a pressure transducer and estimated using an associated rating curve. The fit of each station's rating curve is generally high, as measured by the Coefficient of Determination (r^2) shown in Table 7-7. Full documentation of the measurement methodology and results are available in the NCRWQCB yearly reports (NCRWQCB 2020, 2021, 2022, 2023, 2024). Flow at these stations was generally recorded for the June-September period and were used as additional intermediate points of reference to validate the LSPC model's ability to represent low flow conditions upstream in smaller upstream tributaries. There is some missing data in these records, as shown in Table 7-8; across the stations, May had 42% to 71% missing but later dry season months (June to September) had more complete records with 0% to 40% missing data.

The HRU distributions for the drainage area of each of the four NCRWQCB stations, by land cover, HSG, and slope combinations are shown in Table 7-9 to Table 7-12. Like the Navarro River watershed, the drainage areas for the NCRWQCB stations are generally dominated by high slopes; however, there are some differences in major land cover and soil. The North Fork of the Navarro River is dominated by forest on B type soils. Indian Creek, Anderson Creek, and Upper Rancheria Creek also have significant portions of C and D type soils with forest, scrub, and grassland covers.

Table 7-7. Rating curve coefficient of determination for NCRWQCB stations by year

NCRWQCB Station	Drainage Area (ac)	Rating Curve Coefficient of Determination (r^2)				
		2019	2020	2021	2022	2023
N.F. Navarro River	40,013.8	0.976	0.999	0.986	0.979	0.991
Indian Creek	25,252.4	0.996	0.980	0.975	0.897	0.994
Anderson Creek	26,483.6	0.745	0.977	0.981	0.990	0.911
Upper Rancheria Creek	26,547.6	0.989	0.998	0.993	0.998	N/A

Table 7-8. Percentage of missing daily data by month for NCRWQCB stations

NCRWQCB Station	Missing Observed Data by Month (%)											
	Oct	Nov	Dec	Jan	Feb	Mar	Apr	May	Jun	Jul	Aug	Sep
N.F. Navarro River	67%	46%	76%	100%	100%	100%	87%	54%	0%	15%	25%	38%
Indian Creek	38%	50%	81%	100%	100%	100%	99%	71%	7%	0%	18%	39%
Anderson Creek	56%	75%	100%	100%	100%	100%	99%	53%	24%	23%	40%	40%
Upper Rancheria Creek	16%	50%	76%	100%	100%	100%	98%	42%	3%	0%	0%	0%

Color Gradient: Lowest | Low | Med | High | Highest

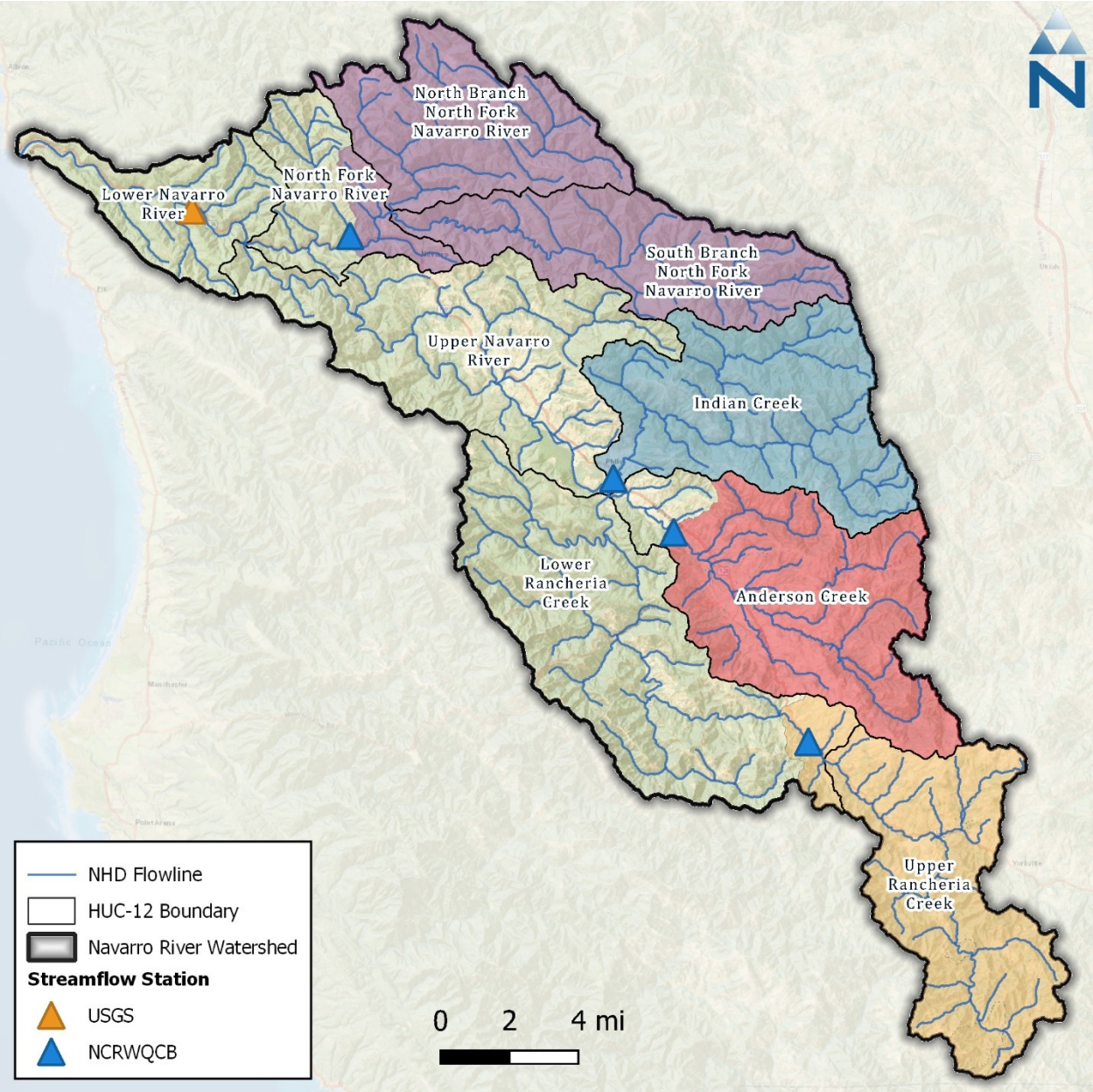

Figure 7-15. North Coast Regional Water Quality Control Board low flow monitoring stations and drainage areas within the Navarro River watershed.

Table 7-9. HRU distribution for the drainage area upstream of the North Fork Navarro River NCRWQCB station, by land cover, HSG, and slope

N.F. Navarro R.	Hydrological Soil Group (ac)					Slope (ac)			
Land Cover	Imp/ Water	A	B	C	D	Imp/ Water	Low	Med	High
Dev. Impervious	4.1	0.0	0.0	0.0	0.0	4.1	0.0	0.0	0.0
Dev. Pervious	0.0	31.2	1953.6	167.4	75.9	0.0	83.9	434.8	1709.4
Barren	0.0	0.0	0.0	0.0	0.4	0.0	0.0	0.0	0.4
Forest	0.0	105.2	32268.0	2218.2	898.9	0.0	389.0	2362.9	32738.4
Scrub	0.0	3.8	898.2	407.2	318.2	0.0	29.1	206.2	1392.2
Grassland	0.0	2.9	207.3	111.0	82.1	0.0	21.8	101.4	280.0
Pasture	0.0	0.0	76.7	130.1	47.4	0.0	27.4	115.2	111.6
Agriculture	0.0	0.0	3.3	1.6	1.1	0.0	0.9	3.3	1.8
Water	0.0	0.0	0.0	0.0	0.0	0.0	0.0	0.0	0.0
Irrigation	0.0	0.0	0.0	0.0	0.0	0.0	0.0	0.0	0.0
Total (ac)	**4.1**	**143.1**	**35407.2**	**3035.3**	**1424.1**	**4.1**	**552.0**	**3223.8**	**36233.8**
Total (%)	**0.0%**	**0.4%**	**88.5%**	**7.6%**	**3.6%**	**0.0%**	**1.4%**	**8.1%**	**90.6%**

Color gradients indicate HRU combinations with more area for Soil Group and Slope, respectively

Table 7-10. HRU distribution for the drainage area upstream of the Indian Creek NCRWQCB station, by land cover, HSG, and slope

Indian Creek	Hydrological Soil Group (ac)					Slope (ac)			
Land Cover	Imp/ Water	A	B	C	D	Imp/ Water	Low	Med	High
Dev. Impervious	7.3	0.0	0.0	0.0	0.0	7.3	0.0	0.0	0.0
Dev. Pervious	0.0	8.7	286.5	361.5	286.7	0.0	50.2	165.7	727.5
Barren	0.0	0.0	0.0	0.9	0.4	0.0	0.9	0.4	0.0
Forest	0.0	14.5	6,296.4	9,420.4	3,496.5	0.0	115.2	721.2	18,391.3
Scrub	0.0	5.6	336.5	1,232.1	2,348.3	0.0	35.8	256.0	3,630.6
Grassland	0.0	6.0	30.9	113.2	390.1	0.0	29.1	55.6	455.5
Pasture	0.0	13.3	26.9	137.4	324.0	0.0	90.7	68.1	342.9
Agriculture	0.0	3.1	11.0	31.1	15.9	0.0	26.1	21.7	13.3
Water	1.8	0.0	0.0	0.0	0.0	1.8	0.0	0.0	0.0
Irrigation	0.0	3.1	0.8	27.6	13.9	0.0	24.1	16.8	4.4
Total (ac)	**9.1**	**54.3**	**6,989.1**	**11,324.2**	**6,875.8**	**9.1**	**372.2**	**1,305.5**	**23,565.6**
Total (%)	**0.0%**	**0.2%**	**27.7%**	**44.8%**	**27.2%**	**0.0%**	**1.5%**	**5.2%**	**93.3%**

Color gradients indicate HRU combinations with more area for Soil Group and Slope, respectively

Table 7-11. HRU distribution for the drainage area upstream of the Anderson Creek NCRWQCB station, by land cover, HSG, and slope

Anderson Creek	Hydrological Soil Group (ac)					Slope (ac)			
Land Cover	Imp/ Water	A	B	C	D	Imp/ Water	Low	Med	High
Dev. Impervious	48.5	0.0	0.0	0.0	0.0	48.5	0.0	0.0	0.0
Dev. Pervious	0.0	34.4	178.0	697.7	208.4	0.0	260.0	304.0	554.6
Barren	0.0	0.0	0.0	0.0	0.0	0.0	0.0	0.0	0.0
Forest	0.0	9.3	2,349.4	7,354.6	1,043.3	0.0	87.4	615.8	10,053.3
Scrub	0.0	11.3	158.6	7,413.5	2,207.0	0.0	216.4	1,176.9	8,397.2
Grassland	0.0	40.7	131.4	1,037.9	589.1	0.0	301.3	433.0	1,064.8
Pasture	0.0	57.4	162.1	1,213.8	862.9	0.0	629.4	434.8	1,232.1
Agriculture	0.0	35.1	48.8	258.1	77.8	0.0	209.3	130.7	80.0
Water	10.9	0.0	0.0	0.0	0.0	10.9	0.0	0.0	0.0
Irrigation	0.0	9.8	35.5	160.9	37.1	0.0	150.3	60.4	32.6
Total (ac)	**59.4**	**198.1**	**3,063.8**	**18,136.5**	**5,025.7**	**59.4**	**1,854.1**	**3,155.6**	**21,414.4**
Total (%)	**0.2%**	**0.7%**	**11.6%**	**68.5%**	**19.0%**	**0.2%**	**7.0%**	**11.9%**	**80.9%**

Color gradients indicate HRU combinations with more area for Soil Group and Slope, respectively

Table 7-12. HRU distribution for the drainage area upstream of the Upper Rancheria Creek NCRWQCB station, by land cover, HSG, and slope

Upper Rancheria Creek	Hydrological Soil Group (ac)					Slope (ac)			
Land Cover	Imp/ Water	A	B	C	D	Imp/ Water	Low	Med	High
Dev. Impervious	17.4	0.0	0.0	0.0	0.0	17.4	0.0	0.0	0.0
Dev. Pervious	0.0	0.0	168.1	692.2	301.7	0.0	67.7	294.9	799.4
Barren	0.0	0.0	0.0	1.1	0.0	0.0	0.0	0.7	0.4
Forest	0.0	0.0	1779.6	9749.1	2316.0	0.0	110.1	905.4	12829.2
Scrub	0.0	0.0	438.3	5742.0	2853.1	0.0	215.5	1301.9	7516.0
Grassland	0.0	0.0	27.6	781.3	314.7	0.0	57.4	201.5	864.7
Pasture	0.0	0.0	24.7	1055.9	193.7	0.0	92.7	242.6	938.9
Agriculture	0.0	0.0	2.6	50.9	17.7	0.0	13.8	26.2	31.1
Water	7.1	0.0	0.0	0.0	0.0	7.1	0.0	0.0	0.0
Irrigation	0.0	0.0	0.8	10.2	1.9	0.0	5.3	4.2	3.3
Total (ac)	**24.5**	**0.0**	**2441.6**	**18082.7**	**5998.8**	**24.5**	**562.5**	**2977.5**	**22983.2**
Total (%)	**0.1%**	**0.0%**	**9.2%**	**68.1%**	**22.6%**	**0.1%**	**2.1%**	**11.2%**	**86.6%**

Color gradients indicate HRU combinations with more area for Soil Group and Slope, respectively

Across the NCRWQCB stations, monthly average streamflow was used to evaluate the LSPC model's ability to represent low flow conditions. Table 7-13 summarizes dry-season observed and simulated flow averaged over all dry-season days and their computed PBIAS statistic alongside R^2 values of observed vs. simulated flow for all seasons. The N.F. Navarro River and Indian Creek had slight overprediction of dry season flows; Anderson Creek and Upper Rancheria Creek had "Unsatisfactory" overprediction of the smallest streamflow values. Across all seasons, Indian Creek, Anderson Creek, and Upper Rancheria Creek had "Good" to "Very Good" values for the monthly average flow coefficient of determination (R^2), as shown in Table 7-13. The R^2 metric describes the degree of linear relationship in the variability of observed and simulated data—the R^2 metric describes how well the model predicts the timing of streamflow. Values for R^2 range from 0 to 1, with 1 indicating a perfect fit; values greater than 0.75 indicate a very good fit to seasonal flows while values ≤ 0.5 indicate a poor match of simulated and observed values (Donigian 2000). Simulating instream low flows can be challenging because small-value differences in low flow values are exaggerated as large percentage differences in model error statistics. For example, a simulated value of 2 cfs versus an observed value of 1 cfs translates to 100% difference even though the difference in flow is a relatively small 1 cfs.

Table 7-13. Comparison of simulated and observed dry season daily average streamflow with monthly average streamflow R^2 for all seasons at low flow stations

Hydrology Monitoring Locations	Dry Season (Apr-Sep) Average Daily Streamflow (cfs)			All Seasons
	Observed	Simulated	PBIAS	R^2
North Fork Navarro	1.15	1.48	-6.1% (n=16 months)	0.22 (n=21)
Indian Creek	2.58	2.83	-9.3% (n=21 months)	0.89 (n=28)
Anderson Creek	0.89	4.21	-358.7% (n=16 months)	0.92 (n=21)
Upper Rancheria Creek	1.03	3.61	-244.2% (n=18 months)	0.85 (n=26)

Very Good Good Fair Poor
\- Overpredicts + Underpredicts

Figure 7-16 to Figure 7-19 present the range of average observed and simulated values by month for each station as well as a 1:1 plot with values for every month. Examination of these plots helps explain the low overall R^2 value for the N.F. Navarro River (Figure 7-16). There is good correspondence between simulated and observed values during the dry season; however, the model overpredicts wet season flows (e.g., October, November, December). Monthly average flows also have a reasonable fit for the dry season months at Indian Creek (Figure 7-17). The model overpredicts flows at Anderson Creek and Upper Rancheria Creek, but in a consistent manner over the time series which leads to the high overall R^2 values. These two stations are predominately C type soils, as opposed to the N.F. Navarro River and Indian Creek which are B dominate and B/C mixed, respectively. The overprediction at these stations may indicate the need to reduce runoff from C type soils, which could be a potential avenue for future refinement, or that there are additional water losses (e.g., groundwater pumping) that are not accounted for in the model.

Figure 7-20 to Figure 7-23 present a comparison of average monthly totals for rainfall, potential ET, OpenET, and simulated total actual ET. In general, OpenET values for these drainage areas (at the HUC-12 scale) are similar to the potential ET and follow the same trends seen at the watershed scale, as discussed in Section 7.1.1. At Anderson Creek and Upper Rancheria Creek, which have a higher percentage of scrub and grassland land covers than the N.F. Navarro River and Indian Creek, OpenET

is lower than potential ET; while OpenET may still be biased high for these land covers, it may indicate the need to slightly increase simulated ET for these land covers.

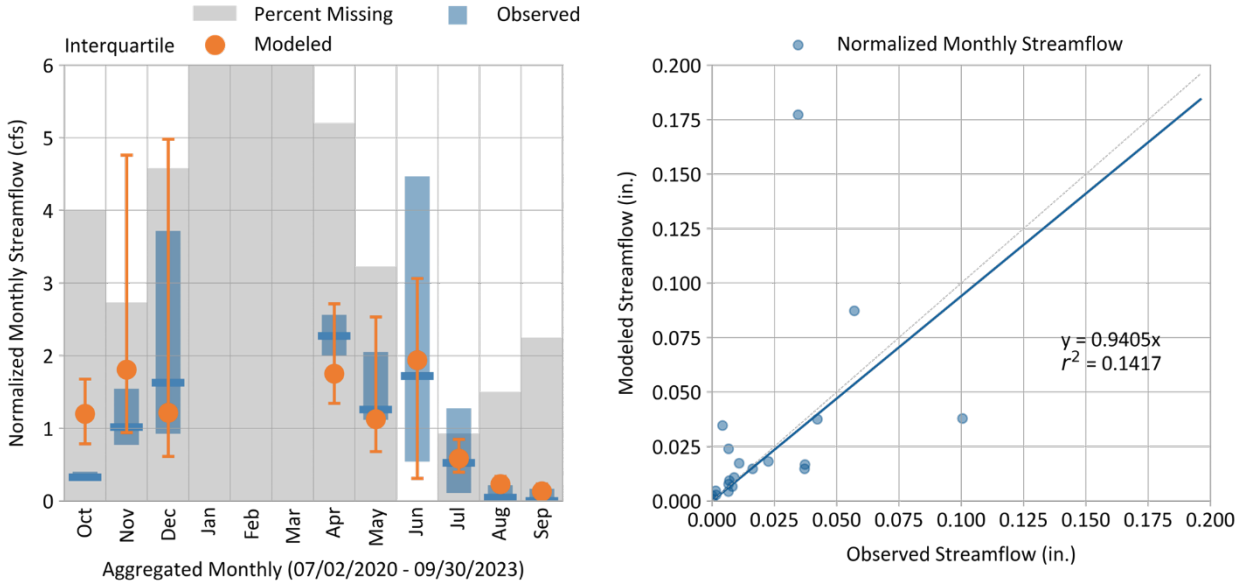

Figure 7-16. Monthly simulated vs. observed streamflow for the North Fork Navarro River NCRWQCB station.

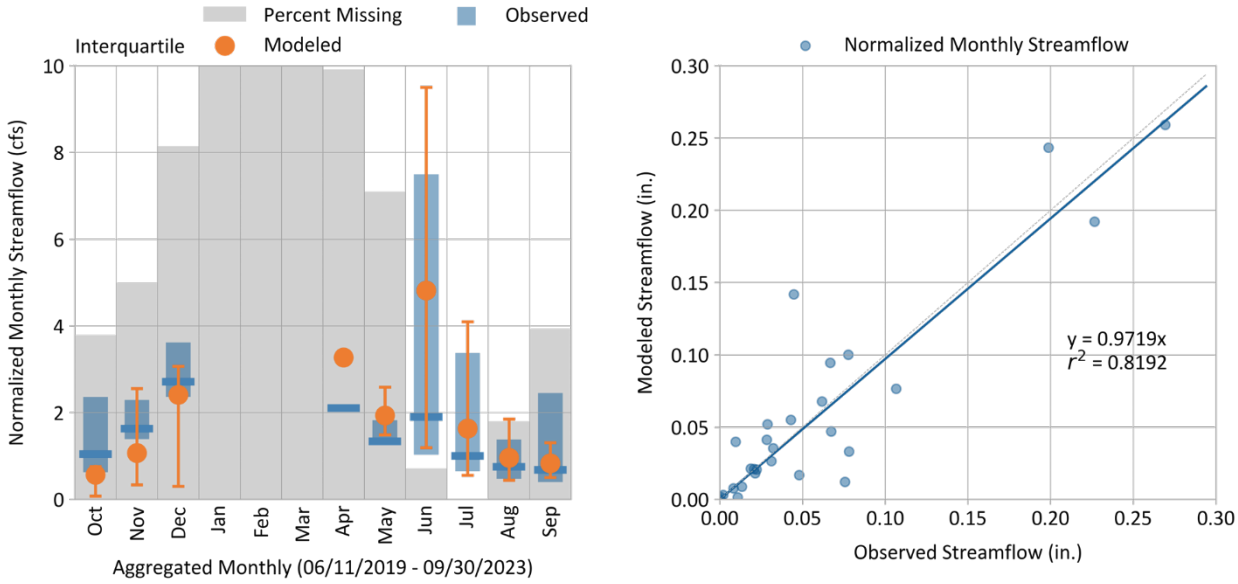

Figure 7-17. Monthly simulated vs. observed streamflow for the Indian Creek NCRWQCB station.

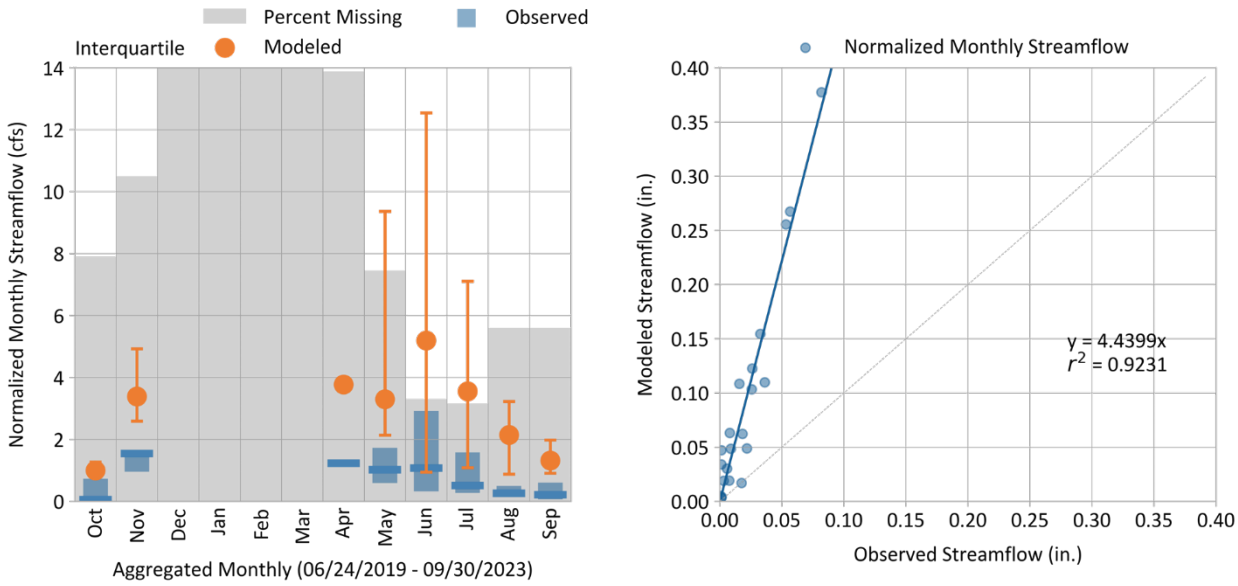

Figure 7-18. Monthly simulated vs. observed streamflow for the Anderson Creek NCRWQCB station.

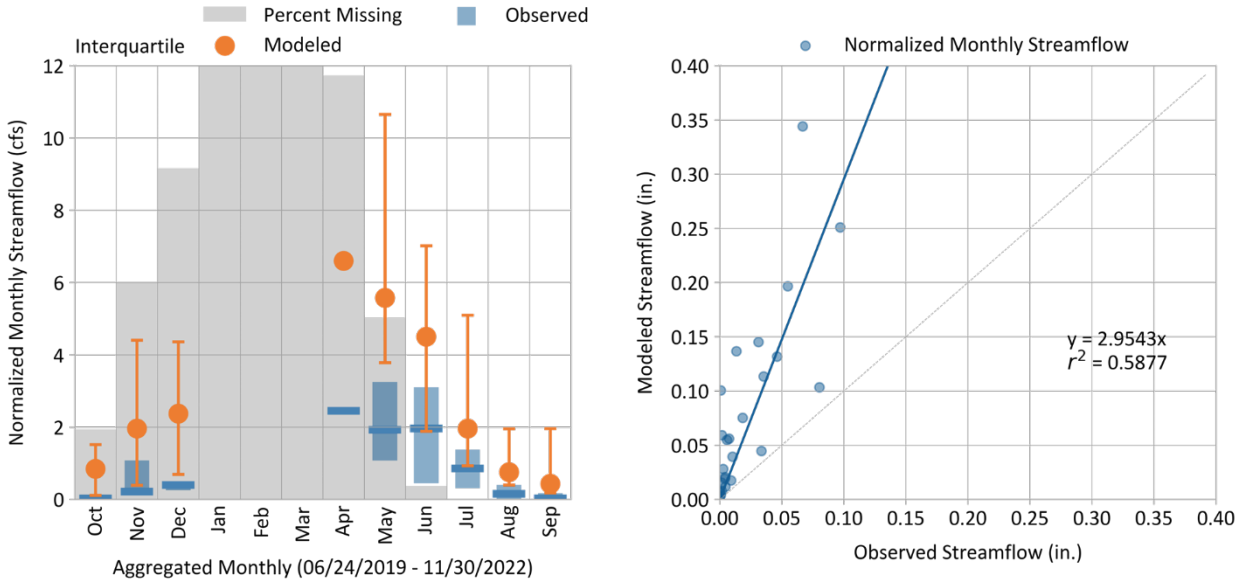

Figure 7-19. Monthly simulated vs. observed streamflow for the Upper Rancheria Creek NCRWQCB station.

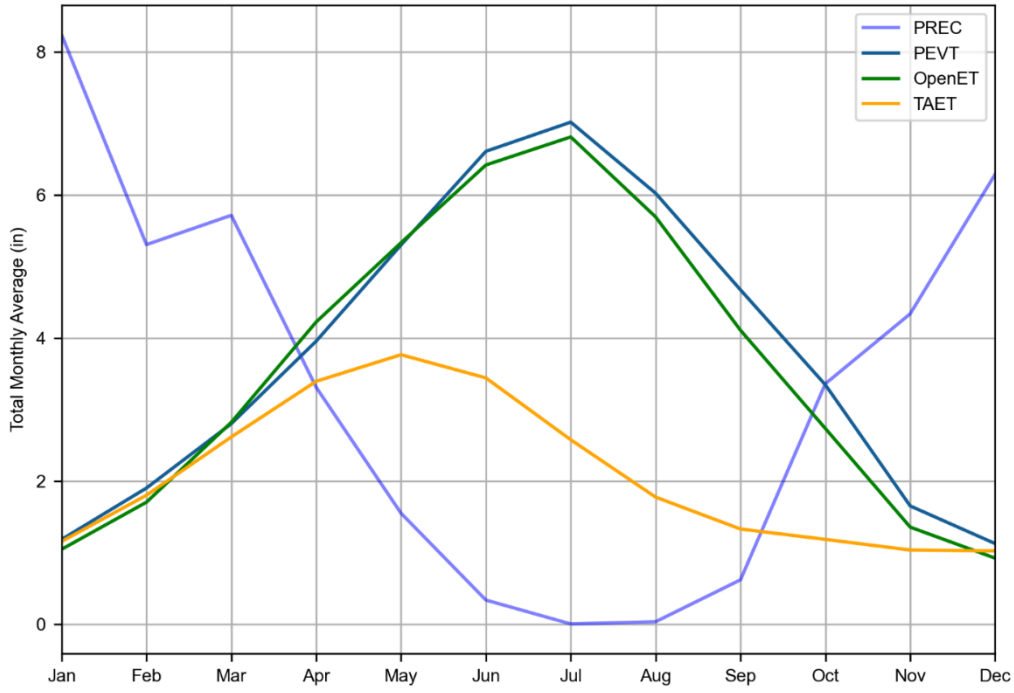

Figure 7-20. Comparison of average monthly totals from February 2016 – September 2022 for rainfall (PREC), potential ET (PEVT), OpenET, and simulated total actual ET (TAET) for the North Fork Navarro River NCRWQCB station (180101080405, 180101080406, 180101080407 HUC-12s).

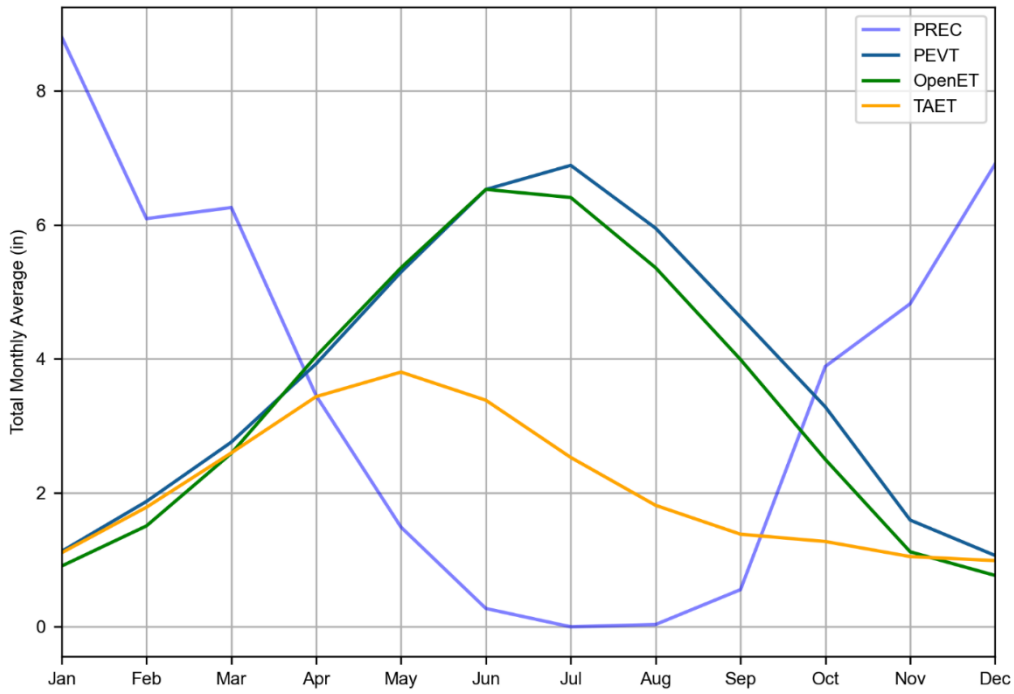

Figure 7-21. Comparison of average monthly totals from February 2016 – September 2022 for rainfall (PREC), potential ET (PEVT), OpenET, and simulated total actual ET (TAET) for the Indian Creek NCRWQCB station (HUC-12 180101080404).

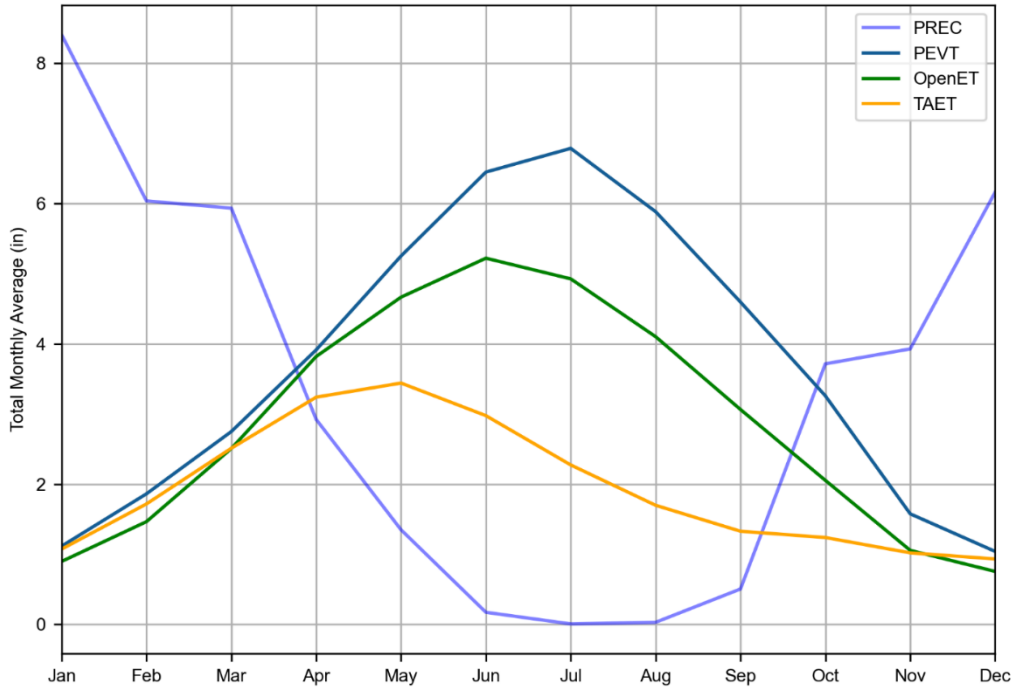

Figure 7-22. Comparison of average monthly totals from February 2016 – September 2022 for rainfall (PREC), potential ET (PEVT), OpenET, and simulated total actual ET (TAET) for the Anderson Creek NCRWQCB station (HUC-12 180101080403).

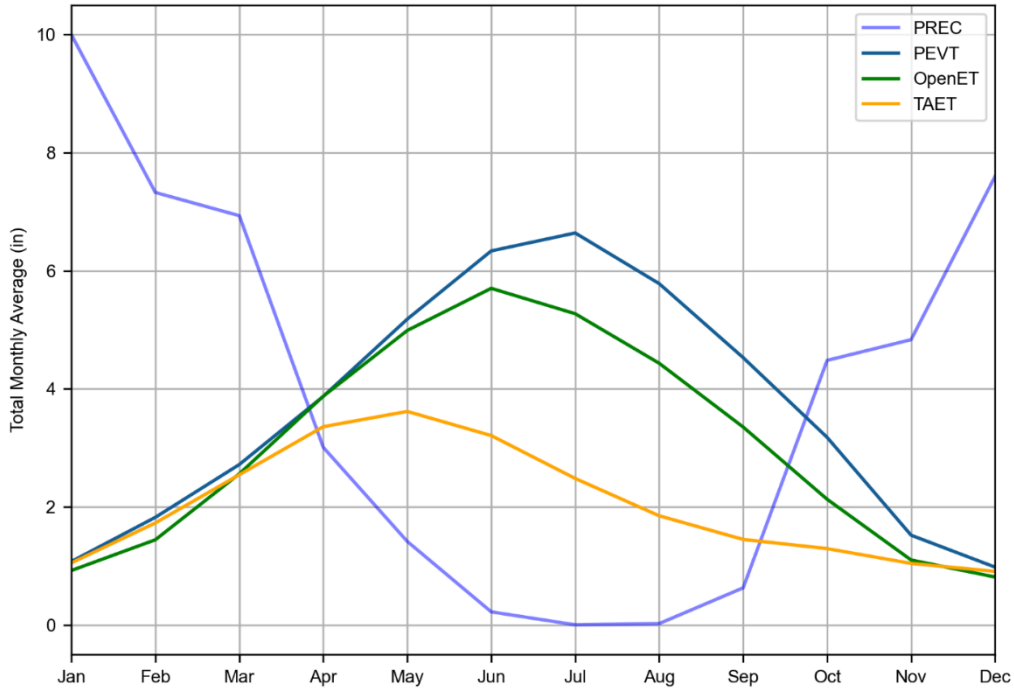

Figure 7-23. Comparison of average monthly totals from February 2016 – September 2022 for rainfall (PREC), potential ET (PEVT), OpenET, and simulated total actual ET (TAET) for the Upper Rancheria Creek NCRWQCB station (HUC-12 180101080401).

8 SUMMARY

This report documented the configuration, calibration, and validation of an LSPC hydrology model for the Navarro River watershed. The Water Board will use this model to help facilitate water use planning to ensure adequate, minimal water supplies for critical purposes. The Navarro River watershed model provides a comprehensive planning and decision-making tool by serving as an evaluation platform for (1) simulating existing instream flows that integrate current water management activities and consumptive uses and (2) evaluating the range of impacts of alternative management scenarios, including water allocation, changes in demand, and the impact of extreme events (e.g., droughts, atmospheric rivers, etc.).

The Navarro River watershed model was configured based on authoritative and comprehensive data sets suitable for characterizing hydrology within the region. The model is based on HRUs, which capture physical attributes controlling the rainfall-runoff response and are driven by long-term meteorological forcing time series representing the spatial and temporal range of precipitation and evapotranspiration conditions in the watershed. The model was calibrated and validated at the USGS streamflow station near the mouth of the river, which is the only long-term streamflow data set corresponding to the modeled period (Water Years 2004-2023). Overall model performance across the evaluated performance metrics was generally "Very Good" to "Good."

The model was also validated at four streamflow stations operated by the NCRWQCB during the dry seasons (e.g., June - September) since 2019. At these stations, the model is able to capture the trends in declining streamflow as the dry season progresses. Monthly dry season flow magnitudes are generally well matched by the model for the N. F. Navarro River and Indian Creek; however, flow is overestimated at Anderson Creek and Upper Rancheria Creek. Those two drainages had more shrub and grassland on C and D type soils, compared to N. F. Navarro River and Indian Creek, where B and C soils were dominant. The project team received the four low-flow stations used for validation after model calibration had been completed and no further adjustments were made to the model parameters after validation. The validation effort highlights possible areas for future improvement in terms of the spatial variability of low-flow model predictions and associated upstream HRU distribution and parameterization. Riparian vegetation impact is another important hydrological consideration currently estimated on average at the HRU level instead of being directly represented within the stream corridor. Some of the variability in low-flow predictions may be impacted by variability in riparian vegetation or from unknown illicit cannabis irrigation.

In conclusion, the Navarro River watershed model is a robust platform for representing existing conditions and setting up future management scenarios. An important benefit of the model development approach used to build the watershed model and described in this report is that it is designed in a modular way where key components can be refined and improved over time as new and better information becomes available.

9 REFERENCES

Arcement, G.J., JR. and V.R. Schneider, 1989. Guide for Selecting Manning's Roughness Coefficients for Natural Channels and Flood Plains. USGS Water-Supply Paper 2339.

Arnold, J.G., P.M. Allen, R. Muttiah, and G. Bernhardt, 1995. Automated Base Flow Separation and Recession Analysis Techniques. Groundwater 33:1010–1018.

Bent, G.C. and A.M. Waite, 2013. Equations for Estimating Bankfull Channel Geometry and Discharge for Streams in Massachusetts. U.S. Geological Survey Scientific Investigations Report 2013–5155. :62.

Cosgrove, B.A., D. Lohmann, K.E. Mitchell, P.R. Houser, E.F. Wood, J.C. Schaake, A. Robock, C. Marshall, J. Sheffield, Q. Duan, L. Luo, R.W. Higgins, R.T. Pinker, J.D. Tarpley, and J. Meng, 2003. Real-Time and Retrospective Forcing in the North American Land Data Assimilation System (NLDAS) Project. Journal of Geophysical Research: Atmospheres 108:8842.

Daly, C., G. H. Taylor, W. P. Gibson, T. W. Parzybok, G. L. Johnson, and P. A. Pasteris, 2000. High-Quality Spatial Climate Data Sets for the United States and Beyond. Transactions of the ASAE 43:1957–1962.

Daly, C., R.P. Neilson, and D.C. Phillips, 1994. A Statistical-Topographic Model for Mapping Climatological Precipitation over Mountainous Terrain. Journal of Applied Meteorology and Climatology 33:140–158.

Daly, C., G. Taylor, and W. Gibson, 1997. The Prism Approach to Mapping Precipitation and Temperature. 10th AMS Conf. on Applied Climatology. Reno, NV, pp. 10–12.

Doherty, J. 2015. Calibration and Uncertainty Analysis for Complex Environmental Models - PEST: complete theory and what it means for modelling the real world. ISBN: 978-0-9943786-0-6

Donigian, A.S., 2000. Watershed Model Calibration and Validation: Issues and Procedures.

Duda, P.B., P.R. Hummel, A.S. Donigian, and J.C. Imhoff, 2012. BASINS/HSPF: Model Use, Calibration, and Validation. Transactions of the ASABE 55:1523–1547.

EPA (U.S. Environmental Protection Agency), 2000. BASINS Technical Note 6 Estimating Hydrology and Hydraulic Parameters for HSPF.

Gibson, W.P., C. Daly, T. Kittel, D. Nychka, C. Johns, N. Rosenbloom, A. McNab, and G.H. Taylor, 2002. Development of a 103-Year High-Resolution Climate Data Set for the Conterminous United States. Proceedings of the 13th AMS Conference on Applied Climatology. Portland, OR, pp. 181–183.

Gupta, H. V., H. Kling, K.K. Yilmaz, and G.F. Martinez, 2009. Decomposition of the Mean Squared Error and NSE Performance Criteria: Implications for Improving Hydrological Modelling. Journal of Hydrology 377:80–91.

Henn, B., A.J. Newman, B. Livneh, C. Daly, and J.D. Lundquist, 2018. An Assessment of Differences in Gridded Precipitation Datasets in Complex Terrain. Journal of Hydrology 556:1205–1219.

Kim, S., K. Paik, F.M. Johnson, and A. Sharma, 2018. Building a Flood-Warning Framework for Ungauged Locations Using Low Resolution, Open-Access Remotely Sensed Surface Soil Moisture, Precipitation, Soil, and Topographic Information. IEEE Journal of Selected Topics in Applied Earth Observations and Remote Sensing 11:375–387.

Knoben, W.J.M., J.E. Freer, and R.A. Woods, 2019. Technical Note: Inherent Benchmark or Not? Comparing Nash–Sutcliffe and Kling–Gupta Efficiency Scores. Hydrology and Earth System Sciences 23:4323–4331.

Kouchi, D.H., K. Esmaili, A. Faridhosseini, S.H. Sanaeinejad, D. Khalili, and K.C. Abbaspour, 2017. Sensitivity of Calibrated Parameters and Water Resource Estimates on Different Objective Functions and Optimization Algorithms. Water 9. doi:10.3390/w9060384.

LACFCD (Los Angeles County Flood Control District), 2020. WMMS Phase I Report: Baseline Hydrology and Water Quality Model. Prepared for the Los Angeles County Flood Control District by Paradigm Environmental. Alhambra, CA.

Looper, J.P. and B.E. Vieux, 2012. An Assessment of Distributed Flash Flood Forecasting Accuracy Using Radar and Rain Gauge Input for a Physics-Based Distributed Hydrologic Model. Journal of Hydrology 412–413:114–132.

McCandless, T.L., 2003a. Maryland Stream Survey: Bankfull Discharge and Channel Characteristics in the Allegheny Plateau and the Valley and Ridge Hydrologic Region. Annapolis, MD.

McCandless, T.L., 2003b. Maryland Stream Survey: Bankfull Discharge and Channel Characteristics in the Coastal Plain Hydrologic Region. Annapolis, MD. www.fws.gov/r5cbfo. Accessed 4 Jul 2021.

McCandless, T.L. and R.A. Everett, 2002. Maryland Stream Survey: Bankfull Discharge and Channel Characteristics in the Piedmont Hydrologic Region. Annapolis, MD.

McGourty, G., et al. 2020. Agricultural water use accounting provides path for surface water use solutions. California Agriculture, 74(1), 46–57. https://doi.org/10.3733/CA.2020A0003

Melton, F.S., J. Huntington, R. Grimm, J. Herring, M. Hall, D. Rollison, T. Erickson, R. Allen, M. Anderson, J.B. Fisher, A. Kilic, G.B. Senay, J. Volk, C. Hain, L. Johnson, A. Ruhoff, P. Blankenau, M. Bromley, W. Carrara, B. Daudert, C. Doherty, C. Dunkerly, M. Friedrichs, A. Guzman, G. Halverson, J. Hansen, J. Harding, Y. Kang, D. Ketchum, B. Minor, C. Morton, S. Ortega-Salazar, T. Ott, M. Ozdogan, P.M. ReVelle, M. Schull, C. Wang, Y. Yang, and R.G. Anderson, 2022. OpenET: Filling a Critical Data Gap in Water Management for the Western United States. JAWRA Journal of the American Water Resources Association 58:971–994.

Mitchell, K.E., D. Lohmann, P.R. Houser, E.F. Wood, J.C. Schaake, A. Robock, B.A. Cosgrove, J. Sheffield, Q. Duan, L. Luo, R.W. Higgins, R.T. Pinker, J.D. Tarpley, D.P. Lettenmaier, C.H. Marshall, J.K. Entin, M. Pan, W. Shi, V. Koren, J. Meng, B.H. Ramsay, and A.A. Bailey, 2004. The Multi-Institution North American Land Data Assimilation System (NLDAS): Utilizing Multiple GCIP Products and Partners in a Continental Distributed Hydrological Modeling System. Journal of Geophysical Research: Atmospheres 109. doi:10.1029/2003jd003823.

Moriasi, D. N., J. G. Arnold, M. W. Van Liew, R. L. Bingner, R. D. Harmel, and T. L. Veith, 2007. Model Evaluation Guidelines for Systematic Quantification of Accuracy in Watershed Simulations. Transactions of the ASABE 50:885–900.

Moriasi, D.N., M.W. Gitau, N. Pai, and P. Daggupati, 2015. Hydrologic and Water Quality Models: Performance Measures and Evaluation Criteria. Transactions of the ASABE 58:1763–1785.

Nash, J.E. and J. V. Sutcliffe, 1970. River Flow Forecasting through Conceptual Models Part I - A Discussion of Principles. Journal of Hydrology 10:282–290.

Nathan, R.J. and T.A. McMahon, 1990. Evaluation of Automated Techniques for Base Flow and Recession Analyses. Water Resources Research 26:1465–1473.

NCRWQCB (North Coast Regional Water Quality Control Board), 2020. Navarro River Watershed Flow Monitoring Memorandum 2019. Santa Rosa.

NCRWQCB (North Coast Regional Water Quality Control Board), 2021. Navarro River Watershed Flow Monitoring Memorandum 2020. Santa Rosa.

NCRWQCB (North Coast Regional Water Quality Control Board), 2022. Navarro River Watershed Flow Monitoring Results 2021. Santa Rosa.

NCRWQCB (North Coast Regional Water Quality Control Board), 2023. Navarro River Watershed Flow Monitoring Results 2022. Santa Rosa.

NCRWQCB (North Coast Regional Water Quality Control Board), 2024. Navarro River Watershed Flow Monitoring Results 2023. Santa Rosa.

OpenET, 2021. Intercomparison and Accuracy Assessment Report. https://etdata.org/wp-content/uploads/2021/10/Intercomparison-and-Accuracy-Assessment-Report.pdf. Accessed 4 Aug 2024.

Quirmbach, M. and G.A. Schultz, 2002. Comparison of Rain Gauge and Radar Data as Input to an Urban Rainfall-Runoff Model. Water Science and Technology 45:27–33.

Sloto, R.A. and M.Y. Crouse, 1996. HYSEP: A Computer Program for Streamflow Hydrograph Separation and Analysis: U.S. Geological Survey Water-Resources Investigations Report 1996–4040. doi:10.3133/wri964040.

Smakhtin, V.U., 2001. Low Flow Hydrology: A Review. Journal of Hydrology 240:147–186.

Sutherland, R.C., 2000. Methods for Estimating the Effective Impervious Area of Urban Watersheds, Technical Note 58. T. R. Scueler and H. K. Holland (Editors). The Practice of Watershed Protection. Center for Watershed Protection, Ellicot City, MD, pp. 193–195.

USDA (United States Department of Agriculture), 2024. Cropland Data Layer. URL https://croplandcros.scinet.usda.gov/ (accessed 4.25.24).

Xia, Y., K. Mitchell, M. Ek, B. Cosgrove, J. Sheffield, L. Luo, C. Alonge, H. Wei, J. Meng, B. Livneh, Q. Duan, and D. Lohmann, 2012. Continental-Scale Water and Energy Flux Analysis and Validation for North American Land Data Assimilation System Project Phase 2 (NLDAS-2): 2. Validation of Model-Simulated Streamflow. Journal of Geophysical Research Atmospheres 117. doi:10.1029/2011JD016051.

Xia, Y., K. Mitchell, M. Ek, J. Sheffield, B. Cosgrove, E. Wood, L. Luo, C. Alonge, H. Wei, J. Meng, B. Livneh, D. Lettenmaier, V. Koren, Q. Duan, K. Mo, Y. Fan, and D. Mocko, 2012. Continental-Scale Water and Energy Flux Analysis and Validation for the North American Land Data Assimilation System Project Phase 2 (NLDAS-2): 1. Intercomparison and Application of Model Products. Journal of Geophysical Research Atmospheres 117:3109.